

University of South Bohemia in České Budějovice

Faculty of Science

# **The Mitochondrial Contact Site and Cristae Organization System and F<sub>1</sub>F<sub>0</sub>-ATP Synthase Crosstalk is a Fundamental Property of Mitochondrial Cristae**

Master thesis

Bc. Lawrence Rudy Cadena III B.Sc.

Supervisor: Mgr. Hassan Hashimi, Ph.D.

Department of Molecular Biology and Genetics, Faculty of Science, University of South Bohemia in České Budějovice  
Institute of Parasitology, Biology Centre CAS, České Budějovice, Czech Republic

České Budějovice 2021

This thesis should be cited as:

**Cadena, L.R.**, (2021): A fundamental property of aerobic mitochondria: The occurrence of crosstalk between the Mitochondrial Contact Site and Cristae Organization System and dimeric F<sub>1</sub>F<sub>0</sub>-ATP Synthase in cristae. Master thesis, in English. – 53 p., Faculty of Science, University of South Bohemia, České Budějovice, Czech Republic.

## ANNOTATION

The acquisition of mitochondria from an endosymbiont closely related to extant alphaproteobacteria occurred prior to the divergence of modern eukaryotes. Since then, diverse eukaryotes have not only developed a number of different mechanisms to adapt to their environment regarding growth and proliferation, but perpetuated certain traits that have persisted for eons. This thesis postulates an ancestral mechanism for cristae development in mitochondria involving interplay between two cristae shaping protein complexes, the Mitochondrial Contact Site and Cristae Organization System and F<sub>1</sub>F<sub>0</sub>-ATP Synthase, that has remained conserved throughout eukaryotic diversification for over 2 billion years.

## **DECLARATION**

I declare that I am the author of this qualification thesis and that in writing it I have used the sources and literature displayed in the list of used sources only.

České Budějovice, 8. 12. 2021

.....  
Bc. Lawrence Rudy Cadena III B.Sc.

## **FINANCIAL SUPPORT**

I acknowledge funding from the following sources: Czech Science Foundation grants 20-23513S, 18-17529S, and 20-01450Y; Czech Ministry of Education grant OPVVV16\_019/0000759; and Czech BioImaging grant LM2015062.

## **ACKNOWLEDGEMENTS**

Firstly, I would like to extend my gratitude to my supervisor, Mgr. Hassan Hashimi, Ph.D., for his insight and helpfulness throughout my 5-year journey under his wing, starting from the point where I was ignorant of even the most basics of molecular biology. It goes without saying that my scientific maturation, the point I find myself in now, would not have been possible without your constant guidance and supervision. It is certain that I would not have achieved what you believed I was capable of achieving without your counsel, and for that you have my everlasting gratitude. I am aware that you expect excellence of me in the future, and I will do my best to strive towards those goals. Rest assured, even in old age I will never forget the sacrifices and headaches you endured for my benefit. Hassan, although we had our scientific disagreements, I always held your opinions in high regard. Thank you for everything, both the bad and the good, as I regard both experiences critical for my development as a scientist. Thank you for your support.

Additionally, I would like to Dr. Alena Zíková Ph.D. and Dr. Ondra Gahura Ph.D. for giving me the opportunity to work alongside them on the MICOS-ATP synthase project. The pleasure and honor was mine. The ability to collaborate with world-class scientists on a passionate topic of mine is something I could not have fathomed. Thank you both for your respective insights and the amazing opportunity to cooperate.

I would also like to extend my gratitude to both prof. Libor Grubhoffer Ph.D. and Mgr. Thomáš Doležal, Ph.D. for providing me the opportunity to pursue a Master of Science at the University of South Bohemia. Without their vouching, this work would not have been possible. Furthermore, I would like to currently thank prof. Julius Lukeš Ph.D. for allowing me to chance to work in his lab and pursue my own interests at the time of writing (a worthwhile investment).

On a more personal note, would like to Dr. Daria Tashyreva Ph.D. not only for her inviolable friendship, but for her support on a personal level. Thank you for being there for me, and thank you for showing me how there exists someone out there with an uninhibited love for the natural sciences.

## LIST OF PUBLICATIONS AND AUTHOR'S CONTRIBUTIONS

- I.     **Cadena, L.R.**, Gahura, O., Panicucci, B., Zíková, A., Hashimi, H. (2021) Mitochondrial Contact Site and Organization System and F<sub>1</sub>F<sub>0</sub>-ATP Synthase crosstalk is a fundamental property of mitochondrial cristae. *mSphere* **16**: e0032721 (IF on acceptance = 4.389).

*Lawrence Rudy Cadena conceived, designed and performed the experiments, analyzed the data and wrote and revised the manuscript.*

## **ABBREVIATIONS**

**CJ** Crista junctions

**CS** Contact sites

**ETC** Electron transport chain

**FECA** First eukaryotic common ancestor

**HMM** Hidden Markov model

**IBM** Inner boundary membrane

**IMS** Intermembrane space

**LECA** Last eukaryotic common ancestor

**MICOS** Mitochondrial Contact Site and Cristae Organization System

**MIB** Mitochondrial intermembrane space bridging complex

**MIM** Mitochondrial inner membrane

**MOM** Mitochondrial outer membrane

**mtDNA** Mitochondrial DNA

**OXPHOS** Oxidative Phosphorylation

**ROS** Reactive oxygen species

**SAM** Sorting and assembly machinery

**SAR** Stamenopiles Alveolates Rhizaria (Eukaryotic supergroup)

**TCA** Tricarboxylic acid

**TOM** Translocase of the outer mitochondrial membrane

1. INTRODUCTION .....	1
1.1. The mitochondrion: A brief summary .....	1
1.1.1. Labyrinthine beginnings: Evolutionary origin of the mitochondrion .....	1
1.1.2. Back to the basics: General structure and function of mitochondria .....	3
1.1.3. Mitochondria: A hub for diverse pathways .....	4
1.1.4. Cristae: Variations on a common theme.....	7
1.2. MICOS: An overview.....	8
1.2.1. MICOS: A multitasking giant .....	8
1.3. F <sub>1</sub> F <sub>o</sub> -ATP Synthase: An overview .....	11
1.3.1. F <sub>1</sub> F <sub>o</sub> -ATP Synthase: A marvelous enzyme .....	11
1.4. Trypanosoma: An enticing model to study mitochondria .....	13
1.4.1. The mitochondrion of <i>Trypanosoma brucei</i> .....	15
1.5. MICOS: A view outside humans and yeast .....	16
1.6. F <sub>1</sub> F <sub>o</sub> -ATP Synthase: Different models for different species .....	18
1.7. MICOS and F <sub>1</sub> F <sub>o</sub> -ATP Synthase crosstalk: A conserved feature? Or a fungal novelty? .....	20
2. AIMS AND TASKS .....	21
3. SUMMARY .....	21
4. ORIGINAL PAPER .....	22
5. CONCLUSION .....	37
6. ADDITIONAL EXPERIMENTS AND FUTURE PERSPECTIVES .....	39
7. REFERENCES .....	42

## 1. INTRODUCTION

*“Let us beware of saying there are laws in nature. There are only necessities: there is no one to command, no one to obey, no one to transgress.” – Friedrich Nietzsche 1882*

### The mitochondrion: A brief summary

Mitochondria are essential double-membrane bound organelles that are commonly referred to as the “powerhouse” of the cell, as they supply aerobic eukaryotes with energy in the form of ATP through respiration to meet bioenergetic needs. These organelles are inferred to have been present in the eukaryote cencestor, *i.e.*, the last eukaryotic common ancestor (LECA) (Roger et al., 2017). The acquisition of mitochondria from an endosymbiont closely related to modern alphaproteobacteria occurred prior to the divergence of modern eukaryotes (Martijn et al., 2018)(Eme et al., 2017). To date, mitochondria has been most well studied in systems belonging to what is referred to as the Opisthokonta supergroup, containing model organisms such as *Mus musculus*, *Drosophila melanogaster* and *Saccharomyces cerevisiae* (Hashimi, 2019). These organisms represent a single clade of the eukaryotic Tree of Life, thus depicting an isolated view of the diversity of mitochondria (Burki et al., 2020).

The philosophy of evolutionary cell biology suggests that a comparative approach to biological systems in different organisms can shed light to their chemical and physical limitations with respect to their evolution (Lynch et al., 2014). This comparative approach allows us to discover flexible features as well as aspects that can give rise to novel properties, as there are pathways not found in model systems but are nevertheless widely distributed throughout eukaryotes. Moreover, by studying mitochondria in diverse organisms outside the opisthokonts, we can discern specific features which have been lost, gained, and retained in multiple lineages, thus completing the picture as to what the ancestral mitochondria in LECA was like.

### Labyrinthine beginnings: Evolutionary origin of the mitochondrion

In 1967, Lynn Sagan (later Margulis) famously published a paper titled *On the Origin of Mitosing Cells*, in which she proposed that mitochondria and chloroplasts derived from endosymbiotic bacteria, building upon the theory of symbiogenesis from Konstantin Mereschkowski at the turn of the 20<sup>th</sup> century (Sagan, 1967). Initially receiving much controversy, phylogenetic analyses of both genes and proteins from both organelles a decade later confirmed their prokaryotic provenance (Bonen et al., 1977)(Schwartz and Dayhoff, 1978)(Yang et al., 1985)(Andersson et al., 1998). Since then, numerous datasets made available through high-throughput sequencing and subsequent bioinformatic analyses has further advanced our understanding of the evolutionary origin of mitochondria (Muñoz-Gómez et al., 2017). These modern phylogenomic analyses have confirmed that the ancestral

protomitochondria endosymbiont was indeed related to what is now known as alphaproteobacteria (Roger et al., 2017).

The acquisition of this alphaproteobacterial endosymbiont by a host related to Asgard archaea laid the groundwork for eukaryogenesis (Martijn et al., 2018)(Eme et al., 2017)(Zaremba-Niedzwiedzka et al., 2017). The origin and early evolution of mitochondria can be depicted in a linear and progressive way (Fig. 1.). The earliest eukaryotic common ancestor of mitochondria is known as the mitochondrial cenancestor, present in LECA. Prior to that, numerous events may have taken place after the initial acquisition of the pre-mitochondrial alphaproteobacterium from FECA (first eukaryotic common ancestor) such as the loss of various “proto-eukaryotes” species that contained this pre-mitochondrial alphaproteobacterium but became extinct, allowing only a single species to survive and ultimately become the forefather to all present-day eukaryotes (Roger et al., 2017). Subsequent investigations of diverse protists and multicellular genomic datasets years later revealed that indeed all currently known eukaryotes descended from this single species mitochondrion-containing ancestor (Roger, 1999)(Embley, 2006)(Dacks et al., 2016). Hence, it is wise to study mitochondria from diverse organisms in order to find commonalities that may shed light into how the mitochondrial cenancestor was like.

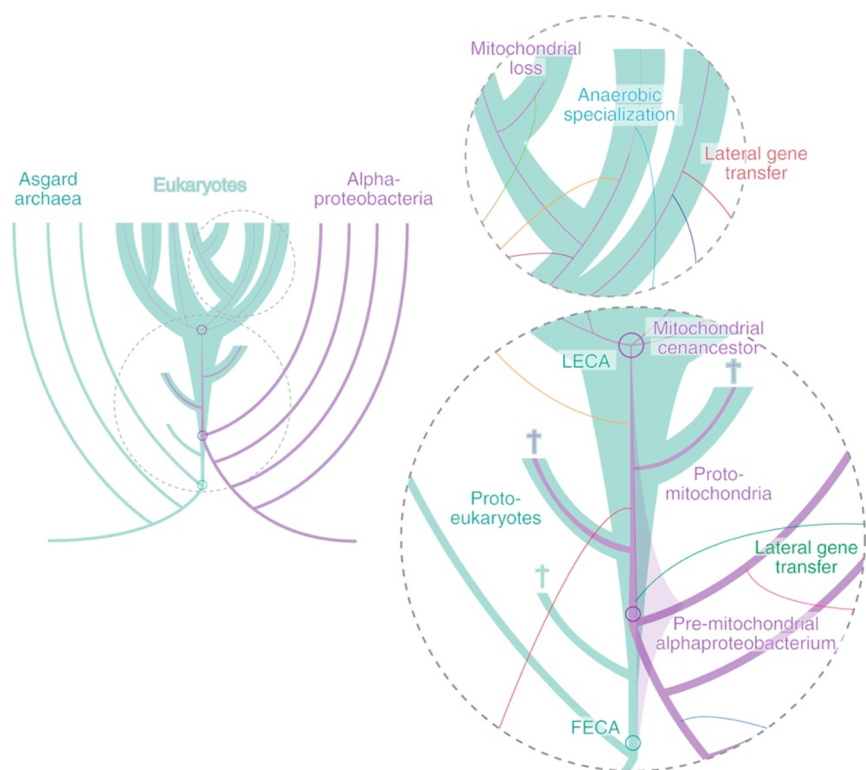


Fig. 1. The origin and evolution of mitochondria and eukaryotes (Roger et al., 2017). Crosses indicate extinct lineages.

## Back to the basics: General structure and function of mitochondria

At the finer level of mitochondrial internal architecture, a tight coupling between function and structure has been observed (Mannella, 2006)(Mannella et al., 2013)(Cogliati et al., 2016)(Iovine et al., 2021). The mitochondrial envelope comprises the mitochondrial outer membrane (MOM) and the mitochondrial inner membrane (MIM), while the space between the MOM and MIM is referred to as the intermembrane space (IMS) (Fig. 2.) (Bornstein et al., 2020).

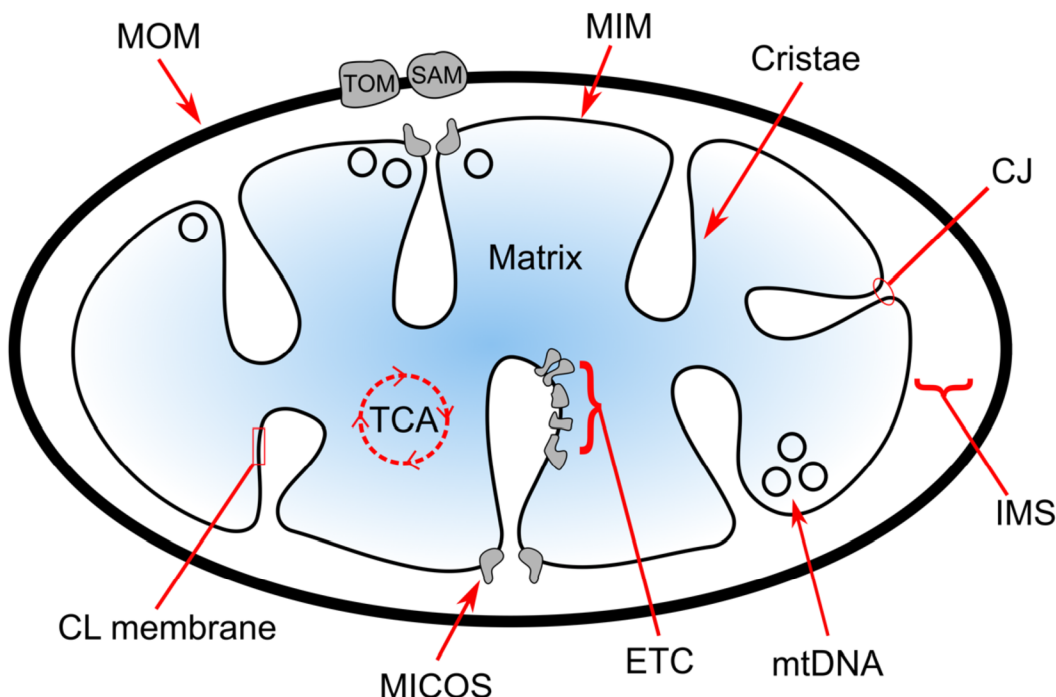


Fig. 2. Schematic illustration of mitochondria. Mitochondrial outer membrane (MOM), Mitochondria inner membrane (MIM), Intermembrane space (IMS), Crista junction (CJ), cardiolipin (CL), Mitochondrial DNA (mtDNA), Electron transport chain (ETC), Tricarboxylic acid cycle (TCA), Mitochondrial Contact Site and Cristae Organization System (MICOS), Translocase of the outer mitochondrial membrane (TOM), Sorting and assembly machinery (SAM).

The MOM serves as a barrier between the organelle and cytoplasm and mediates contact with other cellular organelles (*e.g.*, the endoplasmic reticulum) (Scorrano et al., 2019). Numerous channels and pores allow the MOM to be permeable to ions and small uncharged molecules. Large multiprotein translocases and chaperone structures, including the translocase of the outer membrane (TOM) and the sorting and assembly machinery (SAM) are found throughout the MOM. Nuclear encoded mitochondrial proteins enter the mitochondria via TOM, enabling protein import into different sub compartments, with the aid of N-terminal signal peptides (Neupert, 1997)(Model et al., 2002)(Kunze and Berger, 2015). Whereas large

$\beta$ -barrel proteins destined to be directly inserted into the MOM are folded and translocated by SAM (Paschen et al., 2003)(Wiedemann et al., 2003)(Höhr et al., 2018)(Takeda et al., 2021).

The space between the outer and inner membrane is referred to as the intermembrane space (IMS). Components of the IMS participate in a variety of functions including protein folding and degradation, transport of metabolites (*e.g.*, ATP, fumarate, citrate, camitine, *etc.*) between the cytoplasm and MIM (Herrmann and Riemer, 2010), and reactive oxygen species (ROS) signaling (Bornstein et al., 2020). The IMS is also the most constricted sub-compartment of the mitochondria (Edwards et al., 2021), containing only 5% of the mitochondrial proteome (Rath et al., 2021), yet houses a large variability of import pathways, including the Mia40, cytochrome *b2*, cytochrome *c* heme lysate, and uncoupling protein import pathways (Edwards et al., 2021).

In order to maintain the transmembrane gradient required for respiratory metabolism the MIM is largely impermeable to ions and small molecules, allowing only oxygen, carbon dioxide and water to move freely between the membrane (Lemasters, 2007). Unlike the MOM, the MIM harbors a complex morphology and invaginates into the matrix giving rise to specialized sub-compartments called cristae, which are attached to the MIM by crista junctions (CJs) (Perkins et al., 1997)(Fig. 2.).

The MIM also has a distinct lipid composition, including the specialized phospholipid cardiolipin, which physically contributes to the formation of cristae (Jouhet, 2013)(Pánek et al., 2020)(Tarasenko and Meinecke, 2021). Large multiprotein complexes needed for respiratory metabolism and ATP synthesis, collectively known as the electron transport chain (ETC), are enriched throughout the cristae membranes. Indeed, the manifestation of cristae is linked to the presence of respiratory chain complexes, as anaerobic mitochondria, which commonly lack these complexes, appear with little to no cristae (Muñoz-Gómez et al., 2015a)(Friedman et al., 2015)(Pánek et al., 2020). This reduction of cristae under low oxygen conditions demonstrates the interdependence between function and structure; as membrane morphology modulates the organization and function of the oxidative phosphorylation (OXPHOS) system (Cogliati et al., 2016).

Finally, the matrix is the space contained within the inner membrane. This space harbors the various enzymes needed for pathways including those of the tricarboxylic acid (TCA) cycle, oxidation of pyruvate, and beta oxidation of fatty acids. The matrix also houses mitochondrial ribosomes and mitochondrial DNA (mtDNA), with both being associated in proximity to the MIM (Liu and Spremulli, 2000)(Gerhold et al., 2015)(Colina-Tenorio et al., 2020).

## Mitochondria: A hub for diverse pathways

Respiratory metabolism, the aerobic catabolism of nutrients such as carbohydrates, proteins, and certain fatty acids, for energy production, takes place in mitochondria (Spinelli

and Haigis, 2018). While mitochondria also play other roles, such as signaling pathways that induce intrinsic apoptosis and the biogenesis of iron-sulfur (Fe/S) clusters (Bohovych and Khalimonchuk, 2016)(Lill et al., 2012), the most well-known function is that of the production of ATP via OXPHOS under aerobic conditions. Indeed, the mitochondria has shown to house a variety of different pathways that are integrated into the eukaryotic cell.

Glycolysis, which converts glucose into pyruvate, occurs in the cytoplasm (or within specialized organelles termed ‘glycosomes’ in kinetoplastids, *for details see page 15*)(Michels et al., 2006). Meanwhile, the TCA cycle and OXPHOS occur in the mitochondria to produce ATP, the primary energy currency for enzymatic reactions (Hroudová and Fišar, 2013). Embedded within the MIM, the ETC is comprised of four multiprotein complexes, which couple the transfer of electrons to pump protons across the MIM (Fig. 3.). This generates an electrochemical gradient, ultimately allowing protons to drive back into the matrix through F<sub>1</sub>F<sub>0</sub>-ATP Synthase.

In brief, electron transport begins as Complex I (NADH dehydrogenase) oxidizes the cofactor NADH (generated by the TCA cycle) to NAD<sup>+</sup>. Electrons also enter the ETC at Complex II (succinate dehydrogenase) through oxidation of succinate to fumarate, a complimentary step in the TCA cycle. The electron generated by both Complex I and Complex II is transferred to the coenzyme factor ubiquinone, allowing for the passage of the electron to cytochrome *c* via Complex III (cytochrome *c* reductase). Intriguingly, Complex II is typically found on the IBM and not enriched in cristae, raising questions on how these electrons travel the long way towards the cristae-localized Complex III (Wilkens et al., 2013)(Cogliati et al., 2016). Ultimately, cytochrome *c* shuttles the electron to Complex IV (cytochrome *c* oxidase), where it is then transferred into the matrix and accepted by oxygen as final electron acceptor. During electron transfer, protons are pumped by Complex I/III/IV from the matrix into the IMS. The proton gradient generated subsequently powers ATP production through F<sub>1</sub>F<sub>0</sub>-ATP Synthase, which functions as a molecular rotor to generate ATP from ADP and inorganic phosphate.

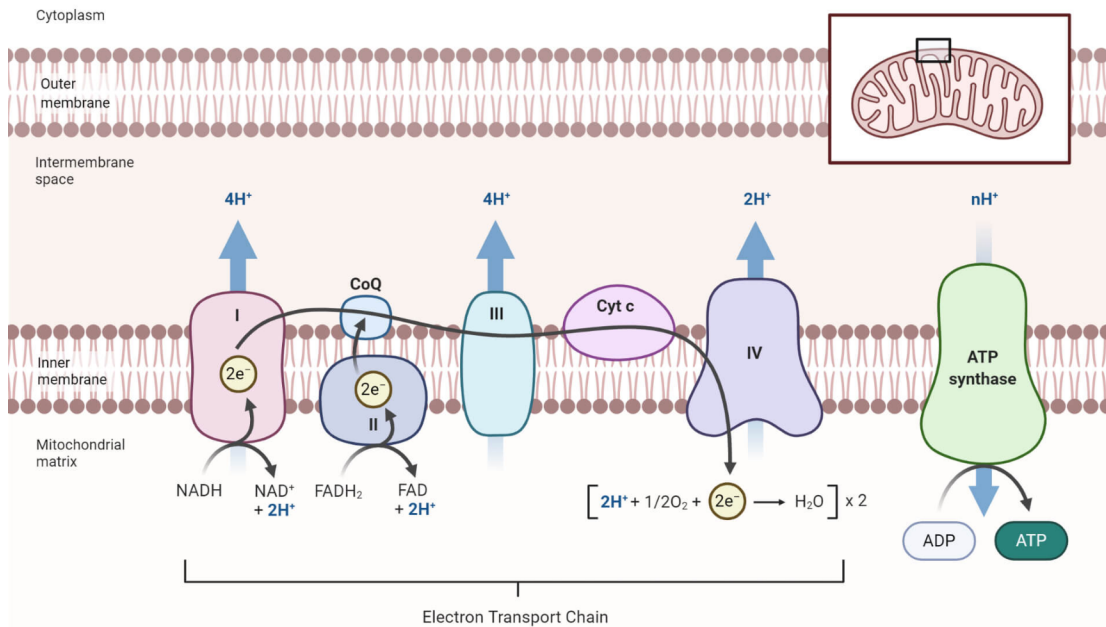


Fig. 3. Diagram of the transfer of electrons via the ETC and movement of protons. Adapted from (Wu et al., 2021).

While OXPHOS is ubiquitous throughout eukaryotes, both unicellular and multicellular, certain commonly studied mitochondrial pathways are found restricted to single monophyletic groups. Intrinsic apoptosis is a highly regulated and controlled process of programmed cell death via membrane blebbing, cell shrinkage, and/or DNA fragmentation and is currently known to solely occur in metazoans (Hengartner, 2000)(Green and Fitzgerald, 2016). This mitochondrial pathway of apoptosis is initiated by a range of exogenous and endogenous stimuli (*e.g.*, DNA damage and oxidative stress caused by chemical toxins/radiation) which activate proteases known as caspases that degrade proteins (Hongmei, 2012). This caspase activation is closely linked to MOM permeabilization by proapoptotic proteins known as Bcl family proteins. These proteins subsequently activate signal-transducing molecules that associate to the MOM and induce permeabilization. Upon disruption of the MOM via Opa1 cleavage, cytochrome *c* (localized within IMS/cristae lumen) is released into the cytosol and triggers the execution of total cell death by activating caspase-3 via the formation of a cytochrome *c*/Apaf-1/caspase-9-containing apoptosome complex (Fulda and Debatin, 2006)(Hongmei, 2012)(Gilkerson et al., 2021).

Iron-sulfur (Fe/S) clusters are essential factors of proteins involved in respiration, DNA replication and repair, and regulation of gene expression (Lill et al., 2012). The assembly of Fe/S clusters is ubiquitous to eukaryotes and is present in nearly all known mitochondria, unlike intrinsic apoptosis. It has been theorized that this particular pathway is the reason why some anaerobic eukaryotes retain relics of mitochondria termed mitosomes that have otherwise lost all components for OXPHOS and other mitochondrial bioenergetic pathways (Shiflett and Johnson, 2010).

## Cristae: Variations on a common theme

Cristae, the structural hallmarks of the MIM, constitute respiratory sub-compartments within the mitochondria (Pánek et al., 2020)(Wolf et al., 2019)(Toth et al., 2020)(Mannella, 2020). Cristae contain the ability to concentrate metabolites (Mannella et al., 2013), prevent the release of signaling molecules (e.g., cytochrome *c* during apoptosis) (Cogliati et al., 2013)(Olichon et al., 2003)(Scorrano et al., 2002), and localize proton gradients by limiting the diffusion of molecules between the intra-cristal space and the IMS (Mannella et al., 2001). This compartmentalization is achieved by means of CJs, which appear as tubular, slot- or neck-like membrane structures that differentiate the MIM into the inner boundary membrane (IMB) and the crista membrane (Barbot et al., 2015)(Colina-Tenorio et al., 2020)(Pánek et al., 2020).

Although cristae are present in all aerobic mitochondria, they exhibit variations among a wide variety of eukaryotes (Pánek et al., 2020). The diversity of cristae has also been witnessed between different tissues and during metabolic changes, indicating their dynamic nature (Zick et al., 2009)(Vafai and Mootha, 2012). Furthermore, the distribution of cristae-shaping proteins (e.g., MICOS, F<sub>1</sub>F<sub>0</sub>-ATP synthase dimers, Opa1) does not correlate with specific cristae morphologies (Muñoz-Gómez et al., 2015a). Two major CJ morphologies have been observed (Pánek et al., 2020). The tubular like structures is the most predominant CJ morphology and is seen in all eukaryotes except in a handful of species. The secondary, rarer type has been observed in ascomycete fungi, and bears a flattened, slot like opening. Nevertheless, the diameter and width of these two types of CJs are the roughly similar although one represents a larger opening (Pánek et al., 2020).

The morphology of the cristae is far more diverse than that of CJs. Five major types of cristae morphologies have been observed and further categorized into 2 classes (Pánek et al., 2020). The tubulo-vesicular class encompasses tubular, vesicular and irregular tubulo-vesicular morphologies, while the flat class contains both discoidal and lamellar cristae (Fig. 4.).

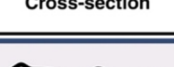
Morphotype	Cross-section	Longitudinal section	Three-dimensional appearance	Crista junctions	Electron tomography study
Tubulo-vesicular	Irregular tubulo-vesicular	 	Long, saccate	1-2	<i>Polytomella</i>
	Tubular	 	Long tubules	1-2	<i>Paramecium</i>
	Vesicular	 	Short; blob-like or ampullar	1?	Not assigned
Flat	Discoidal	 	Disc-like; often pedicellate	1	<i>Trypanosoma</i>
	Lamellar	 	Plate-like or ribbon-like	≥ 1	Chick cerebellum

Fig. 4. Cristae structures are diverse in different eukaryotes. Modified from (Pánek et al., 2020).

## MICOS: An overview

The Mitochondrial Contact Site and Cristae Organization System (MICOS) is a large hetero-oligomeric protein complex that localizes at CJs and has been best studied and characterized in model organisms *Saccharomyces cerevisiae* and *Homo sapiens* (Harner et al., 2011)(Colina-Tenorio et al., 2020). To a lesser extent in recent years, MICOS research has reached outside these two systems and into more esoteric species such as *Trypanosoma brucei* (Kaurov et al., 2018) and *Arabidopsis thaliana* (Michaud et al., 2016). MICOS appears to be responsible for the development and maintenance of CJs, as disruption of the complex results in the complete loss of CJs and the accumulation of internal stacked cristae vesicles detached from the MIM. This defective ultrastructure ultimately leads to impaired aerobic respiration and other secondary consequences such as altered mtDNA inheritance (Paumard et al., 2002)(Colina-Tenorio et al., 2020). Indeed, this drastic disturbance in MIM morphology demonstrates the rigid control that mitochondrial structure exerts on function (Rabl et al., 2009)(Harner et al., 2011).

## MICOS: A multitasking giant

MICOS has been most well characterized in *S. cerevisiae*, and consists of six subunits assembled hierarchically into the subcomplexes Mic60-Mic19 and Mic12-Mic10-Mic26-Mic27 (Friedman et al., 2015)(Muñoz-Gómez et al., 2015b)(Zerbes et al., 2012). Mic60 and Mic10 are the two most functionally important MICOS subunits, as their disruption leads to the most severe mutant phenotypes (Bohnert et al., 2015). Moreover, homologs for both Mic60 and Mic10 are found commonly distributed throughout the eukaryote tree of life in comparison to other *S. cerevisiae* MICOS subunits (Muñoz-Gómez et al., 2015a). Hence, subcomplex organization is based around these two subunits. Overall, MICOS has been shown to perform two major roles: the formation of CJs and contact sites (CS) (Anand et al., 2021).

Mic60, previously annotated as mitofillin/Fcj1, was the first MICOS subunit to be described in detail and was investigated using human cell culture (John et al., 2005). A multifunctional protein, Mic60 is one of the two core subunits of the MICOS complex. It has been shown to directly contribute to CJ formation by actively bending the membrane of the MIM (Hessenberger et al., 2017)(Tarasenko et al., 2017). Studies both *in vivo* and *in vitro* have demonstrated that the intermembrane space (mitofillin) domain of Mic60 has a lipid-bending capacity and induces membrane curvature even in absence of its transmembrane domain (TMD) (Tarasenko et al., 2017)(Hessenberger et al., 2017). It has also been recently shown that the Mic60 subcomplex by itself is sufficient in inducing CJ formation when re-expressed in MICOS knockout cell lines in human cells, demonstrating its critical role in establishing *de novo* CJs (Stephan et al., 2020). Mic19 (including paralog Mic25 in humans/metazoans), part of the Mic60 subcomplex, appears to regulate the mitofillin domain by binding to it directly via

its CHCH (coiled-coil helix coiled-coil helix) domain, thus modulating the membrane shaping activity of Mic60 (Hessenberger et al., 2017). Additionally, Mic19 is the only known MICOS subunit to lack a TMD and thus is not directly attached to the membrane (Sakowska et al., 2015)(Tang et al., 2020).

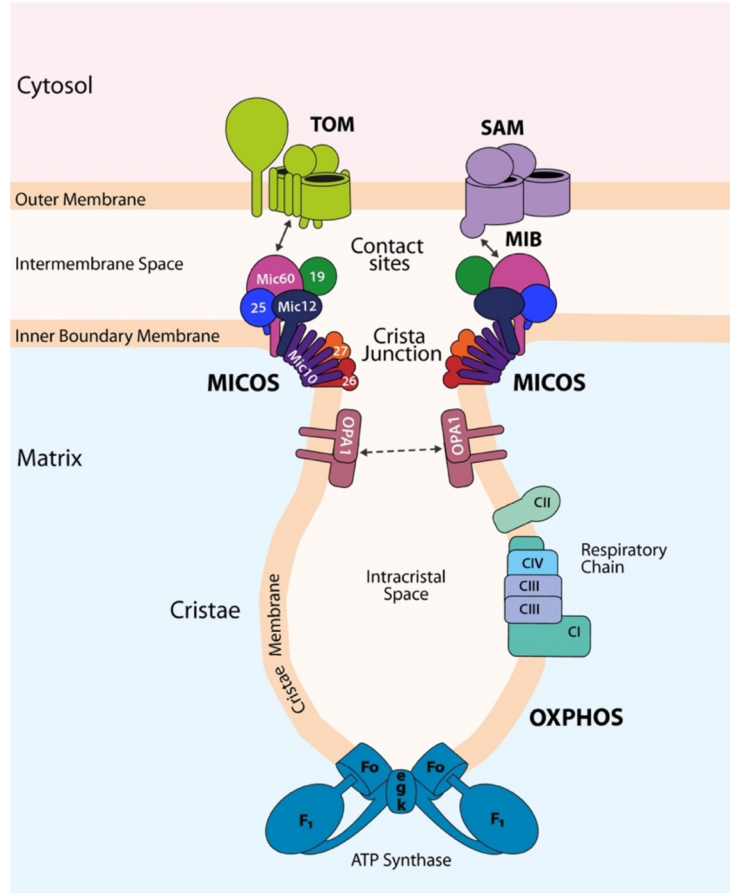


Fig. 5. Determinants of mitochondrial cristae architecture and dynamics (Colina-Tenorio et al., 2020).

Mic10 is the second core morphogenetic factor in the formation of lamellar cristae in human cell culture (Stephan et al., 2020), as it establishes homo-oligomers that induce strong negative curvature at CJs to mature the IBM into cristae (Barbot et al., 2015)(Bohnert et al., 2015). Mic10 is a small protein with two TMDs spanning across the MIM, hypothesized to form a wedge-like topology (Rampelt et al., 2017b). Similar to Mic60, Mic10 has been shown to bend membranes both *in vivo* and *in vitro* (Barbot et al., 2015). It has been speculated that the combination of Mic10's wedge-like topology and ability to homo-oligomerize through the glycine rich motifs present in the TMDs are the main factors contributing to membrane bending, as oligomerization mutants fail to induce curvature (Barbot et al., 2015).

Mic12 (putative metazoan homolog annotated as Qil1) has been reported to act as the intermediary bridge between the Mic60 and Mic10 subcomplexes (Zerbes et al., 2016)(Guarani et al., 2015). The yeast paralogs Mic26/27 are theorized to directly bind to cardiolipin and thus

may play a scaffolding role in the stability of MICOS due to their evolutionary relationship to apolipoproteins (Friedman et al., 2015)(Zerbes et al., 2016). Moreover, it was also reported that in the absence of cardiolipin synthesis, the Mic10 subcomplex has been shown to be affected, suggesting an interaction between cardiolipin and Mic26/27 (Friedman et al., 2015). Additionally, an earlier study revealed that the human homolog of Mic26/27 may serve a similar function (Weber et al., 2013)(Anand et al., 2021). Overall, both Mic26/27 and Mic12 have been shown to influence Mic10 stability differently, indicating independent, non-redundant roles (Zerbes et al., 2016).

The secondary major role of MICOS is the formation of contact sites (CS). Here, CSs are defined as steric interactions between MICOS and other proteins in proximity that play influential roles. In humans, the Mic60 subcomplex has been shown to interact with outer membrane protein Sam50 via Mic19 to establish contact to the MOM, assembling what is known as the mitochondrial intermembrane space bridging (MIB) (Xie et al., 2007)(Ott et al., 2012)(Ding et al., 2015)(Tang et al., 2020). A similar interaction has been reported with both TOM and the major metabolite channel porin/VDAC (voltage dependent anion channel), but not thoroughly investigated (von der Malsburg et al., 2011)(Harner et al., 2011). Depletion of Mic19 has been shown to lead MIB disassembly, as the Mic60-Mic19-Sam50 axis is disrupted. Even in the presence of Mic60 and Sam50, abnormal mitochondrial morphology, reduced CJs, and reduced ATP production were witnessed (Tang et al., 2020). Thus, it has been speculated that Sam50 serves a role as an anchoring point to guide the formation of CJs in conjunction with Mic60 (Ott et al., 2012)(Tang et al., 2020). It is also believed that this interaction between MICOS and MOM proteins supports the import of mitochondrial proteins (Ueda et al., 2019). This bridging of outer and inner mitochondrial membranes also plays a role in phospholipid transfer and biosynthesis (Khosravi and Harner, 2020), as in the case of the MIB enabling Psd1 to decarboxylate phosphatidylserine to phosphatidylethanolamine in the MOM, as precursor lipids need to be imported from the ER into mitochondria before further synthesized in the MIM (Daum and Vance, 1997)(Connerth et al., 2012). Furthermore, cardiolipin precursors are transported and synthesized in a similar fashion (Miyata et al., 2016)(Khosravi and Harner, 2020). In addition, depletion of Sam50 has shown decreased numbers of CJs (Ott et al., 2015)(Ott et al., 2012)(Tang et al., 2020). Considering that the central role of Sam50 is the embedment of  $\beta$ -barrel proteins into the MOM (Klein et al., 2012), it is safe to assume that that this decrease in CJs is the result of the lack of CSs and not a secondary effect caused by decreased mitochondrial import.

Therefore, MICOS has been shown to form the core of a large network of interacting proteins with diverse functions including membrane architecture, lipid biogenesis and metabolism. Aside from steric interactions, MICOS has additionally been reported to transiently interact with the protein Mia40, which is essential for import and oxidative folding of precursors IMS proteins containing disulfide bridges (Peleh et al., 2016). In conclusion, the MICOS network has thus been proposed to play an orchestrating role for the spatial and functional coordination of various mitochondrial activities.

## F<sub>1</sub>F<sub>o</sub>-ATP Synthase: An overview

The F<sub>1</sub>F<sub>o</sub>-ATP Synthase consists of a hydrophilic, matrix-facing ATP-generating F<sub>1</sub> head and the membrane-embedded F<sub>o</sub> subcomplex (Fig. 6.) (Noji et al., 1997)(Yoshida et al., 2001). The primary function of F-type ATP synthase is the synthesis of ATP from ADP and inorganic phosphate coupled with the proton gradient generated by the ETC. Indeed, these F-type ATP synthases are one of the most ancient enzymatic complexes as they are found ubiquitously throughout all living organisms, including anaerobes (Ozawa et al., 2000)(Petri et al., 2019). Predominantly, they are localized to the lumen of mitochondrial cristae, the thylakoid membrane of chloroplasts, and the plasma membrane of bacteria (Kühlbrandt, 2019). Currently, F-type ATP synthases are the only known biological mechanism capable to transduce a membrane potential directly into chemical energy, thus making it one of the most fundamental reactions in the field of biology (Kühlbrandt, 2019).

## F<sub>1</sub>F<sub>o</sub>-ATP Synthase: A marvelous enzyme

F-type ATP synthases, when operating in the forward mode, employ proton motive force generated by the ETC to produce ATP, the universal energy currency of the cell, by rotary catalysis. In the reverse mode, they act as ATP-consuming proton pumps contributing to the generation of electrochemical membrane potential. Prokaryotes have been known to utilize both modes depending on species and the environment (Cotter and Hill, 2003). In contrast, mitochondrial ATP synthases in the majority of aerobes produce cellular ATP and the reserve mode appears as a manifestation of pathophysiological conditions (Campanella et al., 2009)(Gahura et al., 2021). Due to their central role in cell metabolism and bioenergetics, the F<sub>1</sub>F<sub>o</sub>-ATP Synthase has been of key interest to biochemists, molecular biologists, and structural biologists (Kühlbrandt, 2019).

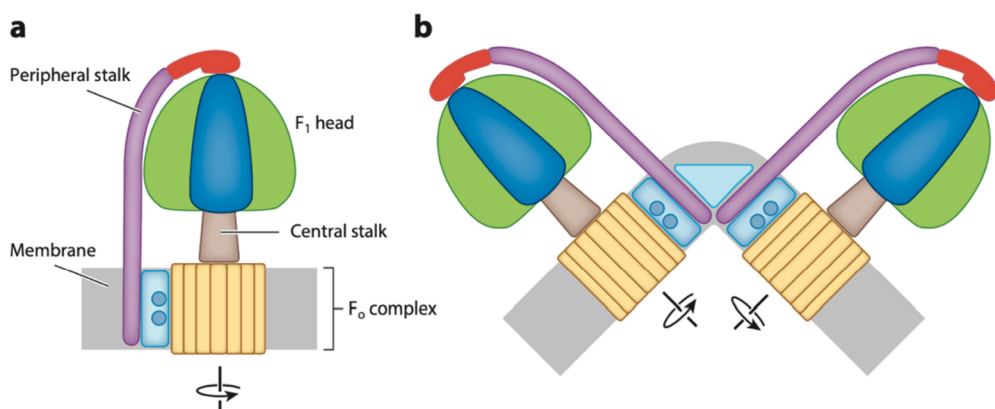


Fig. 6. (a) Schematic overview of F-type ATP synthases. F-type ATP synthases consist of a catalytic F<sub>1</sub> head, and the F<sub>o</sub> motor complex embedded in the membrane. (b) Mitochondrial ATP synthase exists as a dimer (Kühlbrandt, 2019).

In mitochondrial ATP synthase, the F<sub>1</sub> motor consists of a heterohexamer assembly of three  $\alpha$ - and three  $\beta$ - subunits, organized symmetrically around the  $\gamma$ - subunit central shaft (Abrahams et al., 1994). Within the F<sub>1</sub> motor, the  $\beta$ - subunits constitute the catalytic nucleotide binding sites, where empty pockets become occupied by Mg-ADP and inorganic phosphate, which condense to form Mg-ATP. Although both the  $\alpha$  and  $\beta$ - subunits show similar structure and polypeptide sequences, the catalytic site lays embedded within the  $\beta$ - subunits (Kühlbrandt, 2019).

While the F<sub>1</sub> head performs the catalytic function, the F<sub>0</sub> motor either generates the torque required for ADP phosphorylation via proton flow driven from IMS, or actively pumps protons into the matrix to maintain the electrochemical potential under dephosphorylation conditions. The foundation of the F<sub>0</sub> moiety is found within the 8-17 c-ring subunits. The F<sub>1</sub> head is connected to the F<sub>0</sub> motor by the central stock ( $\gamma$ -,  $\varepsilon$ - and  $\delta$ - subunits) and the peripheral stalk (OSCP subunit in mitochondria). The  $\gamma$ - subunit functions as a crankshaft by pressing the F<sub>1</sub>  $\alpha$ - and  $\beta$ - head into different conformations, allowing for different binding affinities for ATP or ADP and inorganic phosphate (Wilkens and Capaldi, 1998).

The mitochondrial ATP synthase differs from that of bacterial and chloroplast ATP synthase (Junge and Nelson, 2015). Among these differences include structure, membrane arrangement and several additional F<sub>0</sub> associated subunits (von Ballmoos et al., 2009)(Kühlbrandt, 2019). Perhaps the most noticeable feature of mitochondrial ATP synthase is that they occur as dimers (Fig. 6.) (Arnold et al., 1998)(Dudkina et al., 2005)(Davies et al., 2012). These ATP synthase dimers have been witnessed to arrange themselves into long rows or short ribbons around the cristae rim membranes (Davies et al., 2012)(Dudkina et al., 2010)(Anselmi et al., 2018). The enrichment of ATP synthase dimers along cristae rims leads to the conclusion that they mediate cristae structure by inducing membrane curvature (Dudkina et al., 2006)(Davies et al., 2012). The exact mechanism how these dimers are formed is still under debate. However, it has been shown in *S. cerevisiae* that ATP synthase dimer maintenance is dependent on the presence of F<sub>0</sub> moiety subunits e- and g- (Guo et al., 2017)(Wagner et al., 2009). Indeed, deletion of either genes encoding for subunits e- or g- was shown to result in disassociation of ATP synthase dimers into monomers (Arnold et al., 1998)(Davies et al., 2012). Additionally, as a result of this loss of dimerization, mitochondria exhibit malformed cristae, giving the appearance of layered, onion-like morphology (Arselin et al., 2004)(Paumard et al., 2002)(Davies et al., 2012). Hence, it has been concluded that the presence of ATP synthase dimers *in vivo* is a prerequisite for proper cristae architecture to take place. Therefore, apart from enzymatic function, ATP synthase affect mitochondrial physiology by shaping submitochondrial ultrastructure.

## **Trypanosoma: An enticing model to study mitochondria**

As previously mentioned, the evolution of the mitochondria from an alphaproteobacterial endosymbiont was achieved via a set of events, including the transfer of genes to the host nucleus, development of a targeting system enabling the transfer of nuclear encoded proteins into the organelle, and host cell control over division (Hewitt et al., 2011)(Ku et al., 2015)(Roger et al., 2017). Given that this singular event occurred prior to the separation of eukaryotic lineages into their present-day major supergroups, it can be said that various evolutionary divergencies have taken place with their mitochondria as well (Roger et al., 2017). Thus, by studying trypanosomal mitochondria, we have the ability to discern specific features that have been lost, gained, and/or retained in comparison to Opisthokont model species.

Trypanosomes are a group of single-flagellum bearing protists belonging to the supergroup Discoba (formally grouped as Excavata along with Metamonada and Malawimonadida) (Fig. 7.) (Adl et al., 2019)(Burki et al., 2020). Trypanosomes are exclusively parasitic with some members being causative agents of diseases such as human African trypanosomiasis (*Trypanosoma brucei*) and Chagas disease (*Trypanosoma cruzi*) (Matthews, 2015). Species encompassing Discoba are believed to diverged early from opisthokonts ~2 Ga ago (Eme et al., 2017) and thus are an enticing model to study both mitochondrial conserved features as well as novel properties when compared to well-studied lineages such as *S. cerevisiae* and *M. musculus* (Hashimi, 2019). Unlike other mitochondria, the trypanosomal mitochondrion contains the genome at a single location near the flagellar basal body (Fig. 8.) (Ogbadoyi et al., 2003). This mitochondrial genome consists of a network of tightly packed circular DNA (kDNA) known as the kinetoplast which contains multiple copies of the genome (Lukeš et al., 2002). Because of this property, trypanosomatids appear bearing only a single mitochondrion (Esseiva et al., 2004). Therefore, species that contain this kinetoplast are commonly referred to as kinetoplastids (Lukes et al., 2005). *T. brucei* is without a doubt the best studied kinetoplastid, as it is easily cultured and amenable to a variety of reverse genetic techniques (Matthews, 2015).

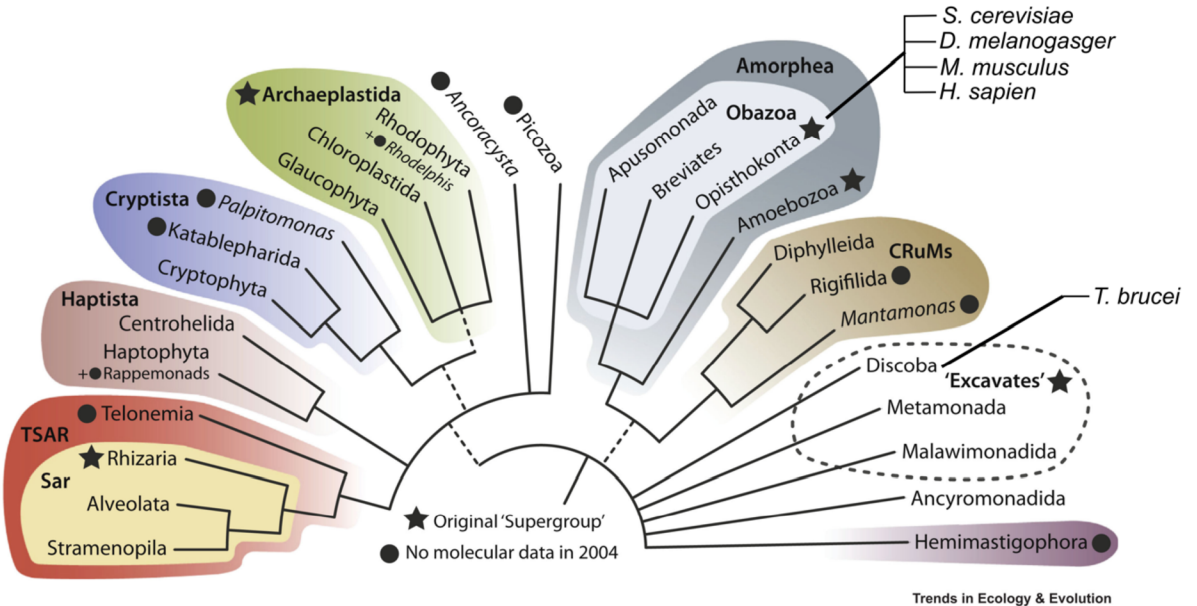


Fig. 7. The latest Tree of Eukaryotes adapted from (Burki et al., 2020). Highlighted are the most frequently studied lineages belonging to the Opisthokonta and the position of *T. brucei* in relation.

An additional property of the amenability of *T. brucei* is the ability to recapitulate parts of their lifecycle under culturable conditions. The life cycle of *T. brucei* is dixenous, involving both a tsetse fly vector (*Glossina* spp.) and a mammalian host (Fig. 8.) (Vickerman, 1985)(Mehlhorn, 2001). Throughout its different life cycle stages, gross morphology and ultrastructure are heavily remodeled alongside drastic metabolomic changes (Vickerman, 1985)(Bíly et al., 2021). A simplistic approach to the lifecycle of *T. brucei* is to state that two major stages exist: the **bloodstream stage** within the mammalian host, while within the tsetse fly midgut it takes form of the **procyclic stage** (Fig. 8.).

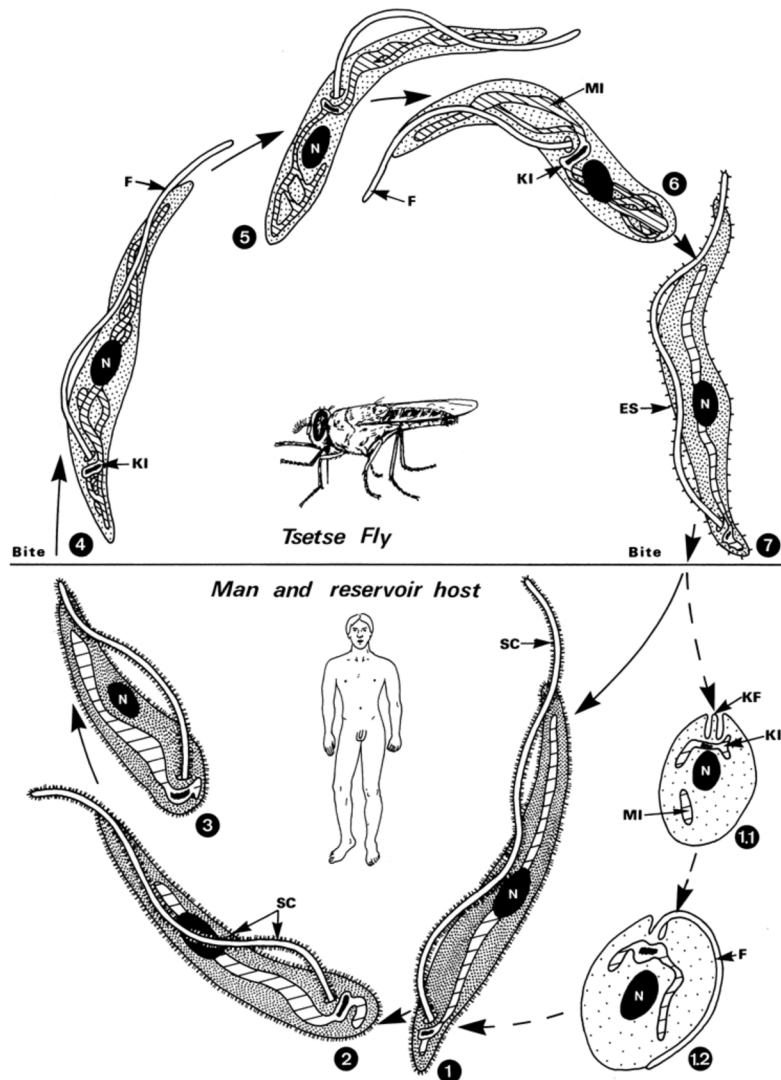


Fig. 8. The complex life cycle of *T. brucei*. Nucleus (N), Mitochondrion (MI), Kinetoplast (KI). Taken from (Mehlhorn, 2001).

### The mitochondrion of *Trypanosoma brucei*

The overall gross morphology of *T. brucei* changes throughout its dixenous life cycle, similar drastic remodeling takes place within its singular mitochondrion to meet the different bioenergetic requirements within host environments (Vickerman, 1985)(Doleželová et al., 2020). Due to the abundance of free glucose found in mammalian blood (Wasserman, 2009), during the bloodstream stage, production of ATP relies exclusively on glycolysis (Doleželová et al., 2020). These glycolytic pathways take place within kinetoplastid specific peroxisome-derived organelles known as ‘glycosomes’, containing glycolytic and gluconeogenic enzymes. (Michels et al., 2006). In the bloodstream stage, OXPHOS does not take place and several components of the ETC (Complex III and Complex VI) are absent (Zíková et al., 2017). During this stage, F<sub>1</sub>F<sub>0</sub>-ATP Synthase is still present and performs ATP to ADP hydrolysis in order to maintain the mitochondrial membrane potential for protein import and Fe/S cluster assembly

(Hierro-Yap et al., 2021). Moreover, the bloodstream form mitochondrial volume is reduced by 36-50 % compared to that of the procyclic stage (Bílý et al., 2021). This reduction in volume is accompanied by low levels of MIM invaginations resembling stub-like cristae (Brown et al., 1973)(Bílý et al., 2021). These nascent cristae-like structures occupy 1-2 % of the overall mitochondrial volume, which is consistent with the lack of ETC complexes that are found typically enriched within cristae (Zíková et al., 2017)(Cogliati et al., 2013)(Bílý et al., 2021).

During the procyclic stage the mitochondrion appears larger and reticulated, reflecting on the upregulation of the TCA cycle and OXPHOS (Verner et al., 2015). Large, discoidal cristae are abundant and appear throughout the mitochondrion, starkly contrasting the bloodstream mitochondrion (Vickerman, 1985). Due to the abundance of proline and lack of free glucose in the tsetse fly midgut, *T. brucei* relies on the catabolism of the former as the main source of carbon for the TCA cycle to produce ATP (L'Hostis et al., 1993)(Lamour et al., 2005)(Mantilla et al., 2017). Strikingly however, the TCA cycle during the procyclic stage does not operate in a conventional cyclic manner but is broken into individual pathways. This is achieved in part that only certain TCA enzymes are used for energy generation while other parts of the “cycle” are utilized for transportation and degradation of mitochondrial substrates (van Hellemond et al., 2005).

Thus, the ability for the trypanosome mitochondrion to undergo extensive remodeling makes it an appealing model to study cristae maturation. In pleomorphic cell lines, the differentiation from bloodstream to procyclic can be induced *in vitro*, thus allowing cristae development to be studied thoroughly and relatively easy. Moreover, the procyclic stage can be easily cultivated with or without fermentable carbon sources to address metabolic and respiration capacities *in vitro*.

## MICOS: A view outside humans and yeast

By 2014, little was known about the evolutionary history of MICOS, save for its presence in yeast and animals (*S. cerevisiae*, *C. elegans*, and *H. sapiens*) (Mun et al., 2010)(Head et al., 2011). A year later, phylogenetic analyses revealed that both Mic10 and Mic60 appeared to be well conserved throughout aerobic mitochondria containing eukaryotes based on BLAST and Hidden Markov Model (HMM) predictions against *S. cerevisiae* MICOS (Muñoz-Gómez et al., 2015b). Additionally, in 2016 Mic60 was first biochemically described in *Arabidopsis thaliana* (Michaud et al., 2016) and in 2018 the entire complex was characterized in *Trypanosoma brucei* (Kaurov et al., 2018).

With the exception of Mic10, *T. brucei* contains no obvious yeast MICOS homologs (Muñoz-Gómez et al., 2015b)(Kaurov et al., 2018). Of noteworthy mention, *T. brucei* Mic10 is present as two paralogs, Mic10-1 and Mic10-2, the former bearing higher similarity to conventional yeast Mic10 in terms of glycine residue amounts within the predicted transmembrane domain (Kaurov et al., 2018). Similar to yeast however, the trypanosomal

MICOS is divided into two subcomplex; the membrane integral subcomplex containing paralogs Mic10-1/2-Mic16-Mic60 and the peripheral IMS soluble complex Mic32-Mic34-Mic17-Mic40-Mic20 (Fig. 9.) (Eichenberger et al., 2019). Interestingly, the integral subcomplex contains a putative Mic60 subunit containing a conserved coil coiled motif, N-terminal transmembrane domain, and mitochondrial signaling sequence, reminiscent of human/yeast Mic60. However, an obvious mitofillin domain remains absent, which is the canonical hallmark of Mic60, ergo why trypanosomal Mic60 was not initially detected bioinformatically (Kaurov et al., 2018)(Muñoz-Gómez et al., 2015b). It is speculated that one of the peripheral subcomplex proteins could provide the role of a cryptic mitofillin domain (Hashimi, 2019). In addition, it should be noted that the integral subcomplex houses the more eukaryote wide conserved MICOS subunits (*i.e.*, Mic10 and Mic60) while the peripheral subunits exhibit kinetoplastid specific proteins. Intriguingly, this occurrence of membrane bound proteins appearing more evolutionary conserved is inconsistent with the hypothesis that soluble proteins are dramatically more conserved than their membrane counterparts (Sojo et al., 2016).

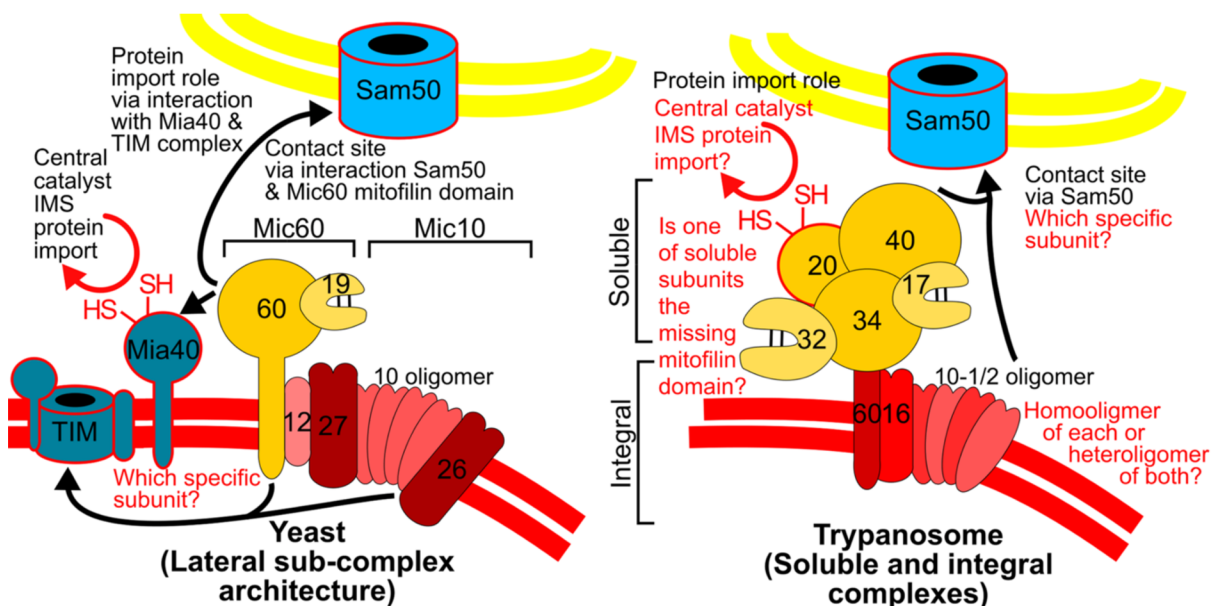


Fig. 9. Illustrative differences between yeast and trypanosomal MICOS. In both systems, MICOS is categorized into two subcomplexes. Taken from (Hashimi, 2019).

Functional analysis of the trypanosomal MICOS has shown that several conserved features remain that have been previously reported in human/yeast MICOS. Depletion of individual subunits results in the detachment of cristae from the MIM and altered mitochondrial ultrastructure, with the exception of Mic16 which was not shown to have a phenotype (Kaurov et al., 2018). This apparent loss of CJ formation is consistent with MICOS mutants witnessed in human and yeast cell cultures. In addition, it has been reported that Mic60 immunoprecipitation pulldowns show enriched amounts of SAM, demonstrating the ability to form contact sites with MOM proteins and possibly establishing a trypanosomal MIB (Kaurov et al., 2018).

et al., 2018)(Tang et al., 2020). The ability for trypanosomal MICOS to aid in protein import into the mitochondria has also been briefly reported. Depletion of the peripheral subunit Mic20 was shown to lead to significant decreased levels of IMS proteins in comparison to Mic60 depletion (Kaurov et al., 2018). Mic20 contains a putative thioredoxin-like domain that has been predicted to aid in oxidative folding of IMS proteins containing CX<sub>3,9</sub>C motifs. Taking the above information into consideration, the trypanosomal MICOS has been proposed to act as a hub for both cristae shaping and IMS protein import. These multi-features found in *T. brucei* MICOS are thus comparable to the diverse functions of MICOS that have been thoroughly described in human and yeast mitochondria.

Although the complex has yet to be characterized, Mic60 has been demonstrated to contribute to the export of phosphatidylethanolamine from mitochondria and import of galactoglycerolipid from plastids in *A. thaliana* (Michaud et al., 2016). Additionally, *A. thaliana* Mic60 has been reported to aid in lipid desorption from membranes and bind to directly TOM, suggesting the ability to form contact sites with the MOM (Michaud et al., 2016). The authors hypothesize that contact sites could mediate lipid trafficking between the MOM and MIM (Michaud et al., 2016). Noteworthy, no interaction with Sam50 was witnessed.

### F<sub>1</sub>F<sub>0</sub>-ATP Synthase: Different models for different species

Comparable to the assortment between conserved and diverged features in MICOS mentioned above, mitochondrial F<sub>1</sub>F<sub>0</sub>-ATP Synthases display similar diversity between species. ATP synthases have been the focal point of interest for structural biologists since the 1970's, and therefore the abundance of structural data from different organisms is extensive compared to other mitochondrial complexes. In order to better differentiate ATP synthase dimer structures, a four class system (Type I-IV) has been established based on dimer angle as determined using cryo-electron imaging (Fig. 10.) (Kühlbrandt, 2019)(Pánek et al., 2020).

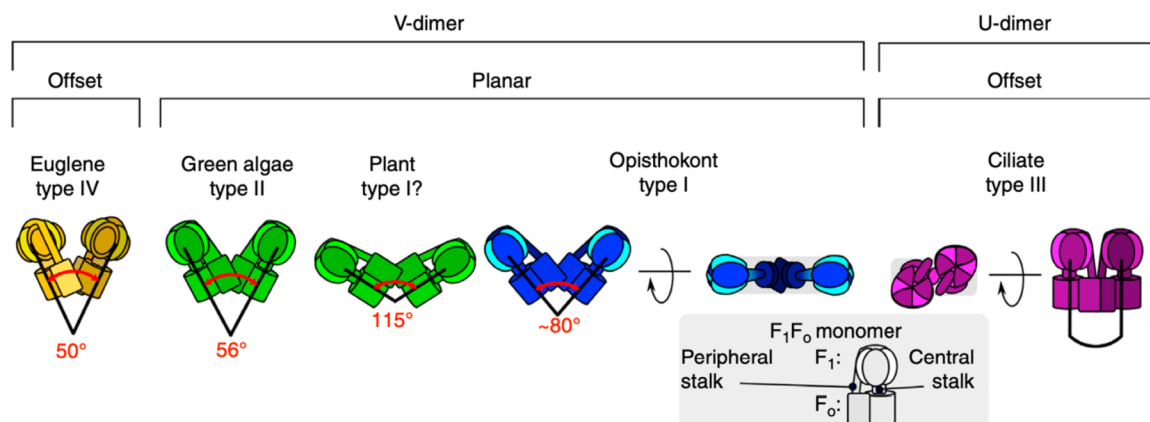


Fig. 10. Different classes of F<sub>1</sub>F<sub>0</sub>-ATP Synthases dimer angles, depicted as Types I-IV, found in different eukaryotes (Pánek et al., 2020).

These structural studies have revealed major difference between ATP synthase dimers among different protists and multicellular organisms. The majority of solved structures exhibit V-shaped dimers, meaning the angle originating from the interface at the F<sub>O</sub> moiety eventually pries apart as the F<sub>I</sub> heads separate (Type I, II, IV). In contrast, Type III dimers exist as U-shaped, with each monomer erected in parallel to each other and are only found in a handful of species including ciliates (SAR family). However, it should not be misinterpreted that Type III dimers are rare in nature given the fact that the SAR family is highly diverse and found in all biomes. Additionally, ATP synthase structures have only been described in detail in a select number of species, thus more than four classifications of dimers may emerge in future studies.

Type I dimers are found in mammals and yeast (Opisthokonta) and are found to exists at an angle of ~86° (Davies et al., 2011)(Davies et al., 2012). This class of dimers appear to associate into long rows along the cristae lumen and generate high local membrane curvature at the edges, ergo producing lamellar shaped cristae (Fig. 4.) (Strauss et al., 2008)(Pánek et al., 2020).

Type II dimers are common in unicellular green algae (Archaeplastida) with the cryo-electron structure being solved in both *Polytomella* sp. and *Chlamydomonas reinhardtii* (van Lis et al., 2007)(Dudkina et al., 2006). Additionally, proteomic data from both organisms revealed a set of unique F<sub>O</sub> subunits that form part of its unusually thick peripheral stalk; the hallmark of Type II dimers (Vázquez-Acevedo et al., 2006)(Vázquez-Acevedo et al., 2016). The typical dimer angle has been calculated at 56° for *Polytomella* sp. However, not all Archaeplastida exhibit Type II dimers, as the multicellular *Solanum tuberosum* (potato) manifests with a dimer angle of 115° (Pánek et al., 2020).

As previously mentioned, Type III are unique as they form an atypical U-shape, with each F<sub>I</sub> monomer slightly a skewed relative to each other when viewed as a plan (*i.e.*, from the top, matrix side), giving this dimer an angle close to 0° (Pánek et al., 2020). This set of unorthodox dimers are found in the tubular cristae of *Paramecium multimicronucleatum* (SAR) (Mühleip et al., 2016). Hence, this specific dimer type may induce different extents of positive curvature *in vivo*, possibly contributing to the diversity of cristae.

Type IV dimers are found in euglenozoans and trypanosomes (Discoba) and share certain features with Type III dimers, as their peripheral stalks appear offset between dimers (Pánek et al., 2020). The angle between monomers has been determined to be ~50° (Kühlbrandt, 2019). Additionally, Type IV dimers have a pyramid shaped F<sub>I</sub> as opposed to the globular shape seen in Type I/II, due to the occurrence of euglenozoan-specific subunit p18 (Gahura et al., 2018)(Montgomery et al., 2018). These dimers have also been witnessed to form a closely packed lattice of interlaced rows, presenting themselves as short ribbons that run a skewed along the cristae edge, due to their offset peripheral stalks (Mühleip et al., 2017). Due to this difference between V-shaped dimer row formation between Type I and Type IV ATP synthases, it is tempting to speculate the role they contribute regarding lamellar and discoidal cristae formation, respectively (Pánek et al., 2020).

## MICOS and F<sub>1</sub>F<sub>0</sub>-ATP Synthase crosstalk: A conserved interaction? Or a fungal novelty?

Crosstalk between crista-shaping factors MICOS and dimeric F<sub>1</sub>F<sub>0</sub>-ATP Synthases has been previously demonstrated in yeast (Rampelt et al., 2017a)(Eydt et al., 2017)(Rampelt and van der Laan, 2017). It has been theorized that a fraction of Mic10 physically interacts with ATP synthase dimers, presumably via subunit e-, and the overexpression of Mic10 leads to stabilization of ATP synthase hyper-oligomers (Rampelt et al., 2017a). An even more pronounced accumulation of ATP synthase hyper-oligomers was witnessed upon deletion of the Mic60 gene, but concrete evidence of a physical interaction between Mic60 and any ATP synthase subunits has yet to be reported (Rabl et al., 2009)(Schweppe et al., 2017). This interplay between MICOS and ATP synthase is a remarkable yet still unexplained phenomenon, as both complexes play critical and antithetical roles in shaping the MOM.

In *T. brucei*, a similar phenomenon was recently reported regarding crosstalk between trypanosomal MICOS and dimeric F<sub>1</sub>F<sub>0</sub>-ATP Synthase (Cadena et al., 2021). Indeed, upon depletion of trypanosomal Mic60, acclimation of ATP synthase hyper-oligomers was witnessed. Additionally, one of the two Mic10 paralogs present in *T. brucei*, Mic10-1, was shown to have physically interact with ATP synthase *in vivo*. Moreover, the identification of trypanosomal ATP synthase subunit e- was also reported in the same study. The appearance of this crosstalk in both *T. brucei* and *S. cerevisiae* is compelling evidence towards the fact that this feature is not simply a fungal novelty but potentially a highly conserved, ancestral feature of mitochondria. Given this statement, three different scenarios of MICOS-ATP synthase crosstalk have been hypothesized (Fig. 11.). The first postulates that a fraction of unbound Mic10 interacts directly to ATP synthase dimers on cristae edges (Rampelt et al., 2017a). The second involves ATP synthase dimers in the proximity of crista junctions, using Mic10 as a bridge between both complexes (Eydt et al., 2017). The third hypothesis proposes that the Mic10-ATP synthase interaction is dynamic and transient, and occurs at the future site of crista junctions in nascent cristae during the process of ATP synthase dimer-induced invagination of the MIM (Cadena et al., 2021).

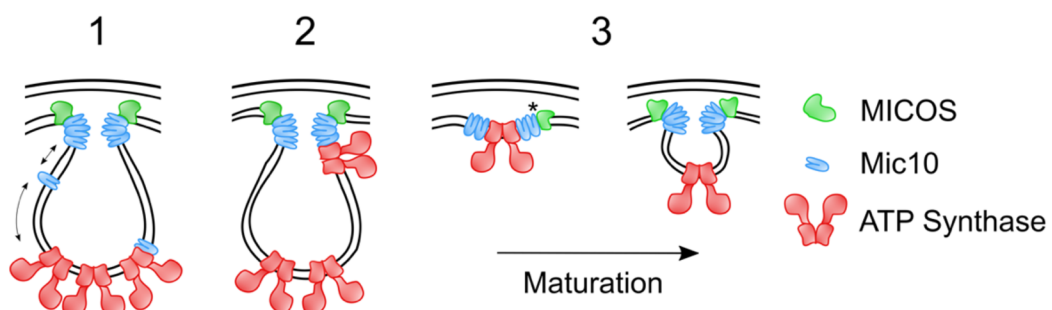


Fig. 11. Three possible scenarios of MICOS-ATP synthase crosstalk in cristae (Cadena et al., 2021).

## 2. AIMS AND TASKS

The main aims of the research were to:

- (i) Identify whether crosstalk between MICOS and F<sub>1</sub>F<sub>o</sub>-ATP Synthase is a conserved eukaryote feature by utilizing model system *T. brucei*;
- (ii) Identify the existence of a kinetoplast specific F<sub>1</sub>F<sub>o</sub>-ATP Synthase subunit capable of stabilizing dimer formation;
- (iii) Propose an alternative mode of action contributing to the maturation of mitochondrial cristae via MICOS and F<sub>1</sub>F<sub>o</sub>-ATP Synthase interplay.

## 3. SUMMARY

As described above, the philosophy of evolutionary cell biology suggests that a comparative approach to biological systems in different organisms can shed light to their chemical and physical limitations with respect to their evolution. Hence, it is wise to study mitochondria from species that are outside the framework of model organisms that receive over 60% of primary research (*i.e.*, Opistokonta model systems). I accepted the notion that the ancient biological machineries of F<sub>1</sub>F<sub>o</sub>-ATP Synthase and MICOS are key in regulating the formation of proper cristae development, and thus enable the aerobic eukaryotic cell to perform the bioenergetic needs to grow and propagate. In addition, given that both F<sub>1</sub>F<sub>o</sub>-ATP Synthase and MICOS are found throughout diverse eukaryotic lineages and found enriched within cristae, I have speculated that crosstalk and coordination between these two complexes may exist. Indeed, I came across previous research concluding that crosstalk between F<sub>1</sub>F<sub>o</sub>-ATP Synthase and MICOS is present in Opistokonta model system *S. cerevisiae*. I took the initiative to investigate whether this crosstalk was a conserved feature of mitochondria or just a fungal novelty by using the parasitic protist *T. brucei* as my system, given that it diverged from humans/yeast some 2 billion years ago and bears an almost alien-like mitochondria in comparison. I was able to conclude that this crosstalk was indeed witnessed in *T. brucei* and thus may very well have been present in the last common ancestor of Opistokonta and Discoba. This and other discoveries are discussed in **Paper I**, which summarizes my findings and proposes a novel scenario in cristae development that utilizes transient crosstalk between F<sub>1</sub>F<sub>o</sub>-ATP Synthase and MICOS, a scenario that may have been applied to ancient mitochondria.

#### **4. ORIGINAL PAPER**



# Mitochondrial Contact Site and Cristae Organization System and F<sub>1</sub>F<sub>O</sub>-ATP Synthase Crosstalk Is a Fundamental Property of Mitochondrial Cristae

Lawrence Rudy Cadena,<sup>a,b</sup> Ondřej Gahura,<sup>a</sup> Brian Panicucci,<sup>a</sup> Alena Zíková,<sup>a,b</sup> Hassan Hashimi<sup>a,b</sup>

<sup>a</sup>Institute of Parasitology, Biology Center, Czech Academy of Sciences, České Budějovice, Czech Republic

<sup>b</sup>Faculty of Science, University of South Bohemia, České Budějovice, Czech Republic

**ABSTRACT** Mitochondrial cristae are polymorphic invaginations of the inner membrane that are the fabric of cellular respiration. Both the mitochondrial contact site and cristae organization system (MICOS) and the F<sub>1</sub>F<sub>O</sub>-ATP synthase are vital for sculpting cristae by opposing membrane-bending forces. While MICOS promotes negative curvature at crista junctions, dimeric F<sub>1</sub>F<sub>O</sub>-ATP synthase is crucial for positive curvature at crista rims. Crosstalk between these two complexes has been observed in baker's yeast, the model organism of the Opisthokonta supergroup. Here, we report that this property is conserved in *Trypanosoma brucei*, a member of the Discoba clade that separated from the Opisthokonta ~2 billion years ago. Specifically, one of the paralogs of the core MICOS subunit Mic10 interacts with dimeric F<sub>1</sub>F<sub>O</sub>-ATP synthase, whereas the other core Mic60 subunit has a counteractive effect on F<sub>1</sub>F<sub>O</sub>-ATP synthase oligomerization. This is evocative of the nature of MICOS–F<sub>1</sub>F<sub>O</sub>-ATP synthase crosstalk in yeast, which is remarkable given the diversification that these two complexes have undergone during almost 2 eons of independent evolution. Furthermore, we identified a highly diverged, putative homolog of subunit e, which is essential for the stability of F<sub>1</sub>F<sub>O</sub>-ATP synthase dimers in yeast. Just like subunit e, it is preferentially associated with dimers and interacts with Mic10, and its silencing results in severe defects to cristae and the disintegration of F<sub>1</sub>F<sub>O</sub>-ATP synthase dimers. Our findings indicate that crosstalk between MICOS and dimeric F<sub>1</sub>F<sub>O</sub>-ATP synthase is a fundamental property impacting crista shape throughout eukaryotes.

**IMPORTANCE** Mitochondria have undergone profound diversification in separate lineages that have radiated since the last common ancestor of eukaryotes some eons ago. Most eukaryotes are unicellular protists, including etiological agents of infectious diseases, like *Trypanosoma brucei*. Thus, the study of a broad range of protists can reveal fundamental features shared by all eukaryotes and lineage-specific innovations. Here, we report that two different protein complexes, MICOS and F<sub>1</sub>F<sub>O</sub>-ATP synthase, known to affect mitochondrial architecture, undergo crosstalk in *T. brucei*, just as in baker's yeast. This is remarkable considering that these complexes have otherwise undergone many changes during their almost 2 billion years of independent evolution. Thus, this crosstalk is a fundamental property needed to maintain proper mitochondrial structure even if the constituent players considerably diverged.

**KEYWORDS** ATP synthase, MICOS, *Trypanosoma*, evolution, mitochondria

Mitochondria are ubiquitous organelles that play a central role in cellular respiration in aerobic eukaryotes alongside other essential processes, some of which are retained in anaerobes (1). These organelles have a complex internal organization. While the mitochondrial outer membrane is smooth, the inner membrane is markedly folded into invaginations called cristae, the morphological hallmark of the organelle in

**Citation** Cadena LR, Gahura O, Panicucci B, Zíková A, Hashimi H. 2021. Mitochondrial contact site and cristae organization system and F<sub>1</sub>F<sub>O</sub>-ATP synthase crosstalk is a fundamental property of mitochondrial cristae. *mSphere* 6:e00327-21. <https://doi.org/10.1128/mSphere.00327-21>.

**Editor** Ira J. Blader, University at Buffalo

**Copyright** © 2021 Cadena et al. This is an open-access article distributed under the terms of the [Creative Commons Attribution 4.0 International license](#).

Address correspondence to Hassan Hashimi, hassan@paru.cas.cz.

**Received** 6 April 2021

**Accepted** 2 June 2021

**Published** 16 June 2021

facultative and obligate aerobes (2, 3). Cristae are enriched with respiratory chain complexes that perform oxidative phosphorylation (4, 5), and eukaryotes that cannot form these complexes lack these ultrastructures (1, 6).

Mitochondrial morphology differs among species, tissues, and metabolic states. Nevertheless, these variations are derived from common structural features, some of which were likely inherited from an endosymbiotic alphaproteobacterium that gave rise to the organelle (1, 7, 8). Cristae contribute to this variety as they can assume different shapes, such as platelike lamellar cristae, which decorate yeast and animal mitochondria, and the paddlelike discoidal cristae seen in discoban protists (9). These shapes are at least in part determined by protein complexes embedded within the crista membranes.

The mitochondrial contact site and cristae organization system (MICOS) is a heterooligomeric protein complex that is responsible for the formation and maintenance of crista junctions, narrow points of attachment of cristae to the rest of the inner membrane (10, 11). Crista junctions serve as diffusion barriers into and out of cristae, as these structures cease to act as autonomous bioenergetic units upon MICOS ablation (12). The two core MICOS subunits Mic10 and Mic60, both of which are well conserved throughout eukaryotes (13, 14), have demonstrated membrane modeling activity that contributes to constriction at crista junctions (15–18).

The  $F_1F_O$ -ATP synthase (here “ATP synthase”) dimers also influence the shape of cristae (19). Throughout eukaryotes, dimeric ATP synthase assembles into rows or other oligomeric configurations that promote positive curvature at crista rims (20–22). In yeast and animals, both belonging to the eukaryotic supergroup Opisthokonta (23), ATP synthase dimerization depends on membrane-embedded  $F_O$  moiety subunits e and g (24–26). Although these subunits do not directly contribute to intermonomer contacts, deletion of either of them hinders dimer formation (20) and subsequently results in the emergence of defective cristae (26, 27).

Crosstalk between the crista-shaping factors MICOS and ATP synthase has been demonstrated in yeast. A fraction of Mic10 physically interacts with ATP synthase dimers, presumably via subunit e, and the overexpression of Mic10 leads to the stabilization of ATP synthase oligomers (28, 29). An even more pronounced accumulation of ATP synthase oligomers was observed upon the deletion of the Mic60 gene, but no physical interaction between Mic60 and any ATP synthase subunits has been reported (30). This interplay between MICOS and ATP synthase is a remarkable and still unexplained phenomenon, as both complexes play critical yet apparently antithetical roles in shaping the inner membrane.

Here, we ask whether crosstalk between MICOS and ATP synthase dimers is a fundamental property of cristae. We employed the protist *Trypanosoma brucei*, a model organism that is part of the clade Discoba, which diverged from the Opisthokonta ~1.8 billion years ago (23, 31). Because of their extended independent evolution, discoban MICOS (31–33) and ATP synthase (22, 34–36) differ radically from their opisthokont counterparts. Discoban MICOS has two Mic10 paralogs and an unconventional Mic60 that lacks the C-terminal mitofillin domain characteristic of other Mic60 orthologs (13, 14). Furthermore, unlike opisthokont MICOS, which is organized into two integral membrane subcomplexes, each assembled around a single core subunit, trypanosome MICOS is composed of one integral and one peripheral subcomplex. Discoban ATP synthase exhibits type IV dimer architecture, different from the canonical type I dimers found in opisthokonts (20–32), and has a dissimilar  $F_O$  moiety, which lacks obvious homologs of subunit e or g (37).

## RESULTS

**Depletion of trypanosome Mic60 affects oligomerization of  $F_1F_O$ -ATP synthase independent of other MICOS proteins.** In *T. brucei*, the ablation of conserved MICOS components, Mic60 or both Mic10 paralogs simultaneously, resulted in impaired sub-mitochondrial morphology characterized by elongated cristae adopting arc-like structures (32). Because in budding yeast, the knockout of Mic60 affects the oligomerization

of ATP synthase (27), a major contributor to crista organization, we asked whether ATP synthase plays a role in the changes in mitochondrial ultrastructure observed after Mic10 and Mic60 depletion. After inducible RNA interference (RNAi) silencing of Mic60 ( $\text{Mic60} \downarrow$ ), we observed increased levels of ATP synthase subunits  $\beta$ , a component of the catalytic  $F_1$  sector; oligomycin sensitivity conferral protein (OSCP), a subunit of the peripheral stalk; and ATPTb2, a distant homolog of opistokont subunit d. Simultaneously, levels of Mic10-1 were mildly reduced (Fig. 1A). Notably, RNAi induction of Mic10-2 in the  $\Delta\text{Mic10-1}$   $\text{Mic10-2} \downarrow$  cell line resulted in the same crista defects as those in  $\text{Mic60} \downarrow$  cells (31) but did not result in detectable changes in steady-state levels of ATP synthase subunits (see Fig. S1A in the supplemental material). Thus, the accumulation of ATP synthase subunits documented upon Mic60 knockdown cannot be explained as a general consequence of morphologically elongated and detached cristae.

The increased abundance of ATP synthase subunits prompted us to investigate if the depletion of Mic60 affects the oligomeric state of ATP synthase by immunodetection of ATP synthase complexes in 1.5% *n*-dodecyl- $\beta$ -D-maltoside (DDM)-solubilized mitochondria resolved by blue native polyacrylamide gel electrophoresis (BN-PAGE) (Fig. 1B). RNAi induction in  $\text{Mic60} \downarrow$  but not in  $\Delta\text{Mic10-1}$   $\text{Mic10-2} \downarrow$  cells led to the stabilization of ATP synthase oligomers, which are labile to nonionic detergents in wild-type (WT) cells (38, 39). ATP hydrolysis in-gel activity staining demonstrated that the oligomers are enzymatically active. To confirm that the accumulation of detergent-resistant ATP synthase oligomers was exclusive to  $\text{Mic60} \downarrow$ , we screened the effect of the depletion of two kinetoplastid-specific subunits of MICOS known to disrupt cristae, Mic32 and Mic20. Upon their depletion, no changes in ATP synthase oligomerization were observed on native gels (Fig. S1B). In conclusion, we present evidence that Mic60 depletion in *T. brucei* alters the oligomeric state of ATP synthase independently of the defects to cristae.

**Trypanosome Mic10-1 interacts with  $F_1F_o$ -ATP synthase.** To analyze whether any of the Mic10 paralogs interact with ATP synthase, the  $F_o$  moiety ATPTb2 was C-terminally V5 epitope tagged and used for coimmunoprecipitation (co-IP) from chemically cross-linked mitochondrial lysates. To facilitate the immunocapture of proteins interacting with the ATPTb2-V5 bait, hypotonically isolated mitochondria were cross-linked with dithiobis(succinimidyl propionate) (DSP) prior to solubilization. These were subsequently incubated with mouse anti-V5 antibody conjugated to protein G Dynabeads to immunoprecipitate the tag. After extensive washing, eluted proteins that coimmunoprecipitate with ATPTb2 were separated via protein electrophoresis and blotted, and the co-IP eluate was probed for the presence of Mic10-1 (the molecular weights of this and other proteins investigated here are given in Table S1). Mic10-1 was shown to coimmunoprecipitate with ATPTb2, yielding two discernible bands at approximately 35 kDa and 70 kDa (Fig. 2A). While un-cross-linked Mic10-1 is prominent in the input, it is completely absent in the eluate, suggesting that the protein can coimmunoprecipitate with ATPTb2 only when permanently linked to an unknown partner. We speculate that the ~35-kDa band corresponds to an adduct between Mic10-1 and the unknown partner, and the ~70-kDa band may represent the same adduct cross-linked to ATPTb2.

In order to verify the interaction between Mic10-1 and ATPTb2, we performed a reciprocal pulldown of C-terminally V5-epitope-tagged Mic10-1. Indeed, we were able to capture ATPTb2 with the Mic10-1-V5 bait in the eluted protein fraction with bands present at 40 kDa and 70 kDa. These bands were not detected in the eluate from Mic10-1-V5 immunoprecipitation (IP) after ATPTb2 was targeted by RNAi (Fig. 2B). The former band corresponds to un-cross-linked ATPTb2, and the latter most likely corresponds to the above-mentioned putative tripartite ATPTb2/Mic10-1/unknown partner adduct. Unlike Mic10-1, C-terminally V5-epitope-tagged Mic10-2 did not coimmunoprecipitate ATPTb2 (Fig. S2A), eliminating this paralog as an interaction partner with ATP synthase.

To investigate if Mic10-1 associates with the entire ATP synthase, rather than with its subcomplex or unassembled ATPTb2, proteins in the eluate from co-IP with Mic10-1-V5 were trypsinized and identified by liquid chromatography-tandem mass spectroscopy (LC-MS/MS). Mock IPs on cell lines lacking the V5 tag were performed in parallel as a negative control. Protein enrichment in comparison to mock IP controls was quantified using

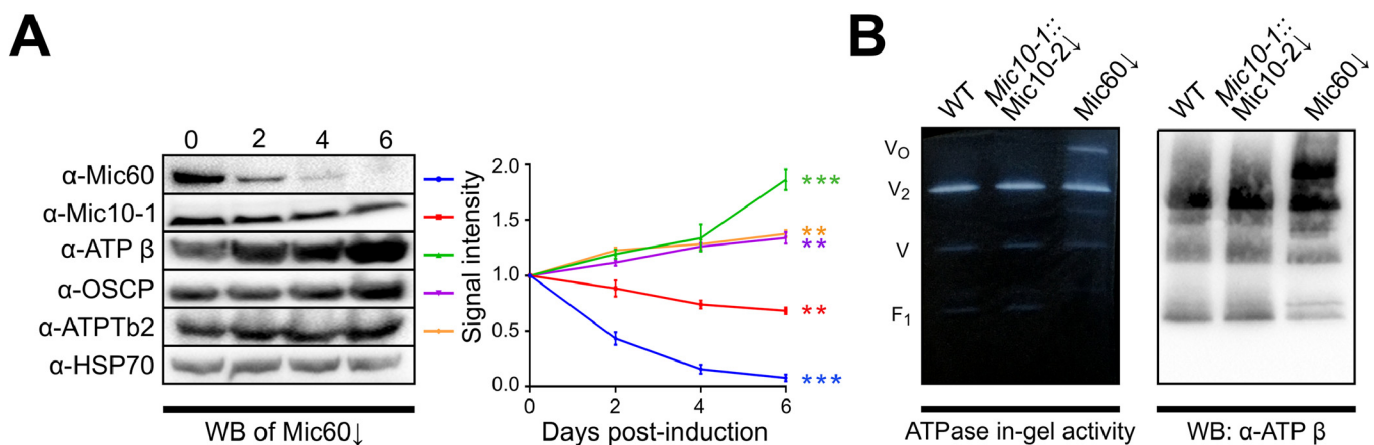


**FIG 1**  $F_1$ - $F_0$ -ATP synthase oligomers are stabilized upon Mic60 depletion. (A) Representative immunoblots of whole-cell lysates from  $\Delta\text{Mic60}$  cells over a 6-day course of RNAi induction with antibodies indicated on the left and densiometric quantification of immunoblots done in triplicate, with the signal normalized to unaffected HSP70 (error bars indicate standard deviations [SD]). Days postinduction are shown above the immunoblots. Line colors to the right of each immunoblot label the antibody signal intensities shown in the graph. The signal intensity is plotted in arbitrary units. The statistical significance of differences in signal intensities between 0 and 6 days after RNAi induction (i.e., the overall change in protein levels over the time course) is shown by asterisks on the right (\*\*,  $P \leq 0.01$ ; \*\*\*,  $P \leq 0.001$ ). (B) Blue native PAGE using 1.5% DDM-solubilized mitochondria from  $\Delta\text{Mic10-1}$   $\Delta\text{Mic10-2}$  and  $\Delta\text{Mic60}$  RNAi cells at 5 days postinduction compared to the wild type (WT). ATP hydrolysis in-gel activity staining is shown on the left, and an immunoblot (WB) probed with anti-ATP synthase  $\beta$ -subunit antibody is shown on the right.  $V_0$ , oligomer;  $V_2$ , dimer;  $V$ , monomer;  $F_1$ , free  $F_1$  moiety.

label-free quantification (LFQ) by a previously described pipeline (40). The identified proteins were filtered to meet the following criteria: (i) presence in all three triplicates, (ii) a mean of each triplicate's log<sub>2</sub>-transformed LFQ intensity score of  $>23$ , (iii) absence from at least two out of three mock IPs, and (iv) presence within the ATOM40 depletome, which indicates that proteins are imported via this outer membrane translocator into the mitochondrion (41). In total, 51 proteins out of 209 detected proteins conformed to these criteria (Fig. 2C and D, Fig. S2B, and Data Set S1). Subunits of the ATP synthase complex and MICOS that are embedded or peripheral to the mitochondrial inner membrane (33) were the most represented proteins in the data set (Fig. 2D). Out of the 23 known subunits that make up the trypanosome ATP synthase, a total of 17 subunits were identified (Fig. 2C), including 5 of 6 subunits of  $F_1$ . As expected, proteins belonging to the MICOS complex were also identified, with all integral subcomplex proteins being present alongside two components of the peripheral moiety; in total, six out of the nine MICOS proteins fit the criteria described above.

In contrast, only 1 protein from electron transport chain (ETC) complex IV (also known as cytochrome *c* oxidase) was recovered using the same criteria out of the 29 proteins that constitute the complex (42). Two other integral inner membrane proteins found to coimmunoprecipitate with the bait were mitochondrial carrier proteins, one of which was an ADP/ATP carrier protein (43). The other 25 proteins found within the set benchmark consisted mainly of highly abundant enzymes affiliated with the tricarboxylic acid (TCA) cycle as well as other prolific soluble mitochondrial matrix proteins (Fig. S2B). To conclude, we present evidence that Mic10-1 interacts with ATP synthase given that the complex's subunits are enriched in Mic10-1–V5 IPs.

**Trypanosome ATPTb8 may be a functional analog of opisthokont  $F_1$ - $F_0$ -ATPase synthase dimer-enriched subunit e.** Previous studies in budding yeast demonstrated that Mic10 directly interacts with ATP synthase dimers via subunit e (28, 29), which is essential for the stability of dimers (20, 44, 45) but does not contribute directly to the monomer-monomer interface (46). In opisthokonts, subunit e contains a conserved GxxxG motif located within its single transmembrane domain (TMD) (45). Analyzing all the ATP synthase subunits identified in the Mic10-1 pulldown (Fig. 2C), we identified a low-molecular-weight protein, termed ATPTb8 (47), that contains this motif (Fig. 3A) and is highly conserved among all kinetoplastids (Fig. S3). A search with HHpred (48) revealed a similarity of the region of ATPTb8 encompassing the TMD to subunit e from yeast and human (also known as ATP5ME) (Fig. 3A). Additionally, a Kyte-Doolittle hydropathy plot comparison of ATPTb8 and human subunit e shows highly similar hydrophobicity

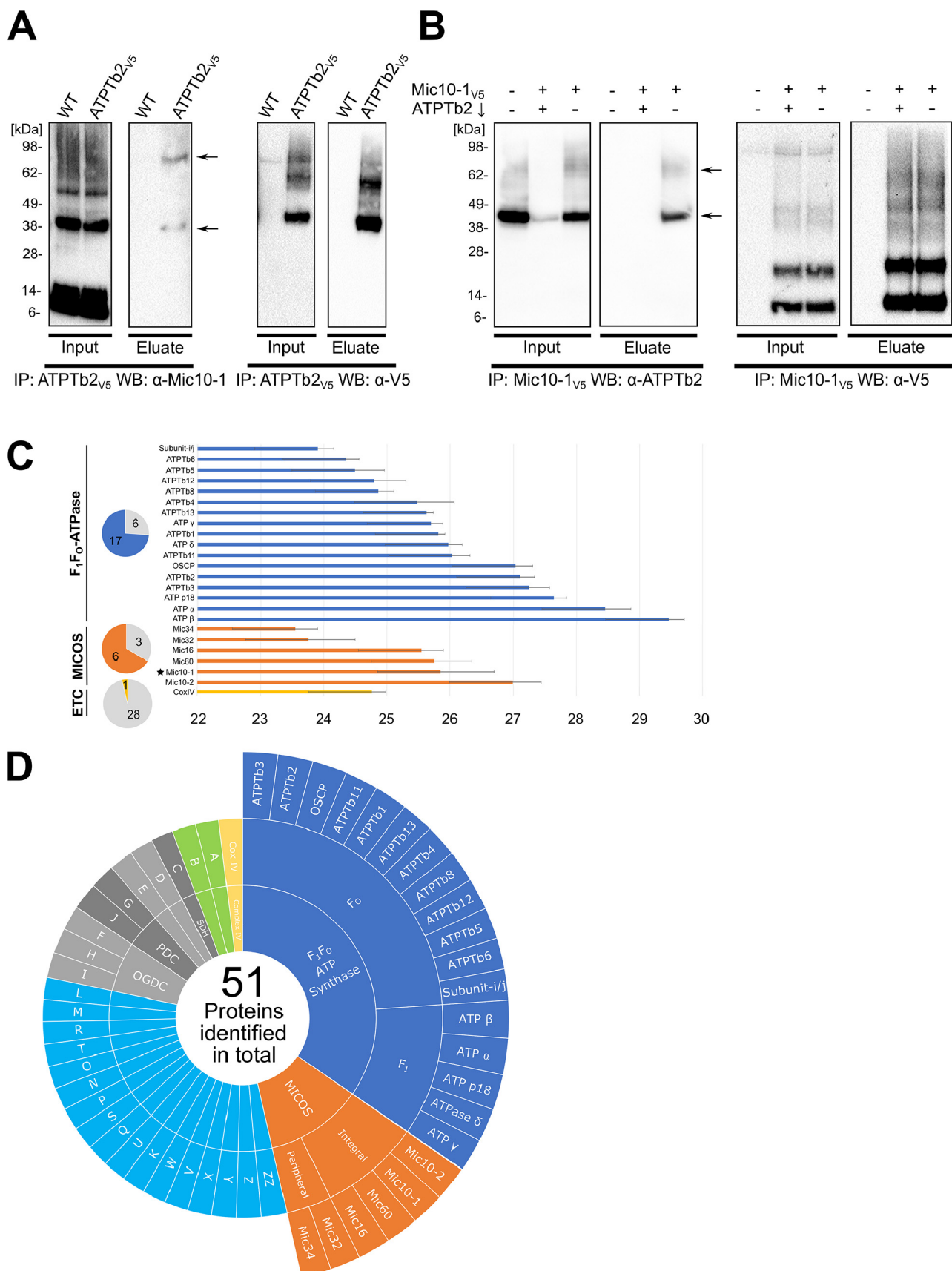


**FIG 2** Mic10-1 interacts with F<sub>o</sub>F<sub>1</sub>-ATP synthase. (A) Immunoprecipitation (IP) with anti-V5 antibody of the wild type (WT) and ATPTb2-V5 from mitochondria cross-linked with 80 μM DSP. The input (10% of the eluate) and eluates were resolved by SDS-PAGE and immunoblotted (WB) with

(Continued on next page)

profiles (Fig. 3B). SWISS-MODEL (49) identified mammalian subunit e among the best templates for structure homology modeling. The modeled part of ATPTb8 corresponds to the transmembrane region of mammalian subunit e, including the GxxxG motif, which homotypically interacts with its counterpart on subunit g (Fig. 3C). Just like subunit e, subunit g was implied in dimer stabilization in yeast (50), but recently, the protein was also proposed to make interdimer contacts in the rows of mammalian ATP synthases (51, 52).

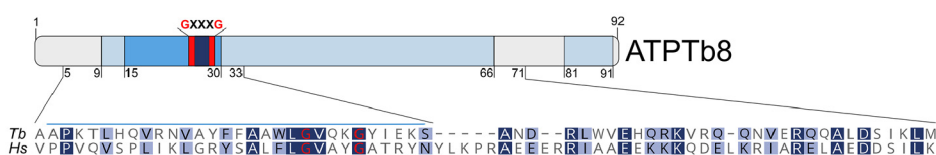
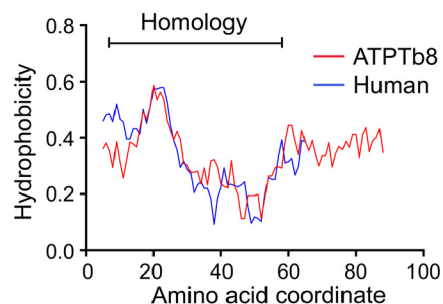
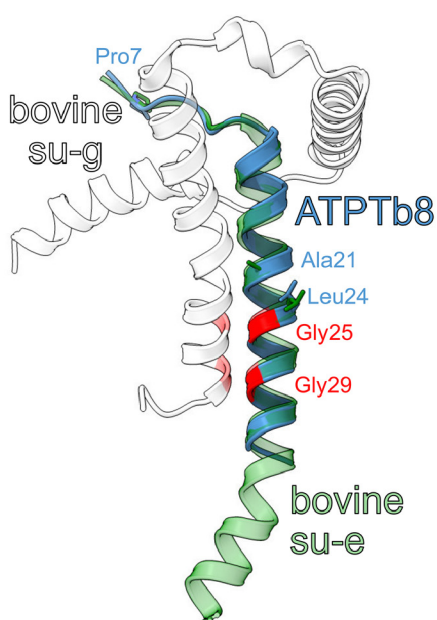
Because the bioinformatic predictions indicated that ATPTb8 might be a distant homolog of opisthokont subunit e, we examined whether this subunit is required for the formation or stability of ATP synthase dimers in *T. brucei*. Utilizing two-dimensional (2D) protein gel electrophoresis, with denaturing SDS-PAGE following the first-dimensional BN-PAGE gel after treatment with 1.5% DDM, we show that C-terminally V5-tagged ATPTb8 is indeed predominantly detected in the dimer fraction (Fig. 4A), which is consistent with the hypothesis that ATPTb8 is involved in dimerization like yeast subunit e (24). Inducible RNAi silencing of ATPTb8 (ATPTb8 $\downarrow$ ) resulted in cellular growth arrest after 72 h (Fig. 4B and C). The growth defect in ATPTb8 $\downarrow$  is likely a consequence of compromised ATP production by oxidative phosphorylation, and it is consistent with growth phenotypes previously observed after silencing of other trypanosomal ATP synthase subunits (38, 39). No alterations in steady-state levels of Mic60 and Mic10-1 were detected in ATPTb8 $\downarrow$  inductions (Fig. S4). Noteworthy, the depletion of ATPTb8 preferentially affected the stability and/or assembly of ATP synthase dimers, as shown by Western blotting (WB) of BN-PAGE-resolved mitochondrial lysates probed with antibodies against subunits  $\beta$  and p18 (Fig. 4D).

To investigate whether the loss of ATPTb8 has an effect on mitochondrial morphology, transmission electron microscopy of cell sections was performed on cells after 3 days of RNAi induction. Mitochondria exhibiting a loss of this subunit depicted anomalous cristae that had circular or semicircular shapes (Fig. 4E), reminiscent of the onion-like structures that appear upon subunit e deletion in budding yeast (20, 26). Collectively, these data suggest that ATPTb8 is a dimer-incorporated subunit much in the same vein as subunit e in budding yeast.

**Trypanosome Mic10-1 interacts with dimeric F<sub>1</sub>F<sub>o</sub>-ATP synthase enriched with ATPTb8.** To confirm that Mic10-1 interacts with fully assembled ATP synthase dimers in *T. brucei*, ATPTb8 was *in situ* C-terminally V5 epitope tagged to perform a cross-link IP. Because ATPTb2 coimmunoprecipitated with ATPTb8-V5, the tag most likely does not interfere with the incorporation of the protein into ATP synthase (Fig. 5A). Next, we probed the IP eluate for the presence of Mic10-1, which was observed mostly as un-cross-linked (Fig. 5B), suggesting that Mic10-1 does not need to be tethered to any interaction partner to coimmunoprecipitate with ATPTb8, unlike with ATPTb2 (Fig. 2A). This further alludes to the possibility that Mic10-1 interacts more firmly with ATP synthase dimers enriched with ATPTb8. Interestingly, a faint band at 40 kDa and a stronger band at 70 kDa were also detected (Fig. 5B, left), reminiscent of the Mic10-1 immunoband pattern seen in the ATPTb2 IP (Fig. 2A).

## FIG 2 Legend (Continued)

antibody against Mic10-1 and V5 peptide. Arrows indicate discernible bands corresponding to ~35 kDa and ~70 kDa. (B) Immunoprecipitation (IP) of WT, Mic10-1-V5:ATPTb2 $\downarrow$ , and Mic10-1-V5 mitochondria cross-linked with 80  $\mu$ M DSP. The input (10% of the eluate) and eluates were resolved by SDS-PAGE and immunoblotted (WB) against anti-ATPTb2 and anti-V5 peptide. Arrows indicate discernible bands corresponding to ~40 kDa and ~70 kDa. (C) Summary of oxidative phosphorylation and MICOS complex subunits that coimmunoprecipitate with Mic10-1-V5 identified by mass spectroscopy. Proteins in dark blue belong to the ATP synthase complex, those in orange belong to the MICOS complex, and those in yellow belong to the electron transport chain (ETC). The naming for the ATP synthase subunits was taken from Gahura et al. and Perez et al. (37, 47). The star indicates bait protein Mic10-1-V5. The intensity score is on the x axis ( $n = 3$ ; error bars indicate SD). Pie charts on the right depict the portion of proteins identified versus the total number of subunits in each respective complex. Other proteins fitting the criteria are given in Fig. S2B in the supplemental material. (D) Sunburst chart of all proteins that coimmunoprecipitate with Mic10-1-V5 identified above the established threshold and criteria described in the text. Subunits of the ATP synthase complex are shown in dark blue and are further distinguished into the F<sub>1</sub> and F<sub>o</sub> moieties. Proteins belonging to the MICOS complex are shown in orange and are further separated into integral or peripheral membrane proteins. All other proteins that met the mass spectroscopy threshold are labeled by letters in boxes in the outside circle, which are defined in Fig. S2B. ETC complex cytochrome c oxidase (complex IV) is shown in yellow, and mitochondrial carriers are shown in green. Components of the tricarboxylic acid (TCA) cycle are in different shades of gray and are distinguished into SDH (succinate dehydrogenase), PDC (pyruvate dehydrogenase complex), and OGDC (oxoglutarate dehydrogenase complex), while those not belonging to any complex lack labels in the innermost circle. Other proteins that could not be categorized into a single group are shown in light blue.

**A****B****C**

**FIG 3** Trypanosome ATPTb8 may be a distant homolog or analog of opisthokont ATP synthase subunit e. (A) Schematic representation of critical features of the ATPTb8 primary structure. The predicted helical regions and the transmembrane domain are shown in pale and dark blue, respectively. The characteristic embedded GxxxG motif is labeled. A sequence alignment with human subunit e is shown for the region with similarity revealed by an HHpred search. The regions of ATPTb8 and mammalian subunit e depicted in panel C are marked with blue and green bars, respectively. (B) Kyte-Doolittle hydrophobicity profile comparison of ATPTb8 and the human homolog of subunit e. The range of homology between both sequences is shown as a bar at the top based on HHpred analysis. (C) Model of ATPTb8 predicted by SWISS-MODEL using the structure of bovine subunit e (su-e) as a template (PDB accession number 6ZPO) (44). The model is superposed with the bovine subunit e and subunit g (su-g) dimer. Glycines of all GxxxG motifs are in red. The conserved residues, which are involved in hydrophobic interactions between subunits e and g, are shown as sticks (44).

## DISCUSSION

Crosstalk between MICOS and ATP synthase was first demonstrated in the budding yeast *Saccharomyces cerevisiae*, a model organism representing the supergroup Opisthokonta, which also encompasses humans. Deletion of Mic60 leads to an accumulation of nonionic-detergent-resistant ATP synthase oligomers, likely connected to the apparent functional

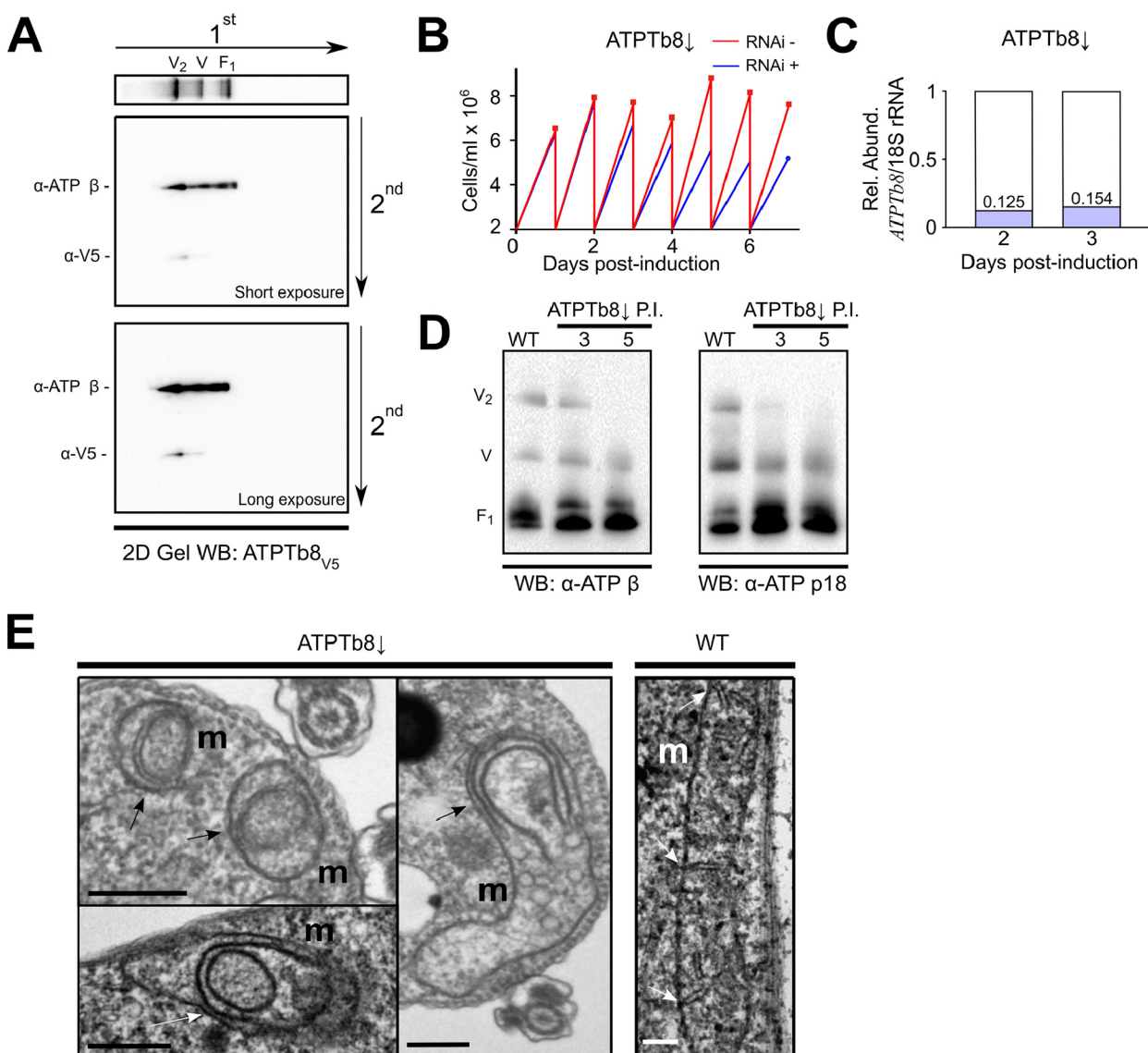


**FIG 4** ATPTb8 is enriched in F<sub>o</sub>F<sub>1</sub>-ATP synthase dimers and crucial for crista formation. (A) Two-dimensional (2D) protein gel electrophoresis of ATPTb8-V5, with denaturing SDS-PAGE following first-dimensional BN-PAGE. (Top) First-dimension immunoblot (WB) against anti-ATP  $\beta$  showing the positions of ATP synthase dimers (V<sub>2</sub>), monomers (V), and the free F<sub>1</sub> moiety. (Middle and bottom) Second-dimension immunoblots against anti-ATP  $\beta$  and anti-V5 at both short (middle) and long (bottom) exposures. (B) Measurement of ATPTb8↓ and negative-control cell growth in glucose-rich medium in which cells were diluted to  $2 \times 10^6$  cells/ml every day ( $n=3$ ; error bars indicate SD). The cell density is on the y axis; days postinduction are on the x axis. (C) Quantitative PCR verification of ATPTb8↓. The relative abundances of ATPTb8 mRNA in RNAi-induced cell lines in comparison to uninduced control cells were normalized to the unaffected 18S rRNA at 2 and 3 days postinduction. (D) BN-PAGE of 1.5% n-dodecyl- $\beta$ -D-maltoside-solubilized mitochondria from ATPTb8↓ cells at 3 and 5 days postinduction (P.I.) compared to the wild type (WT). Immunoblots (WB) against F<sub>1</sub> subunit anti-ATP  $\beta$  and anti-ATP p18 are shown. (E) Transmission electron micrographs of WT *T. brucei* and ATPTb8↓ at 3 days postinduction. Arrows point to cristae of mitochondria (m). Bars, 500 nm.

antagonism between Mic60 and ATP synthase dimerization subunits e and g in yeast (30). At least a fraction of Mic10 interacts with subunit e, which appears to promote ATP synthase dimer oligomerization (28, 29). Indeed, these two phenomena were proposed to be linked in the Mic60 deletion mutants: the cumulative effect of MICOS disruption with the remaining Mic10's stabilizing activity on ATP synthase dimer oligomers resulting in the observed hyperoligomerization phenotype (3, 28).

The physiological role of MICOS-ATP synthase crosstalk in yeast mitochondria remains enigmatic (3), precluding any rational means to hypothesize whether this can be a general eukaryotic phenomenon and not just a fungal novelty. In this work, we have documented the interplay between MICOS and ATP synthase dimers in *T. brucei*,

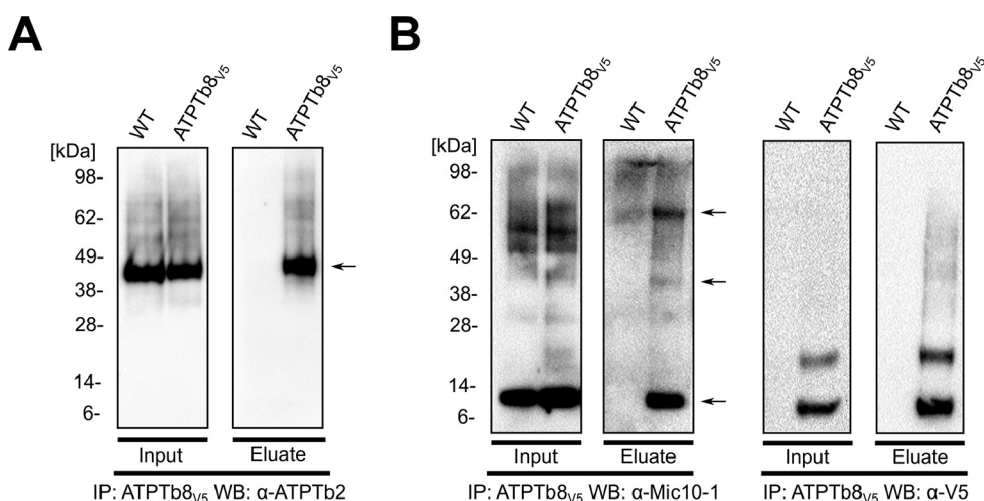


**FIG 5** Mic10-1 interacts with F<sub>o</sub>F<sub>1</sub>-ATP synthase dimers. Immunoprecipitation (IP) of WT and ATPTb8-V5 mitochondria cross-linked as described in the legend of Fig. 2 was performed. (A) The input (10% of the eluate) and eluates were resolved by SDS-PAGE and immunoblotted (WB) using anti-ATPTb2 antibody. The arrow indicates a discernible band corresponding to ~45 kDa (ATPTb2). (B) Same as panel A except using antibody against Mic10-1 and V5 peptide. Arrows indicate discernible bands corresponding to ~10 kDa (Mic10-1), ~40 kDa, and ~70 kDa.

an experimental model belonging to the clade Discoba, which separated from the Opisthokonta ~1.8 billion years ago (23, 31). Even though particular aspects of these complexes are conserved between yeast and trypanosomes, such as MICOS maintaining crista junctions (32) and rows of ATP synthase dimers occurring at the rims of discoidal cristae (22), both complexes exhibit numerous divergent features (30, 37). Based on the early branching of the two lineages and the marked divergence of their MICOS and ATP synthase, we reason that the crosstalk between MICOS and ATP synthase is a fundamental and ancestral property of cristae.

Specifically, we have demonstrated that Mic60 depletion in *T. brucei* phenocopies the stabilization of ATP synthase oligomerization observed in *S. cerevisiae* Mic60 deletion mutants. In addition to being our first indication that there is MICOS-ATP synthase crosstalk in *T. brucei*, this result also supports the putative designation of this subunit as Mic60 despite its lack of a mitofillin domain (32).

We show that crosstalk between MICOS and ATP synthase is mediated by one of the two trypanosome Mic10 paralogs, Mic10-1. We demonstrate that Mic10-1 cross-links to ATPTb2 and ATPTb8, two membrane-associated subunits of the F<sub>o</sub> moiety (34, 37). This observation is consistent with Mic10-1 being an integral membrane protein mostly comprised of two TMDs (32). Furthermore, Mic10-1 coimmunoprecipitates most of the ATP synthase subunits after cross-linking. However, ATP synthase subunits were scarcely detected when MICOS subunits were immunoprecipitated in the absence of any cross-linker (32), suggesting this intercomplex interaction is dynamic and perhaps transient (53).

Our results demonstrate that there are functional differences between Mic10-1 and Mic10-2, as the latter does not interact with ATP synthase. Because Mic10-1 mediates this crosstalk as Mic10 does in yeast, it may represent the conventional Mic10 paralog, while Mic10-2 may be the diversified variant whose precise role in discoidal crista shaping remains undefined. Indeed, trypanosome Mic10-1 has the typical GxGxGxG glycine-rich motif in the C-terminal TMD, a property shared with other Mic10 homologs, whereas Mic10-2's corresponding TMD has a reduced GxGxG motif (32). It is tempting to speculate that this difference may be responsible for Mic10-1 interacting with ATP synthase and may explain why Mic10-2 does not. However, other factors instead of or in synergy with the GxGxGxG motif could possibly mediate Mic10's interaction with ATP synthase.

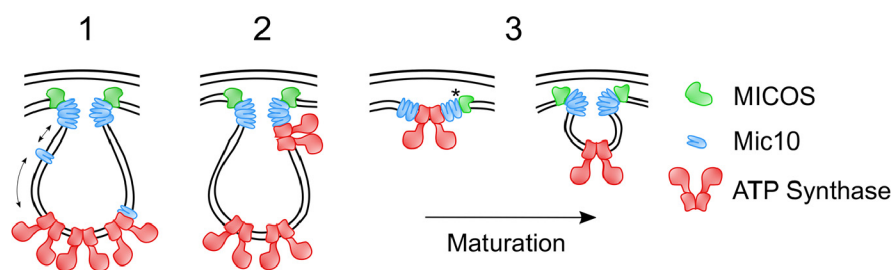


**FIG 6** Possible modes for the functional interplay between MICOS and  $F_0F_1$ -ATP synthase dimers in eukaryotes. Shown is a schematic representation of 3 possible mechanisms of the functional interplay between MICOS (green) and  $F_0F_1$ -ATP synthase (red) in the mitochondrial inner membrane. (1) An extra-MICOS fraction of Mic10 (blue) interacts with ATP synthase dimers at crista rims. Arrows represent crosstalk between MICOS and ATP synthase dimers via Mic10. (2) Mic10 bridges the MICOS complex to ATP synthase dimers directly at crista junctions, enabling dimers to induce positive curvature at the tubular necks of cristae. (3) Transient Mic10-1 interacts with ATP synthase at nascent cristae during ATP synthase dimer-induced invaginations. The asterisk represents a putative MICOS complex subassembly. See Discussion for a more in-depth description of each scenario.

Because yeast Mic10 interacts with ATP synthase dimers, we set out to identify any subunits that may potentially affect dimerization and thus serve as a marker for this higher-order configuration. The  $F_0$  moiety subunits of *T. brucei* ATP synthase identified by mass spectroscopy have not been fully characterized to date (37). Thus, we screened these subunits for the presence of a single-pass TMD with a GxxG motif, a signature of yeast subunit e (24, 45). The protein ATPTb8 emerged from this screen, and outputs of structural modeling and hidden Markov searches support potential homology with human subunit e. ATPTb8 was enriched in dimer fractions, and its ablation phenotype is highly evocative of that of yeast subunit e, in which ATP synthase dimers become sensitive to nonionic detergent treatment along with the correlative emergence of defective cristae (25). Thus, we predict that ATPTb8 may represent a homolog of subunit e. Whether discoban ATPTb8 and opistokont subunit e arose through divergent or convergent evolution remains an open question. Phylogenetic analysis may be precluded by the short lengths of these polypeptides and a high degree of divergence, as observed in human and yeast homologs of subunit e, despite belonging to the same eukaryotic supergroup.

Why is this crosstalk between MICOS and  $F_1F_0$ -ATP synthase present in both opistokonts and discobans, and what role does it play? Two different hypotheses have been previously given, and here, we propose a third (Fig. 6). These hypotheses may not necessarily be mutually exclusive and perhaps may not apply to all lineages. The first hypothesis postulates that an extra-MICOS fraction of Mic10 (15, 16) may relieve membrane tension caused by the positive bending mediated by dimer rows (54), stabilizing the ATP synthase oligomers. In addition, Mic10 binding might enable coordination between MICOS and ATP synthase to temporarily and spatially regulate the shape of cristae (3, 28). In the second hypothesis, Mic10 acts to bridge the MICOS complex with ATP synthase dimers directly at crista junctions (29). In this scenario, the ATP synthase dimers would induce positive curvature of tubular necks of cristae. However, it should be noted that crista junctions in *S. cerevisiae* and other fungi have a predominantly slot-like morphology mainly comprised of flat membranes (9). Our third hypothesis is that we are capturing a transient Mic10-1 interaction with ATP synthase occurring at nascent cristae during the process of ATP synthase dimer-induced invagination of the inner membrane at the future site of crista junctions. This interaction may involve Mic10 alone or as part of a putative MICOS subassembly present on emerging cristae. Why the occurrence of this crosstalk has been preserved throughout the diversification of eukaryotes is still waiting to be answered.

## MATERIALS AND METHODS

**Generation of transgenic cell lines.** All trypanosome cell lines used in this study were derived from *T. brucei* SmOxP927 procyclic-form cells, i.e., TREU 927/4 expressing T7 RNA polymerase and a tetracycline

repressor to allow inducible expression (55), and are listed in Table S2 in the supplemental material. The C-terminally tagged ATPTb8-3×V5 and ATPTb2-3×V5 cell lines were generated using the pPOTv4 vector containing a hygromycin resistance cassette by PCR amplification with the oligonucleotides based on a previously established protocol (56) (Table S2). The underlined sequence anneals to the pPOT vector.

ATPTb8 RNAi constructs were made by PCR amplifying a fragment of the ATPTb8 gene from *T. brucei* strain 927 genomic DNA with the oligonucleotides listed in Table S2. Utilizing the underlined Xhol and BamHI restriction sites within the primer, these fragments were cloned into the pAZ055 stem-loop RNAi vector (Table S2).

**Trypanosome cell culture.** Cells were grown at 27°C in SDM-79 medium supplemented with 10% (vol/vol) fetal bovine serum and 7.5 mg/liter hemin. Cells were grown in the presence and absence of 1 µg/ml doxycycline for RNAi induction. Cell density was measured using the Beckman Coulter Z2 cell and particle counter and maintained at the exponential mid-log growth phase throughout the analyses.

**SDS-PAGE and Western blotting.** Protein samples were separated on a Bolt 4 to 12% Bis-Tris Plus gel (Invitrogen), blotted onto a polyvinylidene difluoride (PVDF) membrane (Amersham), blocked in 5% milk, and probed with the appropriate primary antibody listed in Table S2 diluted in 5% milk in phosphate-buffered saline plus Tween (PBS-T). This was followed by incubation with a secondary horseradish peroxidase (HRP)-conjugated anti-rabbit or anti-mouse antibody (1:2,000; Bio-Rad), depending on the origin of the primary antibody. Proteins were visualized using the Pierce ECL system (Genetica/Bio-Rad) on a ChemiDoc instrument (Bio-Rad).

**Blue native PAGE, in-gel histochemical staining of F<sub>1</sub>-ATPase activity, and 2D electrophoresis.** Blue native PAGE (BN-PAGE) of mitochondrial lysates was adapted from previously reported protocols (34). Briefly, mitochondrial vesicles from ~5 × 10<sup>8</sup> cells were resuspended in 100 µl NativePAGE sample buffer (Invitrogen), lysed with 1.5% (vol/vol) dodecylmaltoside (DDM) for 20 min on ice, and then cleared by centrifugation (18,600 × g for 15 min at 4°C). The protein concentration of each lysate was determined by a Bradford assay (57) so that 50 µg of total protein could be mixed with 5% Coomassie brilliant blue G-250 before loading on a 3 to 12% Bis-Tris BNE gel (Invitrogen). After electrophoresis (2.5 h at 150 V at 4°C), the gel was either blotted onto a PVDF membrane (Amersham) or incubated overnight in an ATPase reaction buffer [35 mM Tris (pH 8.0), 270 mM glycine, 19 mM MgSO<sub>4</sub>, 0.5% Pb(NO<sub>3</sub>)<sub>2</sub>, 15 mM ATP]. For 2D electrophoresis, individual BNE lanes were cut and placed horizontally on a 12% polyacrylamide gel prior to electrophoresis and Western blot analysis.

**Hypotonic mitochondrial isolation.** Mitochondrial vesicles were obtained by hypotonic lysis as described previously (32). Briefly, cell pellets from 5 × 10<sup>8</sup> cells were washed in SBG (150 mM NaCl, 20 mM glucose, 1.6 mM NaHPO<sub>4</sub>), resuspended in DTE (1 mM Tris, 1 mM EDTA [pH 8.0]), and disrupted through a 25-gauge needle. To reintroduce a physiologically isotonic environment, disrupted cells were immediately added to 60% sucrose. Samples were centrifuged (12,300 × g for 15 min at 4°C) to clear the soluble cytoplasmic material from pelleted mitochondrial vesicles. The resulting pellets were resuspended in STM (250 mM sucrose, 20 mM Tris [pH 8.0], 2 mM MgCl<sub>2</sub>) and incubated with 5 µg/ml DNase I for 1 h on ice. An equal volume of STE buffer (250 mM sucrose, 20 mM Tris [pH 8.0], 2 mM EDTA [pH 8.0]) was subsequently added, and the mixture was then centrifuged (18,600 × g for 15 min at 4°C). Pellets enriched with mitochondrial vesicles were then snap-frozen in liquid nitrogen for further analysis or subsequently treated with a chemical cross-linker, as described below.

**Chemical cross-linking.** Hypotonically isolated mitochondrial lysates were resuspended in 1 ml PBS (pH 7.5) and incubated with 80 µM DSP for 2 h on ice. The reaction was stopped by the addition of 20 mM Tris-HCl (pH 7.7) for 15 min at room temperature (RT), and the lysates were then cleared by centrifugation (18,600 × g for 15 min at 4°C). The cross-linked mitochondrial vesicles were then snap-frozen for subsequent immunoprecipitation (IP).

**Immunoprecipitations.** IP of tagged proteins was adapted from previously reported protocols (32). In brief, DSP-cross-linked mitochondrial vesicles from ~5 × 10<sup>8</sup> cells were solubilized in IPP50 (50 mM KCl, 20 mM Tris-HCl [pH 7.7], 3 mM MgCl<sub>2</sub>, 10% glycerol, 1 mM phenylmethanesulfonyl fluoride [PMSF], complete EDTA-free protease inhibitor cocktail [Roche]) supplemented with 1% (vol/vol) Igepal for 20 min on ice. After centrifugation (18,600 × g for 15 min at 4°C), the supernatant was added to 1.5 mg of anti-V5-conjugated magnetic beads, previously washed three times in 200 µl of IPP50 plus 1% Igepal for 5 min at RT. The solubilized mitochondria were rotated with beads for 90 min at 4°C. After the removal of the flowthrough, the beads were washed three times in IPP50 plus 1% Igepal. Prior to elution, the beads were transferred into a new tube. Elution was done in 0.1 M glycine (pH 2.0) for 10 min at 70°C with shaking at 1,000 rpm. The eluate was neutralized with 1 M Tris (pH 8.0). The elution step was repeated to achieve higher recovery. The eluates were further processed for LC-MS/MS analysis or resolved by SDS-PAGE. IPs were performed in triplicate.

**Protein preparation and mass spectroscopy.** Triplicate eluates of coimmunoprecipitated proteins were processed for mass spectroscopy analysis as described previously (58, 59). In brief, samples were resuspended in 100 mM tetraethylammonium bromide (TEAB) containing 2% sodium deoxycholate (SDC). Cysteines were reduced with a final concentration of 10 mM Tris(2-carboxyethyl)phosphine hydrochloride (TCEP) and subsequently cleaved with 1 µg trypsin overnight at 37°C. After digestion, 1% trifluoroacetic acid (TFA) was added to wash twice, and eluates were resuspended in 20 µl of TFA per 100 µg of protein. A nano-reversed-phased column (Easy-Spray column, 50-cm by 75-µm inner diameter, PepMap C<sub>18</sub>, 2-µm particles, 100-Å pore size) was used for LC-MS analysis. Mobile phase buffer A consisted of water and 0.1% formic acid. Mobile phase B consisted of acetonitrile and 0.1% formic acid. Samples were loaded onto the trap column (Acclaim PepMap300 C<sub>18</sub>, 5 µm, 300-Å-wide pore, 300 µm by 5 mm) at a flow rate of 15 µl/min. The loading buffer consisted of water, 2% acetonitrile, and 0.1% TFA. Peptides were eluted using a mobile phase B gradient from 2% to 40% over 60 min at a flow rate of 300 nl/min. The peptide

cations eluted were converted to gas-phase ions via electrospray ionization and analyzed on a Thermo Orbitrap Fusion instrument (Q-OT-qIT; Thermo Fisher). Full MS spectra were acquired in the Orbitrap instrument with a mass range of 350 to 1,400  $m/z$ , at a resolution of 120,000 at 200  $m/z$ , and with a maximum injection time of 50 ms. Tandem MS was performed by isolation at 1.5 Th with the quadrupole, high-energy collisional dissociation (HCD) fragmentation with a normalized collision energy of 30, and rapid-scan MS analysis in the ion trap. The MS/MS ion count target was set to  $10^4$ , and the maximum infection time was set at 35 ms. Only those precursors with a charge state of 2 to 6 were sampled. The dynamic exclusion duration was set to 45 s with a 10-ppm tolerance around the selected precursor and its isotopes. Monoisotopic precursor selection was on with a top-speed mode of 2-s cycles.

**Analysis of mass spectrometry peptides.** Label-free quantification of the data was performed using MaxQuant software (version 1.6.2.1) (60). The false discovery rates for peptides and proteins were set to 1% with a specified minimum peptide length of 7 amino acids. The Andromeda search engine was used for the MS/MS spectra against the *Trypanosoma brucei* database (downloaded from UniProt, November 2018, containing 8,306 entries). Enzyme specificity was set to C-terminal Arg and Lys, alongside cleavage at proline bonds, with a maximum of 2 missed cleavages. Dithiomethylation of cysteine was selected as a fixed modification, with N-terminal protein acetylation and methionine oxidation as variable modifications. The “match between runs” feature in MaxQuant was used to transfer identification to other LC-MS/MS runs based on mass and retention time with a maximum deviation of 0.7 min. Quantifications were performed using a label-free algorithm as described recently (60). Data analysis was performed using Perseus software (version 1.6.1.3). Only proteins identified exclusively alongside a mean  $\log_2$ -transformed LFQ intensity score of  $>23$  and found in the ATOM40 depletome (indicating that proteins are imported into the mitochondria) were considered putative interaction proteins (41). Exclusive identification is defined here as a situation where a given protein was measured in all three replicates of the bait protein pulldown but absent in at least two out of three control replicates.

**Transmission electron microscopy.** For ultrastructural studies, cells were centrifuged at  $620 \times g$  for 10 min at RT and immediately fixed with 2.5% glutaraldehyde in 0.1 M phosphate buffer (pH 7.2). Samples were then postfixed in osmium tetroxide for 2 h at 4°C, washed, dehydrated through an acetone series, and embedded in resin (Polybed 812; Polysciences, Inc.). A series of ultrathin sections were cut using a Leica UCT ultramicrotome (Leica Microsystems) and counterstained with uranyl acetate and lead citrate. Samples were observed using a JEOL 1010 transmission electron microscope operating at an accelerating voltage of 80 kV and equipped with a MegaView III charge-coupled-device (CCD) camera (Emsis).

**Bioinformatic analysis.** The multiple-sequence alignment of ATPTb8 homologs from the order Kinetoplastida was performed by ClustalW using default settings. These alignments were trimmed to remove gaps and regions of poor conservation and rendered in Jalview (version 2.11.1.3) (61). Sequences were obtained from the TriTrypDB database. The regions homologous to human and yeast subunit e were determined using the HHpred toolkit (48), and the helical region and transmembrane domain within the ATPTb8 sequence were predicted by PSIPRED 4.0 and MEMSAT-SVM software (62), respectively. Kyte-Doolittle hydropathy plots for ATPTb8 and the human subunit e sequence were calculated using the ProtScale prediction software courtesy of the ExPASy server (63). The structure of ATPTb8 was homology modeled using SWISS-MODEL (49).

**Data availability.** The mass spectroscopy data have been deposited to the ProteomeXchange Consortium (<http://www.proteomexchange.org>) via the PRIDE partner repository with the data set identifier **PXD025109**.

## SUPPLEMENTAL MATERIAL

Supplemental material is available online only.

**FIG S1**, TIF file, 2.3 MB.

**FIG S2**, TIF file, 2.5 MB.

**FIG S3**, TIF file, 1.9 MB.

**FIG S4**, TIF file, 0.2 MB.

**TABLE S1**, PDF file, 0.05 MB.

**TABLE S2**, PDF file, 0.1 MB.

**DATA SET S1**, XLSX file, 0.1 MB.

## ACKNOWLEDGMENTS

We thank Julius Lukeš for his support in the realization of this project, Karel Harant and Pavel Talacko (Laboratory of Mass Spectrometry, Biocev, Charles University Faculty of Science) for performing LC-MS analysis, and David Hollaus for technical assistance.

We gratefully acknowledge funding from the following sources: Czech Science Foundation grants 20-23513S to H.H., 18-17529S to A.Z., and 20-01450Y to O.G.; Czech Ministry of Education grant OPVVV16\_019/0000759; and Czech Biolimaging grant LM2015062.

## REFERENCES

- Roger AJ, Muñoz-Gómez SA, Kamikawa R. 2017. The origin and diversification of mitochondria. *Curr Biol* 27:R1177–R1192. <https://doi.org/10.1016/j.cub.2017.09.015>.
- Mannella CA. 2020. Consequences of folding the mitochondrial inner membrane. *Front Physiol* 11:536. <https://doi.org/10.3389/fphys.2020.00536>.
- Colina-Tenorio L, Herten P, Pfanner N, Rampelt H. 2020. Shaping the mitochondrial inner membrane in health and disease. *J Intern Med* 287:645–664. <https://doi.org/10.1111/joim.13031>.
- Vogel F, Bornhövd C, Neupert W, Reichert AS. 2006. Dynamic subcompartmentalization of the mitochondrial inner membrane. *J Cell Biol* 175:237–247. <https://doi.org/10.1083/jcb.200605138>.
- Wilkens V, Kohl W, Busch K. 2013. Restricted diffusion of OXPHOS complexes in dynamic mitochondria delays their exchange between cristae and engenders a transient mosaic distribution. *J Cell Sci* 126:103–116. <https://doi.org/10.1242/jcs.108852>.
- Friedman JR, Mourier A, Yamada J, McCaffery JM, Nunnari J. 2015. MICOS coordinates with respiratory complexes and lipids to establish mitochondrial inner membrane architecture. *Elife* 4:e07739. <https://doi.org/10.7554/elife.07739>.
- Martijn J, Vosseberg J, Guy L, Offre P, Ettema TJG. 2018. Deep mitochondrial origin outside the sampled alphaproteobacteria. *Nature* 557:101–105. <https://doi.org/10.1038/s41586-018-0059-5>.
- Lane N, Martin W. 2010. The energetics of genome complexity. *Nature* 467:929–934. <https://doi.org/10.1038/nature09486>.
- Pánek T, Eliáš M, Vancová M, Lukeš J, Hashimi H. 2020. Returning to the fold for lessons in mitochondrial crista diversity and evolution. *Curr Biol* 30:R575–R588. <https://doi.org/10.1016/j.cub.2020.02.053>.
- Wollweber F, von der Malsburg K, van der Laan M. 2017. Mitochondrial contact site and cristae organizing system: a central player in membrane shaping and crosstalk. *Biochim Biophys Acta* 1864:1481–1489. <https://doi.org/10.1016/j.bbampcr.2017.05.004>.
- Rampelt H, Zerbes RM, van der Laan M, Pfanner N. 2017. Role of the mitochondrial contact site and cristae organizing system in membrane architecture and dynamics. *Biochim Biophys Acta* 1864:737–746. <https://doi.org/10.1016/j.bbampcr.2016.05.020>.
- Wolf DM, Segawa M, Kondadi AK, Anand R, Bailey ST, Reichert AS, van der Bliek AM, Shackelford DB, Liesa M, Shirihai OS. 2019. Individual cristae within the same mitochondrion display different membrane potentials and are functionally independent. *EMBO J* 38:e101056. <https://doi.org/10.1522/embj.2018101056>.
- Muñoz-Gómez SA, Slavovits CH, Dacks JB, Baier KA, Spencer KD, Wideman JG. 2015. Ancient homology of the mitochondrial contact site and cristae organizing system points to an endosymbiotic origin of mitochondrial cristae. *Curr Biol* 25:1489–1495. <https://doi.org/10.1016/j.cub.2015.04.006>.
- Huyuen MA, Mühlmeister M, Gotthardt K, Guerrero-Castillo S, Brandt U. 2016. Evolution and structural organization of the mitochondrial contact site (MICOS) complex and the mitochondrial intermembrane space bridging (MIB) complex. *Biochim Biophys Acta* 1863:91–101. <https://doi.org/10.1016/j.bbampcr.2015.10.009>.
- Barbot M, Jans DC, Schulz C, Denkert N, Kroppen B, Hoppert M, Jakobs S, Meinecke M. 2015. Mic10 oligomerizes to bend mitochondrial inner membranes at cristae junctions. *Cell Metab* 21:756–763. <https://doi.org/10.1016/j.cmet.2015.04.006>.
- Bohnert M, Zerbes RM, Davies KM, Mühlleip AW, Rampelt H, Horvath SE, Boenke T, Kram A, Perschil I, Veenhuis M, Kühlbrandt W, van der Klei J, Pfanner N, van der Laan M. 2015. Central role of Mic10 in the mitochondrial contact site and cristae organizing system. *Cell Metab* 21:747–755. <https://doi.org/10.1016/j.cmet.2015.04.007>.
- Tarasenko D, Barbot M, Jans DC, Kroppen B, Sadowski B, Heim G, Möbius W, Jakobs S, Meinecke M. 2017. The MICOS component Mic60 displays a conserved membrane-bending activity that is necessary for normal cristae morphology. *J Cell Biol* 216:889–899. <https://doi.org/10.1083/jcb.201609046>.
- Hessenberger M, Zerbes RM, Rampelt H, Kunz S, Xavier AH, Purfürst B, Lilie H, Pfanner N, van der Laan M, Daumke O. 2017. Regulated membrane remodeling by Mic60 controls formation of mitochondrial crista junctions. *Nat Commun* 8:15258. <https://doi.org/10.1038/ncomms15258>.
- Kühlbrandt W. 2019. Structure and mechanisms of F-type ATP synthases. *Annu Rev Biochem* 88:515–549. <https://doi.org/10.1146/annurev-biochem-013118-110903>.
- Davies KM, Anselmi C, Wittig I, Faraldo-Gomez JD, Kühlbrandt W. 2012. Structure of the yeast  $F_1F_o$ -ATP synthase dimer and its role in shaping the mitochondrial cristae. *Proc Natl Acad Sci U S A* 109:13602–13607. <https://doi.org/10.1073/pnas.1204593109>.
- Mühlleip A, Kock Flygaard R, Ovcáriková J, Lacombe A, Fernandes P, Sheiner L, Amunts A. 2021. ATP synthase hexamer assemblies shape cristae of Toxoplasma mitochondria. *Nat Commun* 12:120. <https://doi.org/10.1038/s41467-020-20381-z>.
- Mühlleip AW, Dewar CE, Schnaufer A, Kühlbrandt W, Davies KM. 2017. In situ structure of trypanosomal ATP synthase dimer reveals a unique arrangement of catalytic subunits. *Proc Natl Acad Sci U S A* 114:992–997. <https://doi.org/10.1073/pnas.1612386114>.
- Keeling PJ, Burki F. 2019. Progress towards the Tree of Eukaryotes. *Curr Biol* 29:R808–R817. <https://doi.org/10.1016/j.cub.2019.07.031>.
- Wagner K, Rehling P, Sanjuán Szklarz LK, Taylor RD, Pfanner N, van der Laan M. 2009. Mitochondrial  $F_1F_o$ -ATP synthase: the small subunits e and g associate with monomeric complexes to trigger dimerization. *J Mol Biol* 392:855–861. <https://doi.org/10.1016/j.jmb.2009.07.059>.
- Arselin G, Vaillier J, Salin B, Schaeffer J, Giraud M-F, Dautant A, Bréthes D, Velours J. 2004. The modulation in subunits e and g amounts of yeast ATP synthase modifies mitochondrial cristae morphology. *J Biol Chem* 279:40392–40399. <https://doi.org/10.1074/jbc.M404316200>.
- Paumard P, Vaillier J, Coulary B, Schaeffer J, Soubannier V, Mueller DM, Bréthes D, di Rago J-P, Velours J. 2002. The ATP synthase is involved in generating mitochondrial cristae morphology. *EMBO J* 21:221–230. <https://doi.org/10.1093/emboj/21.3.221>.
- Harner ME, Unger A-K, Geerts WJ, Mari M, Izawa T, Stenger M, Geimer S, Reggiori F, Westermann B, Neupert W. 2016. An evidence based hypothesis on the existence of two pathways of mitochondrial crista formation. *Elife* 5:e18853. <https://doi.org/10.7554/elife.18853>.
- Rampelt H, Bohnert M, Zerbes RM, Horvath SE, Warscheid B, Pfanner N, van der Laan M. 2017. Mic10, a core subunit of the mitochondrial contact site and cristae organizing system, interacts with the dimeric  $F_1F_o$ -ATP synthase. *J Mol Biol* 429:1162–1170. <https://doi.org/10.1016/j.jmb.2017.03.006>.
- Eydt K, Davies KM, Behrendt C, Wittig I, Reichert AS. 2017. Cristae architecture is determined by an interplay of the MICOS complex and the  $F_1F_o$ -ATP synthase via Mic27 and Mic10. *Microb Cell* 4:259–272. <https://doi.org/10.15698/mic2017.08.585>.
- Rabl R, Soubannier V, Scholz R, Vogel F, Mendl N, Vasiljev-Neumeyer A, Körner C, Jagasia R, Keil T, Baumeister W, Cyrlakoff M, Neupert W, Reichert AS. 2009. Formation of cristae and crista junctions in mitochondria depends on antagonism between Fc1 and Su e/g. *J Cell Biol* 185:1047–1063. <https://doi.org/10.1083/jcb.200811099>.
- Hashimi H. 2019. A parasite's take on the evolutionary cell biology of MICOS. *PLoS Pathog* 15:e1008166. <https://doi.org/10.1371/journal.ppat.1008166>.
- Kaurov I, Vancová M, Schimanski B, Cadena LR, Heller J, Bílý T, Potěšík D, Eichenberger C, Bruce H, Oeljeklaus S, Warscheid B, Zdráhal Z, Schneider A, Lukeš J, Hashimi H. 2018. The diverged trypanosome MICOS complex as a hub for mitochondrial cristae shaping and protein import. *Curr Biol* 28:3393–3407.e5. <https://doi.org/10.1016/j.cub.2018.09.008>.
- Eichenberger C, Oeljeklaus S, Bruggisser J, Mani J, Haenni B, Kaurov I, Niemann M, Zuber B, Lukeš J, Hashimi H, Warscheid B, Schimanski B, Schneider A. 2019. The highly diverged trypanosomal MICOS complex is organized in a nonessential integral membrane and an essential peripheral module. *Mol Microbiol* 112:1731–1743. <https://doi.org/10.1111/mmi.14389>.
- Zíková A, Schnaufer A, Dalley RA, Panigrahi AK, Stuart KD. 2009. The  $F_1F_o$ -ATP synthase complex contains novel subunits and is essential for procyclic *Trypanosoma brucei*. *PLoS Pathog* 5:e1000436. <https://doi.org/10.1371/journal.ppat.1000436>.
- Schnaufer A, Clark-Walker GD, Steinberg AG, Stuart K. 2005. The  $F_1$ -ATP synthase complex in bloodstream stage trypanosomes has an unusual and essential function. *EMBO J* 24:4029–4040. <https://doi.org/10.1038/sj.emboj.7600862>.
- Montgomery MG, Gahura O, Leslie AGW, Zíková A, Walker JE. 2018. ATP synthase from *Trypanosoma brucei* has an elaborated canonical  $F_1$ -domain and conventional catalytic sites. *Proc Natl Acad Sci U S A* 115:2102–2107. <https://doi.org/10.1073/pnas.1720940115>.
- Gahura O, Hierro-Yap C, Zíková A. 8 February 2021. Redesigned and reversed: architectural and functional oddities of the trypanosomal ATP synthase. *Parasitology* <https://doi.org/10.1017/S0031182021000202>.
- Gahura O, Subrtová K, Váčková H, Panicucci B, Fearnley IM, Harbour ME, Walker JE, Zíková A. 2018. The  $F_1$  ATPase from *Trypanosoma brucei* is

- elaborated by three copies of an additional p18-subunit. *FEBS J* 285:614–628. <https://doi.org/10.1111/febs.14364>.
39. Hierro-Yap C, Šubrtová K, Gahura O, Panicucci B, Dewar C, Chinopoulos C, Schnaufer A, Ziková A. 2021. Bioenergetic consequences of  $F_0F_1$ -ATP synthase/ATPase deficiency in two life cycle stages of *Trypanosoma brucei*. *J Biol Chem* 296:100357. <https://doi.org/10.1016/j.jbc.2021.100357>.
  40. Pyrih J, Rašková V, Škodová-Sveráková I, Pánek T, Lukeš J. 2020. ZapE/Afg1 interacts with Oxa1 and its depletion causes a multifaceted phenotype. *PLoS One* 15:e0234918. <https://doi.org/10.1371/journal.pone.0234918>.
  41. Peikert CD, Mani J, Morgenstern M, Käser S, Knapp B, Wenger C, Harsman A, Oeljeklaus S, Schneider A, Warscheid B. 2017. Charting organellar importomes by quantitative mass spectrometry. *Nat Commun* 8:15272. <https://doi.org/10.1038/ncomms15272>.
  42. Panigrahi AK, Ogata Y, Zikova A, Anupama A, Dalley RA, Acestor N, Myler PJ, Stuart KD. 2009. A comprehensive analysis of *Trypanosoma brucei* mitochondrial proteome. *Proteomics* 9:434–450. <https://doi.org/10.1002/pmic.200800477>.
  43. Gnipová A, Šubrtová K, Panicucci B, Horváth A, Lukeš J, Ziková A. 2015. The ADP/ATP carrier and its relationship to oxidative phosphorylation in ancestral protist *Trypanosoma brucei*. *Eukaryot Cell* 14:297–310. <https://doi.org/10.1128/EC.00238-14>.
  44. Arnold I, Pfeiffer K, Neupert W, Stuart RA, Schägger H. 1998. Yeast mitochondrial  $F_0F_1$ -ATP synthase exists as a dimer: identification of three dimer-specific subunits. *EMBO J* 17:7170–7178. <https://doi.org/10.1093/emboj/17.24.7170>.
  45. Arselin G, Giraud M-F, Dautant A, Vaillier J, Brethes D, Coulary-Salin B, Schaeffer J, Velours J. 2003. The GxxxG motif of the transmembrane domain of subunit e is involved in the dimerization/oligomerization of the yeast ATP synthase complex in the mitochondrial membrane. *Eur J Biochem* 270:1875–1884. <https://doi.org/10.1046/j.1432-1033.2003.03557.x>.
  46. Guo H, Bueler SA, Rubinstein JL. 2017. Atomic model for the dimeric Fo region of mitochondrial ATP synthase. *Science* 358:936–940. <https://doi.org/10.1126/science.aoa4815>.
  47. Perez E, Lapaille M, Degand H, Cilibarsi L, Villavicencio-Queijeiro A, Morsomme P, González-Halphen D, Field MC, Remacle C, Baurain D, Cardol P. 2014. The mitochondrial respiratory chain of the secondary green alga *Euglena gracilis* shares many additional subunits with parasitic Trypanosomatidae. *Mitochondrion* 19(Part B): 338–349. <https://doi.org/10.1016/j.mito.2014.02.001>.
  48. Zimmermann L, Stephens A, Nam S-Z, Rau D, Kübler J, Lozajic M, Gabler F, Söding J, Lupas AN, Alva V. 2018. A completely reimplemented MPI bioinformatics toolkit with a new HHpred server at its core. *J Mol Biol* 430:2237–2243. <https://doi.org/10.1016/j.jmb.2017.12.007>.
  49. Waterhouse A, Bertoni M, Bienert S, Studer G, Tauriello G, Gumienny R, Heer FT, de Beer TAP, Rempfer C, Bordoli L, Lepore R, Schwede T. 2018. SWISS-MODEL: homology modelling of protein structures and complexes. *Nucleic Acids Res* 46:W296–W303. <https://doi.org/10.1093/nar/gky427>.
  50. Hahn A, Parey K, Bublitz M, Mills DJ, Zickermann V, Vonck J, Kühlbrandt W, Meier T. 2016. Structure of a complete ATP synthase dimer reveals the molecular basis of inner mitochondrial membrane morphology. *Mol Cell* 63:445–456. <https://doi.org/10.1016/j.molcel.2016.05.037>.
  51. Spikes TE, Montgomery MG, Walker JE. 2021. Interface mobility between monomers in dimeric bovine ATP synthase participates in the ultrastructure of inner mitochondrial membranes. *Proc Natl Acad Sci U S A* 118: e2021012118. <https://doi.org/10.1073/pnas.2021012118>.
  52. Spikes TE, Montgomery MG, Walker JE. 2020. Structure of the dimeric ATP synthase from bovine mitochondria. *Proc Natl Acad Sci U S A* 117:23519–23526. <https://doi.org/10.1073/pnas.2013998117>.
  53. Schweppe DK, Chavez JD, Lee CF, Caudal A, Kruse SE, Stuppard R, Marcinek DJ, Shadel GS, Tian R, Bruce JE. 2017. Mitochondrial protein interactome elucidated by chemical cross-linking mass spectrometry. *Proc Natl Acad Sci U S A* 114:1732–1737. <https://doi.org/10.1073/pnas.1617220114>.
  54. Blum TB, Hahn A, Meier T, Davies KM, Kühlbrandt W. 2019. Dimers of mitochondrial ATP synthase induce membrane curvature and self-assemble into rows. *Proc Natl Acad Sci U S A* 116:4250–4255. <https://doi.org/10.1073/pnas.1816556116>.
  55. Poon SK, Peacock L, Gibson W, Gull K, Kelly S. 2012. A modular and optimized single marker system for generating *Trypanosoma brucei* cell lines expressing T7 RNA polymerase and the tetracycline repressor. *Open Biol* 2:110037. <https://doi.org/10.1098/rsob.110037>.
  56. Dean S, Sunter J, Wheeler RJ, Hodgkinson I, Gluenz E, Gull K. 2015. A toolkit enabling efficient, scalable and reproducible gene tagging in trypanosomatids. *Open Biol* 5:140197. <https://doi.org/10.1098/rsob.140197>.
  57. Bradford MM. 1976. A rapid and sensitive method for the quantitation of microgram quantities of protein utilizing the principle of protein-dye binding. *Anal Biochem* 72:248–254. [https://doi.org/10.1016/0003-2697\(76\)90527-3](https://doi.org/10.1016/0003-2697(76)90527-3).
  58. Hebert AS, Richards AL, Bailey DJ, Ulbrich A, Coughlin EE, Westphall MS, Coon JJ. 2014. The one hour yeast proteome. *Mol Cell Proteomics* 13:339–347. <https://doi.org/10.1074/mcp.M113.034769>.
  59. Rappaport J, Mann M, Ishihama Y. 2007. Protocol for micro-purification, enrichment, pre-fractionation and storage of peptides for proteomics using StageTips. *Nat Protoc* 2:1896–1906. <https://doi.org/10.1038/nprot.2007.261>.
  60. Cox J, Hein MY, Luber CA, Paron I, Nagaraj N, Mann M. 2014. Accurate proteome-wide label-free quantification by delayed normalization and maximal peptide ratio extraction, termed MaxLFQ. *Mol Cell Proteomics* 13:2513–2526. <https://doi.org/10.1074/mcp.M113.031591>.
  61. Waterhouse AM, Procter JB, Martin DMA, Clamp M, Barton GJ. 2009. Jalview version 2—a multiple sequence alignment editor and analysis workbench. *Bioinformatics* 25:1189–1191. <https://doi.org/10.1093/bioinformatics/btp033>.
  62. Jones DT. 2007. Improving the accuracy of transmembrane protein topology prediction using evolutionary information. *Bioinformatics* 23:538–544. <https://doi.org/10.1093/bioinformatics/btl677>.
  63. Duvaud S, Gabella C, Lisacek F, Stockinger H, Ioannidis V, Durinx C. 2021. Expasy, the Swiss Bioinformatics Resource Portal, as designed by its users. *Nucleic Acids Res* gkab225. <https://doi.org/10.1093/nar/gkab225>.

## 5. CONCLUSION

Crosstalk between F<sub>1</sub>F<sub>0</sub>-ATP Synthase and MICOS has been previously demonstrated in yeast, a model system within the supergroup Opisthokonta, which also includes humans (Eydt et al., 2017)(Rampelt et al., 2017a). Deletion of Mic60 leads to increased levels of ATP synthase oligomers, likely the results of functional antagonism between Mic60 and ATP synthase dimer subunits e- and g- in yeast (Rampelt et al., 2017a)(Rabl et al., 2009). It has been reported that a fraction of Mic10 interacts with subunit e- and appears to promote ATP synthase oligomerization. However, this physiological roles of this crosstalk in yeast remains enigmatic, precluding any rational means as to whether this interaction is a general eukaryotic phenomenon or just a fungal novelty.

I was able to document that indeed this interplay between MICOS and ATP synthase dimer is present in *T. brucei*, a model system within the clade Discoba, which separated from Opisthokonta ~1.8 billion years ago (Cadena et al., 2021). Although some aspects of these complexes are conserved in both *S. cerevisiae* and *T. brucei* (*i.e.*, MICOS ability to maintain crista junctions, facilitate protein import and the occurrence of ATP synthase dimer rows at cristae rims) both complexes exhibit divergent features (Hashimi, 2019). Due to their early branching lineages and the marked divergence of their respective MICOS and ATP synthase, I conclude that this crosstalk is a fundamental and ancestral property of cristae (Burki et al., 2020).

It has been demonstrated that trypanosomal Mic60 depletion phenocopies the hyper-oligomerization witnessed in yeast Mic60 deletion mutants (Rampelt et al., 2017a). This is the first indication of a putative MICOS-ATP synthase crosstalk in *T. brucei* (Cadena et al., 2021), in addition, this result supports the putative designation of this subunit as a *bona fide* Mic60 despite the lack of an obvious mitofillin domain (Kaurov et al., 2018). Moreover, crosstalk between MICOS and ATP synthase appears to be mediated by one of the two trypanosome Mic10 paralogs, Mic10-1, as it crosslinks to ATPTb2 and ATPTb8, two membrane-associated subunits of the F<sub>0</sub> moiety (Cadena et al., 2021). This interaction is consistent with Mic10-1 being an integral membrane protein comprised of two transmembrane domains (Kaurov et al., 2018). Additionally, Mic10-1 co-immunoprecipitates with the majority of ATP synthase subunits after cross-linking. However, these ATP synthase subunits are scarcely detected when MICOS is immunoprecipitated in the absence of cross-linker, alluding to the fact that this interaction may be dynamic and/or transient (Cadena et al., 2021).

These results demonstrate that there is functional difference between the Mic10 paralogs, as Mic10-2 appears to not interact with ATP synthase (Cadena et al., 2021). Because Mic10-1 mediates this crosstalk as canonical Mic10 in yeast, it may represent the conventional Mic10 paralog. Whereas Mic10-2 could have arisen as the result of a diversified variant whose precise role in discoidal crista shaping remains unknown. Indeed, Mic10-1 contains the typical GxGxGxG motif in the C-terminal transmembrane domain, a property shared with other Mic10 homologs, whereas Mic10-2 presents a reduced GxGxG motif (Kaurov et al., 2018). One can

speculate that this difference could be the reason why Mic10-1 interacts with ATP synthase as opposed to Mic10-2.

Due to yeast Mic10 interacting with ATP synthase dimers, I set out to identify any subunits that may potentially affect dimerization and thus serve as a marker for hyper-oligomerization. The Fo moiety of *T. brucei* ATP synthase identified by mass spectroscopy has yet to be fully characterized. Thus, proteins containing a single-pass transmembrane domain with a GxxxG motif were screened, a signature motif of yeast subunit e-. The protein ATPTb8 appeared, and outputs of structural modelling, hydropathy plots and Hidden Markov Models supported potential homology with human/yeast subunit e- (Cadena et al., 2021). ATPTb8 is enriched in dimer fractions and its ablation phenocopies that of yeast subunit e-, where defective cristae appear as onion-like structures. Thus, it is predicted that ATPTb8 represents a homolog of subunit e-. However, whether discoban ATPTb8 and opisthokont subunit e- arose through divergent or convergent evolution remains enigmatic, as phylogenetic analysis of the open reading frames and coding regions of both genes are short and highly diverged; a combination lacking the phylogenetic information needed to reconstruct evolutionary relationships.

Why has this crosstalk between MICOS and F<sub>1</sub>F<sub>0</sub>-ATP Synthase prevailed in both opisthokonts and discobans, and what role does it play? Two different hypotheses have been previously established and, in this thesis, a third is proposed (Fig. 11. *Page 20*). These hypotheses may not necessarily be mutually exclusive and perhaps not apply to every lineage. The first hypothesis postulates that unbound Mic10 interacts with ATP synthase dimers. The local negative curvature induced by Mic10 may relieve membrane tension caused by the positive bending mediated by dimer rows, stabilizing ATP synthase oligomers. The second hypothesis speculates Mic10 acts to bridge MICOS and ATP synthase dimers directly at crista junctions. Under these conditions, ATP synthase dimers would induce positive curvature at the tubular necks of cristae. However, crista junctions in *S. cerevisiae* have slot-like morphology and mainly comprised of flat membranes and presents a biophysical problem. This occurrence of flatten membranes at CJs is inconsistent with the co-localization of ATP synthase dimers. Assuming that both MICOS and ATP synthase are evenly distributed along the CJ, the induced curvature would exert forces that would be equal relative to the center of origin, ergo producing a circle, as in the case of tubular CJ morphology. However, under slot-like CJ morphologies, this force is assumed to be an elliptical shaped, thus the forces exerted are eccentric (Fig. 12.). Given the aforementioned reasoning, one would conclude that MICOS and ATP synthase, in conjunction or alone, cannot explain the segregation of tubular and slot-like CJ morphology, therefore, nullifying the basis that MICOS-ATP synthase dimer interaction takes place at CJs and mediates proper CJ morphology.

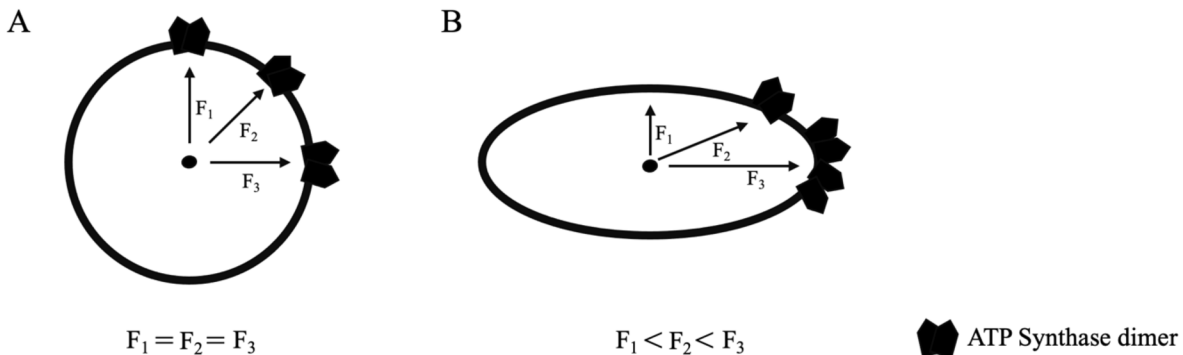


Fig. 12. ATP synthase dimers, with or without MICOS interaction, cannot account for the differentiation of tubular (A) or slot-like (B) crista junctions, unless another factor influences protein complex distribution at crista junction sites. Circle (A) and eclipse (B) show CJ cross sections of tubular and slot-like morphologies, respectively.

The third hypothesis, in which this thesis wishes to propose, is that a transient interaction between Mic10-1 and ATP synthase occurs at nascent cristae during the process of ATP synthase dimer-induced invagination of the MIM at the future site of crista junctions. This interaction may involve Mic10 alone or as a part of a putative MICOS subassembly complex present near emerging crista. As to why this interaction between MICOS and dimeric ATP synthase has been preserved throughout the diversification of eukaryotes has yet to be answered.

## 6. ADDITIONAL EXPERIMENTS AND FURTHER PERSPECTIVES

An enigmatic aspect that has been left unanswered in the three papers investigating MICOS-ATP synthase crosstalk is the discrepancy between Mic60's ability to hyper-oligomerize ATP synthase upon depletion and lack of an obvious interaction between ATP synthase oligomerization and Mic60. Hence, I propose that Mic60 functions either as a cryptic negative regulator in cardiolipin synthesis, or as a negative regulator of cardiolipin incorporation in cristae membranes, as decreased levels of cardiolipin leads of loss of ATP synthase dimers, and artificially increased levels promote hyper-oligomerization (Rampelt et al., 2017a). Given this phenomenon, I assume that under Mic60 deleted/depleted conditions, increased levels of cardiolipin are present in cristae, leading to ATP synthase hyper-oligomerization. A simplistic approach would be to measure levels of cardiolipin in Mic60 depleted/deleted mutants in both *T. brucei* and *S. cerevisiae* via mass spectroscopy compared to both wild type samples (Oemer et al., 2018). Additionally, one should compare the levels of cardiolipin between Mic60 and Mic10 mutants, as both manifest the same ultrastructural phenotype (detached, elongated cristae), but only one exhibits ATP synthase hyper-oligomerization.

Similarly, it has been reported in yeast that overexpression of Mic10 leads to ATP synthase hyper-oligomerization in the same fashion as Mic60 deleted mutants (Rampelt et al., 2017a). Unfortunately, the *T. brucei* system is incapable of overexpressing protein levels to the same extent as in *S. cerevisiae* systems (*e.g.*, pRS426 vector; copy number ~20 per haploid cell)(Johnson et al., 2008) (Fig. 13.). Due to this constraint, I was unable to verify if increased levels of Mic10-1 would lead to ATP synthase hyper-oligomerization (Rampelt et al., 2017a).

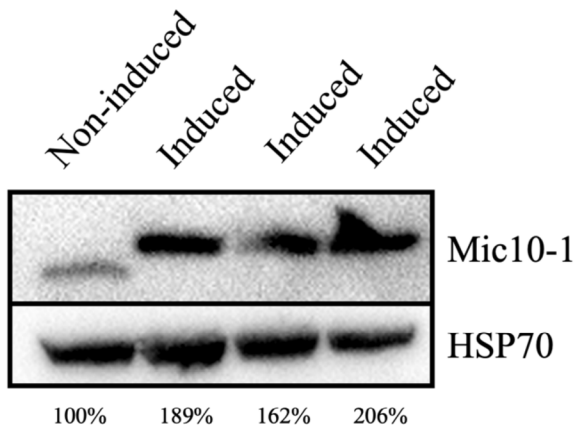


Fig. 13. Verification of Mic10-1 overexpression in *T. brucei* using a modified pLEW111 vector. The steady-state abundance of Mic10-1 in non-induced cells and in cells induced with doxycycline for 5 days was determined by western blot analysis using a specific Mic10-1 antibody. HSP70 serves as a loading control. Percentages on bottom show Mic10-1 signal densiometric quantification relative to non-induced (Unpublished data).

I would be curious whether the MICOS-ATP synthase interaction is present in other eukaryotes outside of Opisthokonta and Discoba. If one were to identify this interaction in organisms from Archaeplastida or SAR, I would assume that this crosstalk is indeed a fundamental feature of cristae development and would go so far as to state that it was perhaps present in the later stages of eukaryogenesis in LECA. However, one would first have to find evidence of possible dimeric ATP synthase present in the mitochondria of LECA, as our hypothesis depends on the ability of ATP synthase to dimerize to facilitate the initial invaginations of cristae at future crista junction sites. Given that ATP synthase dimerization is to date ubiquitous throughout eukaryotes establishes the fact that it is indeed a mitochondrial innovation. The issue that arises from this proposal is the fact that ATP synthase, although present in alphaproteobacteria, does not have the capacity to dimerize. And as such one would assume that ATP synthase dimerization occurred sometime between FECA and LECA. Moreover, recent data suggests that Mic60 homologs are currently present in intracytoplasmic membranes of certain alphaproteobacteria (Muñoz-Gómez et al., 2017), alluding to the fact that the proto-mitochondria held the ability to facilitate inner membrane invaginations. These intracytoplasmic membranes function similar to mitochondrial cristae, as they amplify the cellular membrane for specific energy transduction processes (Fig 14). Moreover, the Light Harvesting Complex II exist as dimers and are found in rows throughout the intracytoplasmic membrane (Liu et al., 2008)(Woronowicz et al., 2013). Indeed, this eerily similarity to ATP

synthase dimer rows and cristae should not go unnoted. Whether the Light Harvesting Complex II is needed for proper intracytoplasmic membrane invagination is still relatively unanswered and suggests an interesting field of research.



Fig. 14. Similarities between intracytoplasmic membranes (ICMs) in alphaproteobacteria (left purple) and cristae in aerobic mitochondria (right: orange). Adapted from (Muñoz-Gómez et al., 2017)

Perhaps I shall go as far as to place forth the idea that modern-day cristae in aerobic mitochondria occurred due to the ability of F<sub>1</sub>F<sub>0</sub>-ATP Synthase to dimerize sometime between the FECA and LECA events with the help of alphaproteobacteria-Mic60.

## 6. REFERENCES

- Abrahams, J.P., Leslie, A.G.W., Lutter, R., Walker, J.E., 1994. Structure at 2.8 Å resolution of F1-ATPase from bovine heart mitochondria. *Nature* 370, 621–628.  
<https://doi.org/10.1038/370621a0>
- Acehan, D., Malhotra, A., Xu, Y., Ren, M., Stokes, D.L., Schlame, M., 2011. Cardiolipin affects the supramolecular organization of ATP synthase in mitochondria. *Biophys. J.* 100, 2184–2192. <https://doi.org/10.1016/j.bpj.2011.03.031>
- Adl, S.M., Bass, D., Lane, C.E., Lukeš, J., Schoch, C.L., Smirnov, A., Agatha, S., Berney, C., Brown, M.W., Burki, F., Cárdenas, P., Čepička, I., Chistyakova, L., Campo, J., Dunthorn, M., Edvardsen, B., Eglit, Y., Guillou, L., Hampl, V., Heiss, A.A., Hoppenrath, M., James, T.Y., Karnkowska, A., Karpov, S., Kim, E., Kolisko, M., Kudryavtsev, A., Lahr, D.J.G., Lara, E., Le Gall, L., Lynn, D.H., Mann, D.G., Massana, R., Mitchell, E.A.D., Morrow, C., Park, J.S., Pawłowski, J.W., Powell, M.J., Richter, D.J., Rueckert, S., Shadwick, L., Shimano, S., Spiegel, F.W., Torruella, G., Youssef, N., Zlatogursky, V., Zhang, Q., 2019. Revisions to the Classification, Nomenclature, and Diversity of Eukaryotes. *J. Eukaryot. Microbiol.* 66, 4–119.  
<https://doi.org/10.1111/jeu.12691>
- Anand, R., Reichert, A.S., Kondadi, A.K., 2021. Emerging Roles of the MICOS Complex in Cristae Dynamics and Biogenesis. *Biology* 10, 600.  
<https://doi.org/10.3390/biology10070600>
- Andersson, S.G.E., Zomorodipour, A., Andersson, J.O., Sicheritz-Pontén, T., Alsmark, U.C.M., Podowski, R.M., Näslund, A.K., Eriksson, A.-S., Winkler, H.H., Kurland, C.G., 1998. The genome sequence of *Rickettsia prowazekii* and the origin of mitochondria. *Nature* 396, 133–140. <https://doi.org/10.1038/24094>
- Anselmi, C., Davies, K.M., Faraldo-Gómez, J.D., 2018. Mitochondrial ATP synthase dimers spontaneously associate due to a long-range membrane-induced force. *J. Gen. Physiol.* 150, 763–770. <https://doi.org/10.1085/jgp.201812033>
- Arnold, I., Pfeiffer, K., Neupert, W., Stuart, R.A., Schägger, H., 1998. Yeast mitochondrial F1F0-ATP synthase exists as a dimer: identification of three dimer-specific subunits. *EMBO J.* 17, 7170–7178. <https://doi.org/10.1093/emboj/17.24.7170>
- Arselin, G., Vaillier, J., Salin, B., Schaeffer, J., Giraud, M.-F., Dautant, A., Brèthes, D., Velours, J., 2004. The modulation in subunits e and g amounts of yeast ATP synthase modifies mitochondrial cristae morphology. *J. Biol. Chem.* 279, 40392–40399.  
<https://doi.org/10.1074/jbc.M404316200>
- Barbot, M., Jans, D.C., Schulz, C., Denkert, N., Kroppen, B., Hoppert, M., Jakobs, S., Meinecke, M., 2015. Mic10 oligomerizes to bend mitochondrial inner membranes at cristae junctions. *Cell Metab.* 21, 756–763.  
<https://doi.org/10.1016/j.cmet.2015.04.006>
- Bílý, T., Sheikh, S., Mallet, A., Bastin, P., Pérez-Morga, D., Lukeš, J., Hashimi, H., 2021. Ultrastructural Changes of the Mitochondrion During the Life Cycle of *Trypanosoma brucei*. *J. Eukaryot. Microbiol.* 68. <https://doi.org/10.1111/jeu.12846>
- Bohnert, M., Zerbes, R.M., Davies, K.M., Mühlleip, A.W., Rampelt, H., Horvath, S.E., Boenke, T., Kram, A., Perschil, I., Veenhuis, M., Kühlbrandt, W., van der Klei, I.J., Pfanner, N., van der Laan, M., 2015. Central role of Mic10 in the mitochondrial contact site and cristae organizing system. *Cell Metab.* 21, 747–755.  
<https://doi.org/10.1016/j.cmet.2015.04.007>
- Bohovych, I., Khalimonchuk, O., 2016. Sending Out an SOS: Mitochondria as a Signaling Hub. *Front. Cell Dev. Biol.* 4. <https://doi.org/10.3389/fcell.2016.00109>

- Bonen, L., Cunningham, R.S., Gray, M.W., Doolittle, W.F., 1977. Wheat embryo mitochondrial 18S ribosomal RNA: evidence for its prokaryotic nature. *Nucleic Acids Res.* 4, 663–671. <https://doi.org/10.1093/nar/4.3.663>
- Bornstein, R., Gonzalez, B., Johnson, S.C., 2020. Mitochondrial pathways in human health and aging. *Mitochondrion* 54, 72–84. <https://doi.org/10.1016/j.mito.2020.07.007>
- Brown, R.C., Evans, D.A., Vickerman, K., 1973. Changes in oxidative metabolism and ultrastructure accompanying differentiation of the mitochondrion in *Trypanosoma brucei*. *Int. J. Parasitol.* 3, 691–704. [https://doi.org/10.1016/0020-7519\(73\)90095-7](https://doi.org/10.1016/0020-7519(73)90095-7)
- Burki, F., Roger, A.J., Brown, M.W., Simpson, A.G.B., 2020. The New Tree of Eukaryotes. *Trends Ecol. Evol.* 35, 43–55. <https://doi.org/10.1016/j.tree.2019.08.008>
- Cadena, L.R., Gahura, O., Panicucci, B., Zíková, A., Hashimi, H., 2021. Mitochondrial Contact Site and Cristae Organization System and F1FO-ATP Synthase Crosstalk Is a Fundamental Property of Mitochondrial Cristae. *mSphere* e0032721. <https://doi.org/10.1128/mSphere.00327-21>
- Campanella, M., Parker, N., Tan, C.H., Hall, A.M., Duchen, M.R., 2009. IF1: setting the pace of the F1Fo-ATP synthase. *Trends Biochem. Sci.* 34, 343–350. <https://doi.org/10.1016/j.tibs.2009.03.006>
- Cogliati, S., Enriquez, J.A., Scorrano, L., 2016. Mitochondrial Cristae: Where Beauty Meets Functionality. *Trends Biochem. Sci.* 41, 261–273. <https://doi.org/10.1016/j.tibs.2016.01.001>
- Cogliati, S., Frezza, C., Soriano, M.E., Varanita, T., Quintana-Cabrera, R., Corrado, M., Cipolat, S., Costa, V., Casarin, A., Gomes, L.C., Perales-Clemente, E., Salviati, L., Fernandez-Silva, P., Enriquez, J.A., Scorrano, L., 2013. Mitochondrial cristae shape determines respiratory chain supercomplexes assembly and respiratory efficiency. *Cell* 155, 160–171. <https://doi.org/10.1016/j.cell.2013.08.032>
- Colina-Tenorio, L., Horten, P., Pfanner, N., Rampelt, H., 2020. Shaping the mitochondrial inner membrane in health and disease. *J. Intern. Med.* 287, 645–664. <https://doi.org/10.1111/joim.13031>
- Connerth, M., Tatsuta, T., Haag, M., Klecker, T., Westermann, B., Langer, T., 2012. Intramitochondrial transport of phosphatidic acid in yeast by a lipid transfer protein. *Science* 338, 815–818. <https://doi.org/10.1126/science.1225625>
- Cotter, P.D., Hill, C., 2003. Surviving the acid test: responses of gram-positive bacteria to low pH. *Microbiol. Mol. Biol. Rev. MMBR* 67, 429–453, table of contents. <https://doi.org/10.1128/MMBR.67.3.429-453.2003>
- Dacks, J.B., Field, M.C., Buick, R., Eme, L., Gribaldo, S., Roger, A.J., Brochier-Armanet, C., Devos, D.P., 2016. The changing view of eukaryogenesis - fossils, cells, lineages and how they all come together. *J. Cell Sci.* 129, 3695–3703. <https://doi.org/10.1242/jcs.178566>
- Daum, G., Vance, J.E., 1997. Import of lipids into mitochondria. *Prog. Lipid Res.* 36, 103–130. [https://doi.org/10.1016/s0163-7827\(97\)00006-4](https://doi.org/10.1016/s0163-7827(97)00006-4)
- Davies, K.M., Anselmi, C., Wittig, I., Faraldo-Gomez, J.D., Kuhlbrandt, W., 2012. Structure of the yeast F1Fo-ATP synthase dimer and its role in shaping the mitochondrial cristae. *Proc. Natl. Acad. Sci.* 109, 13602–13607. <https://doi.org/10.1073/pnas.1204593109>
- Davies, K.M., Strauss, M., Daum, B., Kief, J.H., Osiewacz, H.D., Rycovska, A., Zickermann, V., Kuhlbrandt, W., 2011. Macromolecular organization of ATP synthase and complex I in whole mitochondria. *Proc. Natl. Acad. Sci.* 108, 14121–14126. <https://doi.org/10.1073/pnas.1103621108>

- Ding, C., Wu, Z., Huang, L., Wang, Y., Xue, J., Chen, Si, Deng, Z., Wang, L., Song, Z., Chen, Shi, 2015. Mitofillin and CHCHD6 physically interact with Sam50 to sustain cristae structure. *Sci. Rep.* 5, 16064. <https://doi.org/10.1038/srep16064>
- Doleželová, E., Kunzová, M., Dejung, M., Levin, M., Panicucci, B., Regnault, C., Janzen, C.J., Barrett, M.P., Butter, F., Zíková, A., 2020. Cell-based and multi-omics profiling reveals dynamic metabolic repurposing of mitochondria to drive developmental progression of *Trypanosoma brucei*. *PLOS Biol.* 18, e3000741. <https://doi.org/10.1371/journal.pbio.3000741>
- Dudkina, N.V., Heinemeyer, J., Keegstra, W., Boekema, E.J., Braun, H.-P., 2005. Structure of dimeric ATP synthase from mitochondria: an angular association of monomers induces the strong curvature of the inner membrane. *FEBS Lett.* 579, 5769–5772. <https://doi.org/10.1016/j.febslet.2005.09.065>
- Dudkina, N.V., Oostergetel, G.T., Lewejohann, D., Braun, H.-P., Boekema, E.J., 2010. Row-like organization of ATP synthase in intact mitochondria determined by cryo-electron tomography. *Biochim. Biophys. Acta BBA - Bioenerg.* 1797, 272–277. <https://doi.org/10.1016/j.bbabi.2009.11.004>
- Dudkina, N.V., Sunderhaus, S., Braun, H.-P., Boekema, E.J., 2006. Characterization of dimeric ATP synthase and cristae membrane ultrastructure from *Saccharomyces* and *Polytomella* mitochondria. *FEBS Lett.* 580, 3427–3432. <https://doi.org/10.1016/j.febslet.2006.04.097>
- Edwards, R., Eaglesfield, R., Tokatlidis, K., 2021. The mitochondrial intermembrane space: the most constricted mitochondrial sub-compartment with the largest variety of protein import pathways. *Open Biol.* 11, 210002. <https://doi.org/10.1098/rsob.210002>
- Eichenberger, C., Oeljeklaus, S., Bruggisser, J., Mani, J., Haenni, B., Kaurov, I., Niemann, M., Zuber, B., Lukeš, J., Hashimi, H., Warscheid, B., Schimanski, B., Schneider, A., 2019. The highly diverged trypanosomal MICOS complex is organized in a nonessential integral membrane and an essential peripheral module. *Mol. Microbiol.* 112, 1731–1743. <https://doi.org/10.1111/mmi.14389>
- Embley, T., 2006. Multiple secondary origins of the anaerobic lifestyle in eukaryotes. *Philos. Trans. R. Soc. B Biol. Sci.* 361, 1055–1067. <https://doi.org/10.1098/rstb.2006.1844>
- Eme, L., Spang, A., Lombard, J., Stairs, C.W., Ettema, T.J.G., 2017. Archaea and the origin of eukaryotes. *Nat. Rev. Microbiol.* 15, 711–723. <https://doi.org/10.1038/nrmicro.2017.133>
- Esseiva, A.C., Chanez, A.-L., Bochud-Allemann, N., Martinou, J.-C., Hemphill, A., Schneider, A., 2004. Temporal dissection of Bax-induced events leading to fission of the single mitochondrion in *Trypanosoma brucei*. *EMBO Rep.* 5, 268–273. <https://doi.org/10.1038/sj.embo.7400095>
- Eydt, K., Davis, K.M., Behrendt, C., Wittig, I., Reichert, A.S., 2017. Cristae architecture is determined by an interplay of the MICOS complex and the F1Fo ATP synthase via Mic27 and Mic10. *Microb. Cell* 4, 259–272. <https://doi.org/10.15698/mic2017.08.585>
- Friedman, J.R., Mourier, A., Yamada, J., McCaffery, J.M., Nunnari, J., 2015. MICOS coordinates with respiratory complexes and lipids to establish mitochondrial inner membrane architecture. *eLife* 4. <https://doi.org/10.7554/eLife.07739>
- Fulda, S., Debatin, K.-M., 2006. Extrinsic versus intrinsic apoptosis pathways in anticancer chemotherapy. *Oncogene* 25, 4798–4811. <https://doi.org/10.1038/sj.onc.1209608>
- Gahura, O., Hierro-Yap, C., Zíková, A., 2021. Redesigned and reversed: architectural and functional oddities of the trypanosomal ATP synthase. *Parasitology* 148, 1151–1160. <https://doi.org/10.1017/S0031182021000202>
- Gahura, O., Šubrtová, K., Váčhová, H., Panicucci, B., Fearnley, I.M., Harbour, M.E., Walker, J.E., Zíková, A., 2018. The F1 -ATPase from *Trypanosoma brucei* is elaborated by

- three copies of an additional p18-subunit. *FEBS J.* 285, 614–628.  
<https://doi.org/10.1111/febs.14364>
- Gerhold, J.M., Cansiz-Arda, S., Löhmus, M., Engberg, O., Reyes, A., van Rennes, H., Sanz, A., Holt, I.J., Cooper, H.M., Spelbrink, J.N., 2015. Human Mitochondrial DNA-Protein Complexes Attach to a Cholesterol-Rich Membrane Structure. *Sci. Rep.* 5, 15292. <https://doi.org/10.1038/srep15292>
- Gilkerson, R., De La Torre, P., St. Vallier, S., 2021. Mitochondrial OMA1 and OPA1 as Gatekeepers of Organellar Structure/Function and Cellular Stress Response. *Front. Cell Dev. Biol.* 9, 626117. <https://doi.org/10.3389/fcell.2021.626117>
- Green, D.R., Fitzgerald, P., 2016. Just So Stories about the Evolution of Apoptosis. *Curr. Biol.* CB 26, R620–R627. <https://doi.org/10.1016/j.cub.2016.05.023>
- Guarani, V., McNeill, E.M., Paulo, J.A., Huttlin, E.L., Fröhlich, F., Gygi, S.P., Van Vactor, D., Harper, J.W., 2015. QIL1 is a novel mitochondrial protein required for MICOS complex stability and cristae morphology. *eLife* 4, e06265. <https://doi.org/10.7554/eLife.06265>
- Guo, H., Bueler, S.A., Rubinstein, J.L., 2017. Atomic model for the dimeric FO region of mitochondrial ATP synthase. *Science* 358, 936–940. <https://doi.org/10.1126/science.aao4815>
- Harner, M., Körner, C., Walther, D., Mokranjac, D., Kaesmacher, J., Welsch, U., Griffith, J., Mann, M., Reggiori, F., Neupert, W., 2011. The mitochondrial contact site complex, a determinant of mitochondrial architecture. *EMBO J.* 30, 4356–4370. <https://doi.org/10.1038/emboj.2011.379>
- Hashimi, H., 2019. A parasite's take on the evolutionary cell biology of MICOS. *PLoS Pathog.* 15, e1008166. <https://doi.org/10.1371/journal.ppat.1008166>
- Head, B.P., Zulaika, M., Ryazantsev, S., van der Bliek, A.M., 2011. A novel mitochondrial outer membrane protein, MOMA-1, that affects cristae morphology in *Caenorhabditis elegans*. *Mol. Biol. Cell* 22, 831–841. <https://doi.org/10.1091/mbc.E10-07-0600>
- Hengartner, M.O., 2000. The biochemistry of apoptosis. *Nature* 407, 770–776. <https://doi.org/10.1038/35037710>
- Herrmann, J.M., Riemer, J., 2010. The Intermembrane Space of Mitochondria. *Antioxid. Redox Signal.* 13, 1341–1358. <https://doi.org/10.1089/ars.2009.3063>
- Hessenberger, M., Zerbes, R.M., Rampelt, H., Kunz, S., Xavier, A.H., Purfürst, B., Lilie, H., Pfanner, N., van der Laan, M., Daumke, O., 2017. Regulated membrane remodeling by Mic60 controls formation of mitochondrial crista junctions. *Nat. Commun.* 8, 15258. <https://doi.org/10.1038/ncomms15258>
- Hewitt, V., Alcock, F., Lithgow, T., 2011. Minor modifications and major adaptations: The evolution of molecular machines driving mitochondrial protein import. *Biochim. Biophys. Acta BBA - Biomembr.* 1808, 947–954. <https://doi.org/10.1016/j.bbamem.2010.07.019>
- Hierro-Yap, C., Šubrtová, K., Gahura, O., Panicucci, B., Dewar, C., Chinopoulos, C., Schnaufer, A., Zíková, A., 2021. Bioenergetic consequences of FoF1-ATP synthase/ATPase deficiency in two life cycle stages of *Trypanosoma brucei*. *J. Biol. Chem.* 296, 100357. <https://doi.org/10.1016/j.jbc.2021.100357>
- Höhr, A.I.C., Lindau, C., Wirth, C., Qiu, J., Stroud, D.A., Kutik, S., Guiard, B., Hunte, C., Becker, T., Pfanner, N., Wiedemann, N., 2018. Membrane protein insertion through a mitochondrial β-barrel gate. *Science* 359, eaah6834. <https://doi.org/10.1126/science.aah6834>
- Hongmei, Z., 2012. Extrinsic and Intrinsic Apoptosis Signal Pathway Review, in: Ntuli, T. (Ed.), *Apoptosis and Medicine*. InTech. <https://doi.org/10.5772/50129>

- Hroudová, J., Fišar, Z., 2013. Control mechanisms in mitochondrial oxidative phosphorylation. *Neural Regen. Res.* 8, 363–375. <https://doi.org/10.3969/j.issn.1673-5374.2013.04.009>
- Iovine, J.C., Claypool, S.M., Alder, N.N., 2021. Mitochondrial compartmentalization: emerging themes in structure and function. *Trends Biochem. Sci.* 46, 902–917. <https://doi.org/10.1016/j.tibs.2021.06.003>
- John, G.B., Shang, Y., Li, L., Renken, C., Mannella, C.A., Selker, J.M.L., Rangell, L., Bennett, M.J., Zha, J., 2005. The mitochondrial inner membrane protein mitoflin controls cristae morphology. *Mol. Biol. Cell* 16, 1543–1554. <https://doi.org/10.1091/mbc.e04-08-0697>
- Johnson, B.S., McCaffery, J.M., Lindquist, S., Gitler, A.D., 2008. A yeast TDP-43 proteinopathy model: Exploring the molecular determinants of TDP-43 aggregation and cellular toxicity. *Proc. Natl. Acad. Sci. U. S. A.* 105, 6439–6444. <https://doi.org/10.1073/pnas.0802082105>
- Jouhet, J., 2013. Importance of the hexagonal lipid phase in biological membrane organization. *Front. Plant Sci.* 4, 494. <https://doi.org/10.3389/fpls.2013.00494>
- Junge, W., Nelson, N., 2015. ATP Synthase. *Annu. Rev. Biochem.* 84, 631–657. <https://doi.org/10.1146/annurev-biochem-060614-034124>
- Kaurov, I., Vancová, M., Schimanski, B., Cadena, L.R., Heller, J., Bílý, T., Potěšil, D., Eichenberger, C., Bruce, H., Oeljeklaus, S., Warscheid, B., Zdráhal, Z., Schneider, A., Lukeš, J., Hashimi, H., 2018. The Diverged Trypanosome MICOS Complex as a Hub for Mitochondrial Cristae Shaping and Protein Import. *Curr. Biol.* 28, 3393–3407.e5. <https://doi.org/10.1016/j.cub.2018.09.008>
- Khosravi, S., Harner, M.E., 2020. The MICOS complex, a structural element of mitochondria with versatile functions. *Biol. Chem.* 401, 765–778. <https://doi.org/10.1515/hsz-2020-0103>
- Klein, A., Israel, L., Lackey, S.W.K., Nargang, F.E., Imhof, A., Baumeister, W., Neupert, W., Thomas, D.R., 2012. Characterization of the insertase for β-barrel proteins of the outer mitochondrial membrane. *J. Cell Biol.* 199, 599–611. <https://doi.org/10.1083/jcb.201207161>
- Ku, C., Nelson-Sathi, S., Roettger, M., Sousa, F.L., Lockhart, P.J., Bryant, D., Hazkani-Covo, E., McInerney, J.O., Landan, G., Martin, W.F., 2015. Endosymbiotic origin and differential loss of eukaryotic genes. *Nature* 524, 427–432. <https://doi.org/10.1038/nature14963>
- Kühlbrandt, W., 2019. Structure and Mechanisms of F-Type ATP Synthases. *Annu. Rev. Biochem.* 88, 515–549. <https://doi.org/10.1146/annurev-biochem-013118-110903>
- Kunze, M., Berger, J., 2015. The similarity between N-terminal targeting signals for protein import into different organelles and its evolutionary relevance. *Front. Physiol.* 6. <https://doi.org/10.3389/fphys.2015.00259>
- Lamour, N., Rivière, L., Coustou, V., Coombs, G.H., Barrett, M.P., Bringaud, F., 2005. Proline Metabolism in Procyclic *Trypanosoma brucei* Is Down-regulated in the Presence of Glucose. *J. Biol. Chem.* 280, 11902–11910. <https://doi.org/10.1074/jbc.M414274200>
- Lemasters, J.J., 2007. Modulation of mitochondrial membrane permeability in pathogenesis, autophagy and control of metabolism. *J. Gastroenterol. Hepatol.* 22 Suppl 1, S31–37. <https://doi.org/10.1111/j.1440-1746.2006.04643.x>
- L'Hostis, C., Geindre, M., Deshusses, J., 1993. Active transport of L-proline in the protozoan parasite *Trypanosoma brucei brucei*. *Biochem. J.* 291 ( Pt 1), 297–301. <https://doi.org/10.1042/bj2910297>

- Lill, R., Hoffmann, B., Molik, S., Pierik, A.J., Rietzschel, N., Stehling, O., Uzarska, M.A., Webert, H., Wilbrecht, C., Mühlenhoff, U., 2012. The role of mitochondria in cellular iron-sulfur protein biogenesis and iron metabolism. *Biochim. Biophys. Acta* 1823, 1491–1508. <https://doi.org/10.1016/j.bbamcr.2012.05.009>
- Liu, L.-N., Aartsma, T.J., Frese, R.N., 2008. Dimers of light-harvesting complex 2 from Rhodobacter sphaeroides characterized in reconstituted 2D crystals with atomic force microscopy. *FEBS J.* 275, 3157–3166. <https://doi.org/10.1111/j.1742-4658.2008.06469.x>
- Liu, M., Spremulli, L., 2000. Interaction of Mammalian Mitochondrial Ribosomes with the Inner Membrane. *J. Biol. Chem.* 275, 29400–29406. <https://doi.org/10.1074/jbc.M002173200>
- Lukes, J., Hashimi, H., Zíková, A., 2005. Unexplained complexity of the mitochondrial genome and transcriptome in kinetoplastid flagellates. *Curr. Genet.* 48, 277–299. <https://doi.org/10.1007/s00294-005-0027-0>
- Lukeš, J., Lys Guilbride, D., Votýpka, J., Zíková, A., Benne, R., Englund, P.T., 2002. Kinetoplast DNA Network: Evolution of an Improbable Structure. *Eukaryot. Cell* 1, 495–502. <https://doi.org/10.1128/EC.1.4.495-502.2002>
- Mannella, C.A., 2020. Consequences of Folding the Mitochondrial Inner Membrane. *Front. Physiol.* 11, 536. <https://doi.org/10.3389/fphys.2020.00536>
- Mannella, C.A., 2006. Structure and dynamics of the mitochondrial inner membrane cristae. *Biochim. Biophys. Acta* 1763, 542–548. <https://doi.org/10.1016/j.bbamcr.2006.04.006>
- Mannella, C.A., Lederer, W.J., Jafri, M.S., 2013. The connection between inner membrane topology and mitochondrial function. *J. Mol. Cell. Cardiol.* 62, 51–57. <https://doi.org/10.1016/j.yjmcc.2013.05.001>
- Mannella, C.A., Pfeiffer, D.R., Bradshaw, P.C., Moraru, I.I., Slepchenko, B., Loew, L.M., Hsieh, C., Buttle, K., Marko, M., 2001. Topology of the Mitochondrial Inner Membrane: Dynamics and Bioenergetic Implications. *IUBMB Life Int. Union Biochem. Mol. Biol. Life* 52, 93–100. <https://doi.org/10.1080/15216540152845885>
- Mantilla, B.S., Marchese, L., Casas-Sánchez, A., Dyer, N.A., Ejeh, N., Biran, M., Bringaud, F., Lehane, M.J., Acosta-Serrano, A., Silber, A.M., 2017. Proline Metabolism is Essential for Trypanosoma brucei brucei Survival in the Tsetse Vector. *PLOS Pathog.* 13, e1006158. <https://doi.org/10.1371/journal.ppat.1006158>
- Martijn, J., Vosseberg, J., Guy, L., Offre, P., Ettema, T.J.G., 2018. Deep mitochondrial origin outside the sampled alphaproteobacteria. *Nature* 557, 101–105. <https://doi.org/10.1038/s41586-018-0059-5>
- Matthews, K.R., 2015. 25 years of African trypanosome research: From description to molecular dissection and new drug discovery. *Mol. Biochem. Parasitol.* 200, 30–40. <https://doi.org/10.1016/j.molbiopara.2015.01.006>
- Mehlhorn, H. (Ed.), 2001. Trypanosoma, in: *Encyclopedic Reference of Parasitology*. Springer Berlin Heidelberg, Berlin, Heidelberg, pp. 653–654. [https://doi.org/10.1007/3-540-29834-7\\_1501](https://doi.org/10.1007/3-540-29834-7_1501)
- Michaud, M., Gros, V., Tardif, M., Brugiére, S., Ferro, M., Prinz, W.A., Toulmay, A., Mathur, J., Wozny, M., Falconet, D., Maréchal, E., Block, M.A., Jouhet, J., 2016. AtMic60 Is Involved in Plant Mitochondria Lipid Trafficking and Is Part of a Large Complex. *Curr. Biol. CB* 26, 627–639. <https://doi.org/10.1016/j.cub.2016.01.011>
- Michels, P.A.M., Bringaud, F., Herman, M., Hannaert, V., 2006. Metabolic functions of glycosomes in trypanosomatids. *Biochim. Biophys. Acta* 1763, 1463–1477. <https://doi.org/10.1016/j.bbamcr.2006.08.019>

- Miyata, N., Watanabe, Y., Tamura, Y., Endo, T., Kuge, O., 2016. Phosphatidylserine transport by Ups2-Mdm35 in respiration-active mitochondria. *J. Cell Biol.* 214, 77–88. <https://doi.org/10.1083/jcb.201601082>
- Model, K., Prinz, T., Ruiz, T., Radermacher, M., Krimmer, T., Kühlbrandt, W., Pfanner, N., Meisinger, C., 2002. Protein translocase of the outer mitochondrial membrane: role of import receptors in the structural organization of the TOM complex. *J. Mol. Biol.* 316, 657–666. <https://doi.org/10.1006/jmbi.2001.5365>
- Montgomery, M.G., Gahura, O., Leslie, A.G.W., Zíková, A., Walker, J.E., 2018. ATP synthase from *Trypanosoma brucei* has an elaborated canonical F1 -domain and conventional catalytic sites. *Proc. Natl. Acad. Sci.* 115, 2102–2107. <https://doi.org/10.1073/pnas.1720940115>
- Mühleip, A.W., Dewar, C.E., Schnaufer, A., Kühlbrandt, W., Davies, K.M., 2017. In situ structure of trypanosomal ATP synthase dimer reveals a unique arrangement of catalytic subunits. *Proc. Natl. Acad. Sci.* 114, 992–997. <https://doi.org/10.1073/pnas.1612386114>
- Mühleip, A.W., Joos, F., Wigge, C., Frangakis, A.S., Kühlbrandt, W., Davies, K.M., 2016. Helical arrays of U-shaped ATP synthase dimers form tubular cristae in ciliate mitochondria. *Proc. Natl. Acad. Sci.* 113, 8442–8447. <https://doi.org/10.1073/pnas.1525430113>
- Mun, J.Y., Lee, T.H., Kim, J.H., Yoo, B.H., Bahk, Y.Y., Koo, H.-S., Han, S.S., 2010. *Caenorhabditis elegans* mitofillin homologs control the morphology of mitochondrial cristae and influence reproduction and physiology. *J. Cell. Physiol.* 224, 748–756. <https://doi.org/10.1002/jcp.22177>
- Muñoz-Gómez, S.A., Slamovits, C.H., Dacks, J.B., Baier, K.A., Spencer, K.D., Wideman, J.G., 2015a. Ancient homology of the mitochondrial contact site and cristae organizing system points to an endosymbiotic origin of mitochondrial cristae. *Curr. Biol. CB* 25, 1489–1495. <https://doi.org/10.1016/j.cub.2015.04.006>
- Muñoz-Gómez, S.A., Slamovits, C.H., Dacks, J.B., Wideman, J.G., 2015b. The evolution of MICOS: Ancestral and derived functions and interactions. *Commun. Integr. Biol.* 8, e1094593. <https://doi.org/10.1080/19420889.2015.1094593>
- Muñoz-Gómez, S.A., Wideman, J.G., Roger, A.J., Slamovits, C.H., 2017. The Origin of Mitochondrial Cristae from Alphaproteobacteria. *Mol. Biol. Evol.* 34, 943–956. <https://doi.org/10.1093/molbev/msw298>
- Neupert, W., 1997. Protein import into mitochondria. *Annu. Rev. Biochem.* 66, 863–917. <https://doi.org/10.1146/annurev.biochem.66.1.863>
- Noji, H., Yasuda, R., Yoshida, M., Kinoshita, K., 1997. Direct observation of the rotation of F1-ATPase. *Nature* 386, 299–302. <https://doi.org/10.1038/386299a0>
- Oemer, G., Lackner, K., Muigg, K., Krumschnabel, G., Watschinger, K., Sailer, S., Lindner, H., Gnaiger, E., Wortmann, S.B., Werner, E.R., Zschocke, J., Keller, M.A., 2018. Molecular structural diversity of mitochondrial cardiolipins. *Proc. Natl. Acad. Sci. U. S. A.* 115, 4158–4163. <https://doi.org/10.1073/pnas.1719407115>
- Ogbadoyi, E.O., Robinson, D.R., Gull, K., 2003. A High-Order *Trans*-Membrane Structural Linkage Is Responsible for Mitochondrial Genome Positioning and Segregation by Flagellar Basal Bodies in Trypanosomes. *Mol. Biol. Cell* 14, 1769–1779. <https://doi.org/10.1091/mbc.e02-08-0525>
- Olichon, A., Baricault, L., Gas, N., Guillou, E., Valette, A., Belenguer, P., Lenaers, G., 2003. Loss of OPA1 perturbs the mitochondrial inner membrane structure and integrity, leading to cytochrome c release and apoptosis. *J. Biol. Chem.* 278, 7743–7746. <https://doi.org/10.1074/jbc.C200677200>

- Ott, C., Dorsch, E., Fraunholz, M., Straub, S., Kozjak-Pavlovic, V., 2015. Detailed Analysis of the Human Mitochondrial Contact Site Complex Indicate a Hierarchy of Subunits. PLOS ONE 10, e0120213. <https://doi.org/10.1371/journal.pone.0120213>
- Ott, C., Ross, K., Straub, S., Thiede, B., Götz, M., Goosmann, C., Krischke, M., Mueller, M.J., Krohne, G., Rudel, T., Kozjak-Pavlovic, V., 2012. Sam50 functions in mitochondrial intermembrane space bridging and biogenesis of respiratory complexes. Mol. Cell. Biol. 32, 1173–1188. <https://doi.org/10.1128/MCB.06388-11>
- Ozawa, K., Meikari, T., Motohashi, K., Yoshida, M., Akutsu, H., 2000. Evidence for the presence of an F-type ATP synthase involved in sulfate respiration in *Desulfovibrio vulgaris*. J. Bacteriol. 182, 2200–2206. <https://doi.org/10.1128/JB.182.8.2200-2206.2000>
- Pánek, T., Eliáš, M., Vancová, M., Lukeš, J., Hashimi, H., 2020. Returning to the Fold for Lessons in Mitochondrial Crista Diversity and Evolution. Curr. Biol. 30, R575–R588. <https://doi.org/10.1016/j.cub.2020.02.053>
- Paschen, S.A., Waizenegger, T., Stan, T., Preuss, M., Cyrklaff, M., Hell, K., Rapaport, D., Neupert, W., 2003. Evolutionary conservation of biogenesis of beta-barrel membrane proteins. Nature 426, 862–866. <https://doi.org/10.1038/nature02208>
- Paumard, P., Vaillier, J., Coulary, B., Schaeffer, J., Soubannier, V., Mueller, D.M., Brèthes, D., di Rago, J.-P., Velours, J., 2002. The ATP synthase is involved in generating mitochondrial cristae morphology. EMBO J. 21, 221–230. <https://doi.org/10.1093/emboj/21.3.221>
- Peleh, V., Cordat, E., Herrmann, J.M., 2016. Mia40 is a trans-site receptor that drives protein import into the mitochondrial intermembrane space by hydrophobic substrate binding. eLife 5, e16177. <https://doi.org/10.7554/eLife.16177>
- Perkins, G., Renken, C., Martone, M.E., Young, S.J., Ellisman, M., Frey, T., 1997. Electron Tomography of Neuronal Mitochondria: Three-Dimensional Structure and Organization of Cristae and Membrane Contacts. J. Struct. Biol. 119, 260–272. <https://doi.org/10.1006/jsbi.1997.3885>
- Petri, J., Nakatani, Y., Montgomery, M.G., Ferguson, S.A., Aragão, D., Leslie, A.G.W., Heikal, A., Walker, J.E., Cook, G.M., 2019. Structure of F<sub>1</sub>-ATPase from the obligate anaerobe *Fusobacterium nucleatum*. Open Biol. 9, 190066. <https://doi.org/10.1098/rsob.190066>
- Rabl, R., Soubannier, V., Scholz, R., Vogel, F., Mendl, N., Vasiljev-Neumeyer, A., Körner, C., Jagasia, R., Keil, T., Baumeister, W., Cyrklaff, M., Neupert, W., Reichert, A.S., 2009. Formation of cristae and crista junctions in mitochondria depends on antagonism between Fcj1 and Su e/g. J. Cell Biol. 185, 1047–1063. <https://doi.org/10.1083/jcb.200811099>
- Rampelt, H., Bohnert, M., Zerbes, R.M., Horvath, S.E., Warscheid, B., Pfanner, N., van der Laan, M., 2017a. Mic10, a Core Subunit of the Mitochondrial Contact Site and Cristae Organizing System, Interacts with the Dimeric F1Fo-ATP Synthase. J. Mol. Biol. 429, 1162–1170. <https://doi.org/10.1016/j.jmb.2017.03.006>
- Rampelt, H., van der Laan, M., 2017. The Yin & Yang of Mitochondrial Architecture - Interplay of MICOS and F1Fo-ATP synthase in cristae formation. Microb. Cell Graz Austria 4, 236–239. <https://doi.org/10.15698/mic2017.08.583>
- Rampelt, H., Zerbes, R.M., van der Laan, M., Pfanner, N., 2017b. Role of the mitochondrial contact site and cristae organizing system in membrane architecture and dynamics. Biochim. Biophys. Acta BBA - Mol. Cell Res. 1864, 737–746. <https://doi.org/10.1016/j.bbamcr.2016.05.020>
- Rath, S., Sharma, R., Gupta, R., Ast, T., Chan, C., Durham, T.J., Goodman, R.P., Grabarek, Z., Haas, M.E., Hung, W.H.W., Joshi, P.R., Jourdain, A.A., Kim, S.H., Kotrys, A.V.,

- Lam, S.S., McCoy, J.G., Meisel, J.D., Miranda, M., Panda, A., Patgiri, A., Rogers, R., Sadre, S., Shah, H., Skinner, O.S., To, T.-L., Walker, M.A., Wang, H., Ward, P.S., Wengrod, J., Yuan, C.-C., Calvo, S.E., Mootha, V.K., 2021. MitoCarta3.0: an updated mitochondrial proteome now with sub-organelle localization and pathway annotations. *Nucleic Acids Res.* 49, D1541–D1547.  
<https://doi.org/10.1093/nar/gkaa1011>
- Roger, A.J., 1999. Reconstructing Early Events in Eukaryotic Evolution. *Am. Nat.* 154, S146–S163. <https://doi.org/10.1086/303290>
- Roger, A.J., Muñoz-Gómez, S.A., Kamikawa, R., 2017. The Origin and Diversification of Mitochondria. *Curr. Biol. CB* 27, R1177–R1192.  
<https://doi.org/10.1016/j.cub.2017.09.015>
- Sagan, L., 1967. On the origin of mitosing cells. *J. Theor. Biol.* 14, 225-IN6.  
[https://doi.org/10.1016/0022-5193\(67\)90079-3](https://doi.org/10.1016/0022-5193(67)90079-3)
- Sakowska, P., Jans, D.C., Mohanraj, K., Riedel, D., Jakobs, S., Chacinska, A., 2015. The Oxidation Status of Mic19 Regulates MICOS Assembly. *Mol. Cell. Biol.* 35, 4222–4237. <https://doi.org/10.1128/MCB.00578-15>
- Schwartz, R.M., Dayhoff, M.O., 1978. Origins of prokaryotes, eukaryotes, mitochondria, and chloroplasts. *Science* 199, 395–403. <https://doi.org/10.1126/science.202030>
- Schwepppe, D.K., Chavez, J.D., Lee, C.F., Caudal, A., Kruse, S.E., Stuppard, R., Marcinek, D.J., Shadel, G.S., Tian, R., Bruce, J.E., 2017. Mitochondrial protein interactome elucidated by chemical cross-linking mass spectrometry. *Proc. Natl. Acad. Sci. U. S. A.* 114, 1732–1737. <https://doi.org/10.1073/pnas.1617220114>
- Scorrano, L., Ashiya, M., Buttle, K., Weiler, S., Oakes, S.A., Mannella, C.A., Korsmeyer, S.J., 2002. A Distinct Pathway Remodels Mitochondrial Cristae and Mobilizes Cytochrome c during Apoptosis. *Dev. Cell* 2, 55–67. [https://doi.org/10.1016/S1534-5807\(01\)00116-2](https://doi.org/10.1016/S1534-5807(01)00116-2)
- Scorrano, L., De Matteis, M.A., Emr, S., Giordano, F., Hajnóczky, G., Kornmann, B., Lackner, L.L., Levine, T.P., Pellegrini, L., Reinisch, K., Rizzuto, R., Simmen, T., Stenmark, H., Ungermaann, C., Schuldiner, M., 2019. Coming together to define membrane contact sites. *Nat. Commun.* 10, 1287. <https://doi.org/10.1038/s41467-019-09253-3>
- Shiflett, A.M., Johnson, P.J., 2010. Mitochondrion-related organelles in eukaryotic protists. *Annu. Rev. Microbiol.* 64, 409–429.  
<https://doi.org/10.1146/annurev.micro.62.081307.162826>
- Sojo, V., Dessimoz, C., Pomiankowski, A., Lane, N., 2016. Membrane Proteins Are Dramatically Less Conserved than Water-Soluble Proteins across the Tree of Life. *Mol. Biol. Evol.* 33, 2874–2884. <https://doi.org/10.1093/molbev/msw164>
- Spinelli, J.B., Haigis, M.C., 2018. The multifaceted contributions of mitochondria to cellular metabolism. *Nat. Cell Biol.* 20, 745–754. <https://doi.org/10.1038/s41556-018-0124-1>
- Stephan, T., Brüser, C., Deckers, M., Steyer, A.M., Balzarotti, F., Barbot, M., Behr, T.S., Heim, G., Hübner, W., Ilgen, P., Lange, F., Pacheu-Grau, D., Pape, J.K., Stoldt, S., Huser, T., Hell, S.W., Möbius, W., Rehling, P., Riedel, D., Jakobs, S., 2020. MICOS assembly controls mitochondrial inner membrane remodeling and crista junction redistribution to mediate cristae formation. *EMBO J.* 39.  
<https://doi.org/10.15252/embj.2019104105>
- Strauss, M., Hofhaus, G., Schröder, R.R., Kühlbrandt, W., 2008. Dimer ribbons of ATP synthase shape the inner mitochondrial membrane. *EMBO J.* 27, 1154–1160.  
<https://doi.org/10.1038/emboj.2008.35>
- Takeda, H., Tsutsumi, A., Nishizawa, T., Lindau, C., Bustos, J.V., Wenz, L.-S., Ellenrieder, L., Imai, K., Straub, S.P., Moessmann, W., Qiu, J., Yamamori, Y., Tomii, K., Suzuki,

- J., Murata, T., Ogasawara, S., Nureki, O., Becker, T., Pfanner, N., Wiedemann, N., Kikkawa, M., Endo, T., 2021. Mitochondrial sorting and assembly machinery operates by  $\beta$ -barrel switching. *Nature* 590, 163–169. <https://doi.org/10.1038/s41586-020-03113-7>
- Tang, J., Zhang, K., Dong, J., Yan, C., Hu, C., Ji, H., Chen, L., Chen, S., Zhao, H., Song, Z., 2020. Sam50-Mic19-Mic60 axis determines mitochondrial cristae architecture by mediating mitochondrial outer and inner membrane contact. *Cell Death Differ.* 27, 146–160. <https://doi.org/10.1038/s41418-019-0345-2>
- Tarasenko, D., Barbot, M., Jans, D.C., Kroppen, B., Sadowski, B., Heim, G., Möbius, W., Jakobs, S., Meinecke, M., 2017. The MICOS component Mic60 displays a conserved membrane-bending activity that is necessary for normal cristae morphology. *J. Cell Biol.* 216, 889–899. <https://doi.org/10.1083/jcb.201609046>
- Tarasenko, D., Meinecke, M., 2021. Protein-dependent membrane remodeling in mitochondrial morphology and clathrin-mediated endocytosis. *Eur. Biophys. J.* 50, 295–306. <https://doi.org/10.1007/s00249-021-01501-z>
- Toth, A., Meyrat, A., Stoldt, S., Santiago, R., Wenzel, D., Jakobs, S., von Ballmoos, C., Ott, M., 2020. Kinetic coupling of the respiratory chain with ATP synthase, but not proton gradients, drives ATP production in cristae membranes. *Proc. Natl. Acad. Sci.* 117, 2412–2421. <https://doi.org/10.1073/pnas.1917968117>
- Ueda, E., Tamura, Y., Sakaue, H., Kawano, S., Kakuta, C., Matsumoto, S., Endo, T., 2019. Myristoyl group-aided protein import into the mitochondrial intermembrane space. *Sci. Rep.* 9, 1185. <https://doi.org/10.1038/s41598-018-38016-1>
- Vafai, S.B., Mootha, V.K., 2012. Mitochondrial disorders as windows into an ancient organelle. *Nature* 491, 374–383. <https://doi.org/10.1038/nature11707>
- van Hellemond, J.J., Opperdoes, F.R., Tielens, A.G.M., 2005. The extraordinary mitochondrion and unusual citric acid cycle in *Trypanosoma brucei*. *Biochem. Soc. Trans.* 33, 967–971. <https://doi.org/10.1042/BST20050967>
- van Lis, R., Mendoza-Hernández, G., Groth, G., Atteia, A., 2007. New insights into the unique structure of the FOF1-ATP synthase from the chlamydomonad algae *Polytomella* sp. and *Chlamydomonas reinhardtii*. *Plant Physiol.* 144, 1190–1199. <https://doi.org/10.1104/pp.106.094060>
- Vázquez-Acevedo, M., Cardol, P., Cano-Estrada, A., Lapaille, M., Remacle, C., González-Halphen, D., 2006. The mitochondrial ATP synthase of chlorophycean algae contains eight subunits of unknown origin involved in the formation of an atypical stator-stalk and in the dimerization of the complex. *J. Bioenerg. Biomembr.* 38, 271–282. <https://doi.org/10.1007/s10863-006-9046-x>
- Vázquez-Acevedo, M., Vega-deLuna, F., Sánchez-Vásquez, L., Colina-Tenorio, L., Remacle, C., Cardol, P., Miranda-Astudillo, H., González-Halphen, D., 2016. Dissecting the peripheral stalk of the mitochondrial ATP synthase of chlorophycean algae. *Biochim. Biophys. Acta* 1857, 1183–1190. <https://doi.org/10.1016/j.bbabi.2016.02.003>
- Verner, Z., Basu, S., Benz, C., Dixit, S., Dobáková, E., Faktorová, D., Hashimi, H., Horáková, E., Huang, Z., Paris, Z., Peña-Díaz, P., Ridlon, L., Týč, J., Wildridge, D., Zíková, A., Lukeš, J., 2015. Malleable Mitochondrion of *Trypanosoma brucei*, in: International Review of Cell and Molecular Biology. Elsevier, pp. 73–151. <https://doi.org/10.1016/bsircmb.2014.11.001>
- Vickerman, K., 1985. DEVELOPMENTAL CYCLES AND BIOLOGY OF PATHOGENIC TRYPANOSOMES. *Br. Med. Bull.* 41, 105–114. <https://doi.org/10.1093/oxfordjournals.bmb.a072036>

- von Ballmoos, C., Wiedenmann, A., Dimroth, P., 2009. Essentials for ATP synthesis by F1F0 ATP synthases. *Annu. Rev. Biochem.* 78, 649–672.  
<https://doi.org/10.1146/annurev.biochem.78.081307.104803>
- von der Malsburg, K., Müller, J.M., Bohnert, M., Oeljeklaus, S., Kwiatkowska, P., Becker, T., Loniewska-Lwowska, A., Wiese, S., Rao, S., Milenkovic, D., Hutu, D.P., Zerbes, R.M., Schulze-Specking, A., Meyer, H.E., Martinou, J.-C., Rospert, S., Rehling, P., Meisinger, C., Veenhuis, M., Warscheid, B., van der Klei, I.J., Pfanner, N., Chacinska, A., van der Laan, M., 2011. Dual Role of Mitoflin in Mitochondrial Membrane Organization and Protein Biogenesis. *Dev. Cell* 21, 694–707.  
<https://doi.org/10.1016/j.devcel.2011.08.026>
- Wagner, K., Rehling, P., Sanjuán Szklarz, L.K., Taylor, R.D., Pfanner, N., van der Laan, M., 2009. Mitochondrial F1Fo-ATP synthase: the small subunits e and g associate with monomeric complexes to trigger dimerization. *J. Mol. Biol.* 392, 855–861.  
<https://doi.org/10.1016/j.jmb.2009.07.059>
- Wasserman, D.H., 2009. Four grams of glucose. *Am. J. Physiol.-Endocrinol. Metab.* 296, E11–E21. <https://doi.org/10.1152/ajpendo.90563.2008>
- Weber, T.A., Koob, S., Heide, H., Wittig, I., Head, B., van der Bliek, A., Brandt, U., Mittelbronn, M., Reichert, A.S., 2013. APOOL Is a Cardiolipin-Binding Constituent of the Mitoflin/MINOS Protein Complex Determining Cristae Morphology in Mammalian Mitochondria. *PLoS ONE* 8, e63683.  
<https://doi.org/10.1371/journal.pone.0063683>
- Wiedemann, N., Kozjak, V., Chacinska, A., Schönfisch, B., Rospert, S., Ryan, M.T., Pfanner, N., Meisinger, C., 2003. Machinery for protein sorting and assembly in the mitochondrial outer membrane. *Nature* 424, 565–571.  
<https://doi.org/10.1038/nature01753>
- Wilkens, S., Capaldi, R.A., 1998. ATP synthase's second stalk comes into focus. *Nature* 393, 29. <https://doi.org/10.1038/29908>
- Wilkens, V., Kohl, W., Busch, K., 2013. Restricted diffusion of OXPHOS complexes in dynamic mitochondria delays their exchange between cristae and engenders a transitory mosaic distribution. *J. Cell Sci.* 126, 103–116.  
<https://doi.org/10.1242/jcs.108852>
- Wolf, D.M., Segawa, M., Kondadi, A.K., Anand, R., Bailey, S.T., Reichert, A.S., van der Bliek, A.M., Shackelford, D.B., Liesa, M., Shirihai, O.S., 2019. Individual cristae within the same mitochondrion display different membrane potentials and are functionally independent. *EMBO J.* 38, e101056.  
<https://doi.org/10.15252/embj.2018101056>
- Woronowicz, K., Harrold, J.W., Kay, J.M., Niederman, R.A., 2013. Structural and functional proteomics of intracytoplasmic membrane assembly in Rhodobacter sphaeroides. *J. Mol. Microbiol. Biotechnol.* 23, 48–62. <https://doi.org/10.1159/000346520>
- Wu, Z., Ho, W.S., Lu, R., 2021. Targeting Mitochondrial Oxidative Phosphorylation in Glioblastoma Therapy. *Neuromolecular Med.* <https://doi.org/10.1007/s12017-021-08678-8>
- Xie, J., Marusich, M.F., Souda, P., Whitelegge, J., Capaldi, R.A., 2007. The mitochondrial inner membrane protein mitoflin exists as a complex with SAM50, metaxins 1 and 2, coiled-coil-helix coiled-coil-helix domain-containing protein 3 and 6 and DnaJC11. *FEBS Lett.* 581, 3545–3549. <https://doi.org/10.1016/j.febslet.2007.06.052>
- Yang, D., Oyaizu, Y., Oyaizu, H., Olsen, G.J., Woese, C.R., 1985. Mitochondrial origins. *Proc. Natl. Acad. Sci. U. S. A.* 82, 4443–4447.  
<https://doi.org/10.1073/pnas.82.13.4443>

- Yoshida, M., Muneyuki, E., Hisabori, T., 2001. ATP synthase--a marvellous rotary engine of the cell. *Nat. Rev. Mol. Cell Biol.* 2, 669–677. <https://doi.org/10.1038/35089509>
- Zaremba-Niedzwiedzka, K., Caceres, E.F., Saw, J.H., Bäckström, D., Juzokaite, L., Vancaester, E., Seitz, K.W., Anantharaman, K., Starnawski, P., Kjeldsen, K.U., Stott, M.B., Nunoura, T., Banfield, J.F., Schramm, A., Baker, B.J., Spang, A., Ettema, T.J.G., 2017. Asgard archaea illuminate the origin of eukaryotic cellular complexity. *Nature* 541, 353–358. <https://doi.org/10.1038/nature21031>
- Zerbes, R.M., Höß, P., Pfanner, N., van der Laan, M., Bohnert, M., 2016. Distinct Roles of Mic12 and Mic27 in the Mitochondrial Contact Site and Cristae Organizing System. *J. Mol. Biol.* 428, 1485–1492. <https://doi.org/10.1016/j.jmb.2016.02.031>
- Zerbes, R.M., van der Klei, I.J., Veenhuis, M., Pfanner, N., van der Laan, M., Bohnert, M., 2012. Mitofillin complexes: conserved organizers of mitochondrial membrane architecture. *Biol. Chem.* 393, 1247–1261. <https://doi.org/10.1515/hsz-2012-0239>
- Zick, M., Rabl, R., Reichert, A.S., 2009. Cristae formation—linking ultrastructure and function of mitochondria. *Biochim. Biophys. Acta BBA - Mol. Cell Res.* 1793, 5–19. <https://doi.org/10.1016/j.bbamcr.2008.06.013>
- Zíková, A., Verner, Z., Nenarokova, A., Michels, P.A.M., Lukeš, J., 2017. A paradigm shift: The mitoproteomes of procyclic and bloodstream *Trypanosoma brucei* are comparably complex. *PLOS Pathog.* 13, e1006679. <https://doi.org/10.1371/journal.ppat.1006679>